Computational Simulation of the Mechanobiological Response of Arterial Tissue

Colin James Boyle, B.A., B.A.I.

A thesis submitted to the University of Dublin in partial fulfilment of the requirements for the degree of

Doctor in Philosophy

September 2011

Supervisor

Prof. Patrick J. Prendergast

Prof. G. Dubini **Politecnico di Milano**	**Dr. D. Kelly**
External examiner	Internal examiner

Declaration

I declare that this thesis has not been submitted as an exercise for a degree at this or any other university and it is entirely my own work.

I agree to deposit this thesis in the University's open access institutional repository or allow the library to do so on my behalf, subject to Irish Copyright Legislation and Trinity College Library conditions of use and acknowledgement.

Colin Boyle
September 2011

Abstract

Ischaemic heart disease, causing restriction of arterial blood flow to the heart tissue, can be treated with mechanical revascularisation treatments such as balloon angioplasty and stent implantation. One remaining limitation to the success of these treatments is the re-blockage of the treated artery, termed restenosis. The paradigm of re-blockage as the tissue's response to injury has been proposed to explain restenosis in stents and corroborated with pathological studies. This paradigm has never been used to form the basis of a predictive theoretical model of restenosis. In this thesis, the hypothesis that mechanically-induced injury stimulates restenosis is tested by developing a simulation technique based on this paradigm. The model explicitly simulates the response of individual cells to injury-induced inflammation.

A model based on a vessel-wall stress threshold for injury and smooth muscle cell phenotype modulation was developed and tested by applying it to two stents known to induce differing amounts of restenosis *in vivo*. The model predicted similar differences between stents, but only when a low-level inflammation response was prescribed, demonstrating the importance of inflammation on restenosis prediction.

The algorithms for injury prediction, inflammation and smooth muscle cell phenotype were then refined in a two dimensional model. The new simulation procedure was capable of being calibrated to human balloon angioplasty data, and predicted a correlation between stent expansion and restenosis. Inflammation intensity was found to increase this correlation.

The refined model was then re-implemented in three dimensions, and tested on three clinically-available coronary stents of differing design. The model predicted a relative difference between stents similar to that found in clinical trials.

These results corroborate the paradigm that neointimal hyperplasia is injury-induced. The technique can differentiate between stent designs based on a prediction of long-term lumen geometry, rather than solely on a mechanical analysis. The technique could be applied to novel revascularisation treatments and device designs.

Acknowledgements

I count myself very lucky to have had Prof. Patrick Prendergast as my supervisor. His enthusiasm for bioengineering, his immense knowledge of mechanobiology, and his skill in all aspects of academic life have been essential to my success during my PhD. I greatly appreciated having the academic freedom that he encouraged so early in my career. I cannot count how many times even the briefest meetings have brought a clarity and sense of purpose to often chaotic work!

I would like to thank all the technical and administrative staff in the department. I would especially like to thank Sheena, for giving so generously so much time and effort in all manner of organising throughout my time in Trinity. I am grateful to Alex who provided immense help and advice with the computational methods used in this thesis. Many others have helped me with the work in my thesis, including Damien Byrne, Pavel Galibarov, Bruce Murphy, Triona Lally, Danny Kelly, Eoghan Maher and Michael Early.

I am also very lucky to have spent time in the company of such fun and friendly people in Trinity, and I will always remember with fondness all of the great company at tea-breaks, lunches, conferences, nights out and hikes: Hanifeh, Steve T, Michael, Eoghan, Feng, Katey, Steve W, Brianne, Louise, Fionn, Pavel, Sara, Oana, Jessica, Damien, Kevin, Conor, Alanna, Thomas, Tatiana, Eamonn, Tariq, Darren, Grainne, Iratxe, Nathalie, Karen, Geraldine, Jennifer, Matt and Colm.

A special thanks must go to Niamh for her love, unrelenting support and constant optimism. Her ability to put supposed research catastrophes into perspective has surely prevented untold numbers of myocardial infarctions. I also greatly appreciate the support of all the Nowlans.

Finally, I would like to thank my family, Heather and Kevin, and especially my parents. Their faith in my ability and their unconditional support have made it possible to complete this work. I hope they will be as proud of me as I am of them.

I would like to acknowledge the funding of Science Foundation Ireland (SFI), Medtronic Galway and Enterprise Ireland.

Contents

Publications and presentations resulting from this study

Journal Papers

Boyle, C.J., Lennon, A.B., Prendergast, P.J., "In silico prediction of the mechanobiological response of arterial tissue: application to angioplasty and stenting," *Journal of Biomechanical Engineering*, 2011, 133, 081001.

Boyle, C.J., Lennon, A.B., Early, M., Kelly, D.J., Lally, C., Prendergast, P.J., "Computational simulation methodologies for mechanobiological modelling: a cell-centred approach to neointima development in stents," *Philosophical Transactions of the Royal Society A*, 2010, 368, 2919-2935.

Conference Papers

Boyle, C. J., Lennon, A. B., Prendergast, P. J., "Predicting Restenosis: Simulating Neointima Formation in Stented Arteries", *2nd International Conference on Particle-based Methods, Fundamentals and Applications*, Barcelona, Spain, 26-28th October 2011.

Boyle, C. J., Lennon, A. B., Prendergast, P. J., "Predicting Restenosis in Arteries using a Mechanobiological Model", *17th Annual Conference of the Bioengineering Section of the Royal Academy of Medicine in Ireland*, Galway, Ireland, 28-29th January 2011.

Boyle, C. J., Lennon, A. B., Prendergast, P. J., "A Computational Technique for Simulating Restenosis in Arteries due to Stenting Using the Lattice Based Approach," *6th World Congress of Biomechanics*, Singapore, 1-6th August 2010.

Boyle, C. J., Lennon, A. B., Prendergast, P. J., "Difference in neointima formation between stents depends on aggressiveness of inflammatory response," *17th Congress of the European Society of Biomechanics*, Edinburgh, U.K., 5-8th July 2010.

Boyle, C. J., Lennon, A. B., Prendergast, P. J., "A computational model of tissue formation in arteries due to stent-induced injury," *Symposium of Endocardiac Biomechanics Research*, Marseille, France, 6-7th May 2010.

Boyle, C. J., Lennon, A. B., Prendergast, P. J., "Inflammation response intensity affects differences between stents," *16th Annual Conference of the Bioengineering Section of the Royal Academy of Medicine in Ireland*, Dublin, Ireland, 22-23rd January 2010.

Boyle, C. J., Lennon, A. B., Prendergast, P. J., "Rule-based simulation of restenosis within stents," *4th International Conference on Computational Bioengineering*, Bertinoro, Italy, 16-18th September 2009.

Boyle, C. J., Lennon, A. B., Prendergast, P. J., "Injury driven biological model of restenotic lesion development predicts the effects of stent geometry on restenosis," *American Society of Mechanical Engineers Summer Bioengineering Conference*, Lake Tahoe, USA, 17-21st June 2009.

Boyle, C. J., Lennon, A. B., Prendergast, P. J., "Rule-based simulation of the development of restenosis within stents," *Northern Ireland Biomedical Engineering Society Spring Meeting*, Belfast, Ireland 8th April 2009.

Boyle, C. J., Lennon, A. B., Prendergast, P. J., "A simulation of in-stent restenosis in a cardiovascular stent," *15th Annual Conference of the Bioengineering Section of the Royal Academy of Medicine in Ireland*, Limerick, Ireland, 30-31st January 2009.

Boyle, C. J., Lennon, A. B., Prendergast, P. J., "A Method for Simulating Restenosis Around a Stent using Injury Criteria and Biological Rules," *16th Congress of the European Society of Biomechanics*, Lucerne, Switzerland, 6-9th July 2008.

Boyle, C. J., Lennon, A. B., Prendergast, P. J., "A method for simulating arterial tissue growth in response to mechanically-induced injury," *Symposium of Endocardiac Biomechanics Research*, Marseille, France, 10-11th

April 2008.

Boyle, C. J., Lennon, A. B., Prendergast, P. J., "Neointima formation around a stent: Simulating Restenosis using injury criteria and biological rules," *14th Annual Conference of the Bioengineering Section of the Royal Academy of Medicine in Ireland*, Sligo, Ireland, 25-26$^{\text{th}}$ January 2008.

List of Figures

List of Tables

List of Algorithms

Nomenclature

Latin letters

a_{ij}	Mooney Rivlin material constant
c_{SMC}	SMC concentration
d_g	Growth factor decay rate
D	Damage
e	Extracellular matrix
$e_{\min}$	Minimum extracellular matrix to support cell occupation
g	Growth factor
I_i	Stress Invariant
k_{deg}	ECM degradation rate
k_d	Phenotype modulation rate
k_e	Extracellular matrix production rate
k_g	Growth factor production rate
k_m	Matrix degrading factor production rate
m	Matrix degrading factor
N	Number of loading cycles
N_f	Number of cycles to failure
p_{EC}	EC proliferation rate
p_{SMC}	SMC proliferation rate
$r_{\max}$	Maximum radius of ECM deposition region around a cell
v_{SMC}	SMC migration speed

Greek letters

α	Damage material constant
Δt	Simulation time increment
Δx	Lattice point spacing
ϕ	Cell phenotype
ϕ^*	Homeostatic cell phenotype
ψ	Strain energy function
σ_0	Fatigue Limit
σ_{crit}	Minimum principal stress injury threshold
σ_{f}	Failure strength

Acronyms

cSMC	Contractile smooth muscle cell
EC	Endothelial cell
ECM	Extracellular matrix
FEA	Finite Element Analysis
SMC	Smooth muscle cell
sSMC	Synthetic smooth muscle cell
MBTK	MechanoBiology ToolKit
MDF	Matrix degrading factor
MMP	Matrix metalloproteinase
PCI	Percutaneous coronary intervention
PTCA	Percutaneous translumenal coronary angioplasty
VTK	Visualization Toolkit

Chapter 1

Introduction

Cardiovascular disease is responsible for 4.3 million deaths in the EU, and 48 % of deaths in Europe every year, with a total healthcare cost of €110 billion in 2006 (Allender et al., 2008). In Ireland, cardiovascular disease was responsible for 35 % of deaths in 2006 (Central Statistics Office of Ireland, 2006). Half of these deaths are as a result of ischaemic heart disease, characterised by a restriction of blood flow to the heart muscle tissue, which can result in myocardial infarction. The removal of the restriction to blood flow can help prevent ischaemia, treat it when it occurs, and extend longevity.

Mechanical dilatation of the arterial tissue from within the arteries is

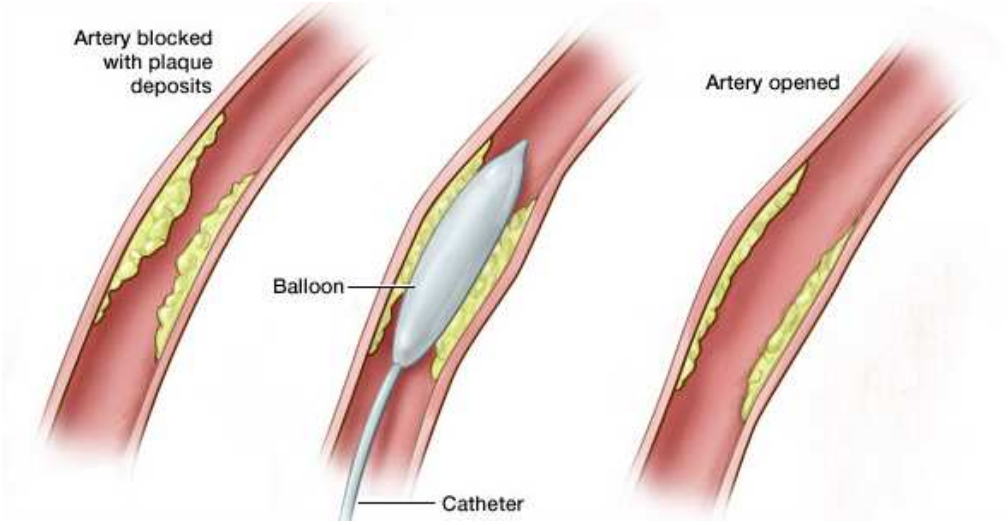

Figure 1.1: Schematic diagram of percutaneous transluminal coronary angioplasty (PTCA). From http://www.virchicago.com/peripheral-artery-disease.htm

routinely used to permanently deform the plaques that cause the restriction of blood flow. Percutaneous translumenal coronary angioplasty (PTCA), for example, is performed by inflating a balloon mounted on a catheter at the occlusion site, deforming the plaque tissue against the arterial wall (Fig. 1.1).

These procedures induce mechanical forces in the arterial tissue, which provoke a growth and remodelling adaptive response. This mechanobiological response can give rise to a re-blockage of the artery, which is termed restenosis. A major contributor to restenosis is the production of new cellular tissue within the artery by smooth muscle cells (SMC), which reside in the artery wall. This growth response is called neointimal hyperplasia, and it leads to a compromise in treatment where the increase in post-procedural lumen size must be balanced with the stimulus to cause

restenosis. In order to engineer optimal long-term outcomes of any biomechanical procedure performed on arterial tissue, it is critical to have an understanding of the mechanobiology of the process, and a model capable of predicting the tissue growth response.

1.1 Mechanobiology of Arterial Tissue

The growth of tissue within the vessel lumen (neointimal hyperplasia) is brought about by the actions of smooth muscle cells (SMCs), the main cell type populating the vessel wall, which produce and maintain the extracellular components of the vessel wall. The phenotype of SMCs can vary from quiescent, with very little tissue turnover, to synthetic, with a large amount of tissue production. The regulation mechanism behind phenotype modulation is not yet fully understood, but biophysical stimuli may play a direct role in regulating SMC behaviour through stretch-activated ion channels and other mechanotransduction pathways (Humphrey, 2008). There is significant evidence to suggest that SMC phenotype is also regulated substantially by the chemical composition of the extracellular matrix surrounding the cell (Thyberg et al., 1990), rather than solely by the mechanical stress it experiences. The extracellular environment is altered by mechanical forces through injury and inflammation. During this process, inflammatory cells are recruited to injured or damages tissue, which resorb the damaged tissue and stimulate tissue repair. Inflammation, when brought about by mechanically-induced injury, could play a key role in linking the mechanical perturbation to the restenotic response of arterial

tissue, and has been proposed as a key stimulus for restenosis (Schulz et al., 2000; Gunn et al., 2002; Dean et al., 2005). In this respect, the mechanobiology of arterial tissue is considered to be a complex process of tissue alteration through SMC activity and mechanically-induced inflammation.

1.2 Mechanobiological Models

Mechanobiological models are used to relate the mechanical stimuli induced in a tissue to the biological responses of the tissue. Biological systems such as arterial tissue are hierarchical and made up of many interacting components. Interactions and dynamics can be seen at length scales from the molecular level to the whole organism level, and over time-courses from seconds to years (Merks and Glazier, 2005). At the highest levels, models take the form of phenomenological, mathematical constructs, which seek to predict the experimental data in a statistical sense, with no underlying mechanisms (Peck, 2004). Early mechanobiological models represented tissue adaptation as a system striving to achieve a homeostatic mechanical state by altering its geometry (growth/resorption) or material properties (stiffness, porosity, etc.). This concept has been successfully applied to bone remodelling (Cowin and Hegedus, 1976; Huiskes et al., 1987) and arterial remodelling (Alastrué et al., 2008; Kuhl et al., 2003; Rachev et al., 2000). Alastrué et al. (2008) assumed a homeostatic value of circumferential stress, and an adaptive response whereby a deviation from this stress induced a growth in the radial direction. Rachev et al. (2000) included an

axial component to the stress response when modelling the adaptation of stent grafts. Lally and Prendergast (2006) introduced a model in which tissue growth was a function of damage, calculated using a remaining life approach. However, it could not capture the fact that some patients do not develop restenosis, and that neointimal growth can stop or reduce. These phenomenological modelling approaches hide the complexities of the link between stress and arterial wall remodelling. This can lead to a lack of generality, where the model needs to be recalibrated to each new situation, making it difficult to correlate new experimental data, and signifies a low predictive power.

While the phenomenological approach proved useful in physics, it becomes much more complex in biology, where the organ-level behaviour is a product of many smaller interacting components, and in fact may be impossible. Lander (2004) has written that

> there is little reason to expect to discern fundamental laws in [large, complex networks of elements]. To do so would be like expecting to discern the fundamental laws of electromagnetism in the output of a personal computer.

Rather it is better to represent the system using a simulation, a discrete dynamical system, which is made up of smaller interacting components (Prendergast et al., 2010). In this way, simulations can go further than phenomenological, statistical models aiming to fit to data, becoming an analogue for the *in vivo* situation, one which is more amenable to exploration. The complexity of tissue mechanoregulation led to the explicit

inclusion of cell activity in mechanobiology, where cell behaviours such as proliferation, differentiation and migration were modelled with differential equations (Bailón-Plaza and van der Meulen, 2003; Lacroix et al., 2002), or where cell activity was indirectly modelled through evolution equations (Zohdi et al., 2004; Ruimerman et al., 2005). Cells present an ideal level of abstraction (Merks and Glazier, 2005) as we have a wealth of information on their behaviour and they are physically discrete, making them ideal for computational simulation.

1.3 Objectives of the Thesis

In this study it is hypothesised that arterial tissue is mechanoregulated by biophysical stimuli. Specifically, it is hypothesised that mechanically induced injury stimulates neointimal hyperplasia of arterial tissue, and that the growth of neointima can be simulated by accounting for the response of cells within the tissue to extracellular inflammatory factors released due to tissue injury.

It is further hypothesised that the level of inflammation response to a given injury (which varies considerably within a population) affects the correlation between injury and neointima quantity.

This leads to the objectives of the thesis:

- To develop a model of the injury-driven response of arterial tissue
- To test if such a model produces biologically realistic results, and under what circumstances

- To quantify the effect of inflammation on the prediction of neointima formation
- To apply the model to clinically available stents, in order to evaluate the ability of the method for predicting long-term treatment outcomes.

If the aims of this thesis are met, the simulation technique can be used to study the design of stents with respect to long-term restenosis rates. The technique provides the flexibility to incorporate new biological phenomena, such as drug-eluting devices, and has the capacity to account for inter-patient variability in tissue response. This could provide a pre-clinical technique to model stent performance which would be cost and time-effective, and reduce the need for animal testing.

Chapter 2

Literature Review

2.1 Biology of Restenosis

2.1.1 Structure of the Artery

Arteries are composed of three distinct concentric layers, the intima, media and adventitia (Holzapfel et al., 2000). The intima is the innermost layer and consists of a mono-layer of endothelial cells covering a basal membrane. The intima in healthy arteries is usually superficial, but can thicken with age and disease to become mechanically important (Holzapfel et al., 2005). The media is the most structurally significant layer, and consists of a network of smooth muscle cells, elastin and collagen, arranged in helical fibre structures (Fig. 2.1). The outermost layer, the adventitia, consists of connective tissue and fibroblasts. The media is separated from the intima and the adventitia by the internal and external elastic laminae, respectively. The endothelium is a key regulator of underlying tissue form and function. It provides an anti-thrombogenic barrier between the tissue and circulating cells and growth-promoting factors, and it can both inhibit and stimulate smooth muscle proliferation and extracellular matrix turnover (Kipshidze et al., 2004). The behaviour of the endothelium is in turn regulated by hemodynamically-induced shear stress, with turbulent or low-flow regimes inducing dysfunction (Wentzel et al., 2001; Esper et al., 2006).

2.1.2 Atherosclerosis

Atherosclerosis is characterised as the focal thickening of the intima, blocking blood flow through the artery (Hansson, 2005). It is caused by the

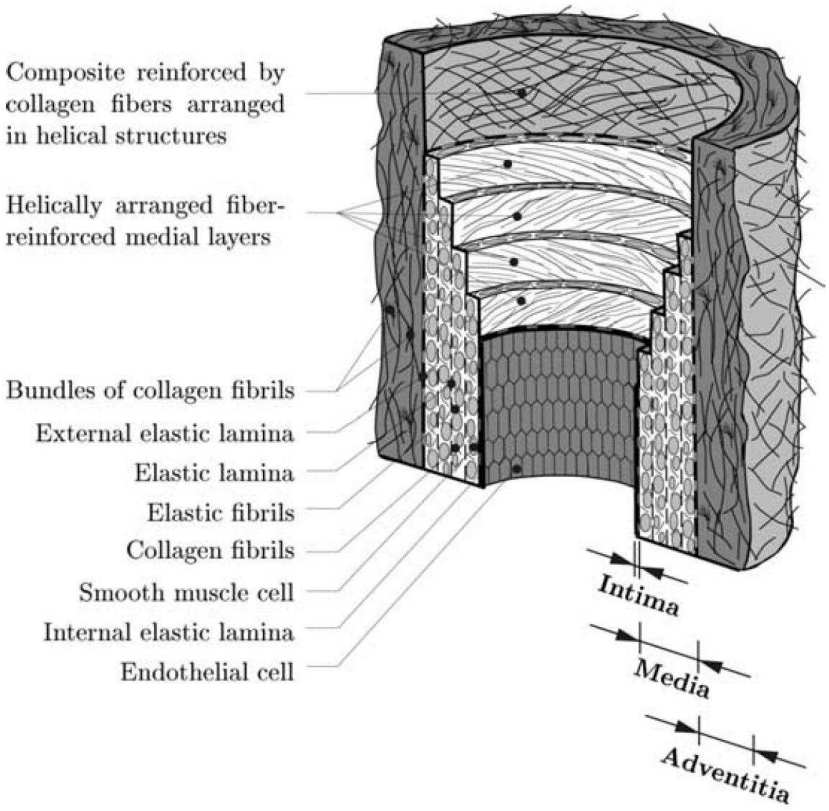

Figure 2.1: The structure and composition of muscular arteries. The artery is composed of three layers: the intima, the media and the adventitia. The arterial tissue is composed of elastin and collagen fibres, organised in helical structures. From Holzapfel et al. (2000).

build-up of fatty streaks in the intima, leading to growth of a lesion consisting of cells (macrophages and smooth muscle cells), fibrous tissue and lipids. The pathology of atherosclerosis is not fully understood, but localised injury or unfavourable haemodynamic forces is thought to induce endothelial dysfunction, which reduces its effectiveness as a selective barrier to the underlying intima and stimulates lesion growth. This may lead to stenosis, where the arterial blood flow is restricted, leading to angina, myocardial infarction, or stroke.

2.1.3 Damage and Injury

Stent placement alters the mechanical environment in the artery. Upon expansion of the stent, the endothelium becomes denuded within the stent region, exposing the underlying tissue and producing a thrombogenic surface. The stresses within the arterial wall are altered, tissue is stretched circumferentially and compressed radially beneath the stent struts, and rupture of the laminae and/or the media can occur. Tearing and stretch have been shown to correlate to neointima development (Kornowski et al., 1998; Gunn et al., 2002). A wound healing response is initialised in response to this injury (Scott, 2006), and SMCs may become apoptotic or necrotic. Lindner and Reidy (1991) showed that inhibiting bFGF (basic fibroblast growth factor, a growth factor released by dead SMCs) significantly reduced SMC proliferation after injury, suggesting that cell death could be a mechanism by which the tissue reacts. Liu et al. (2002) showed that exposing vein grafts to arterial flow produced excessive stretch and

cell death. They also showed that restricting the stretch of the graft with a sheath reduced cell death and subsequent restenosis. Cellular proliferation positively correlated with ruptured internal elastic lamina and medial tearing in a pig carotid model of balloon angioplasty (Groves et al., 1995). Fingerle et al. (1990) showed that a much higher restenotic response was found after balloon injury than after gentle endothelial denudation, indicating the relative importance of endothelial denudation versus tissue injury.

2.1.4 Inflammation

Inflammation plays a key role in the restenotic response of arteries to injury (Libby et al., 1992; Welt and Rogers, 2002). It is usually a beneficial process, which aims to remove damaged or injured tissue through the degradation actions of inflammatory cells, and stimulation of repair through the activation and proliferation of tissue-depositing cells. However, what begins as a healing process can become detrimental, triggering an over-zealous healing response (Davis et al., 2003). Rogers et al. (1996) showed that the number of monocytes at injury sites in a rabbit model correlated well with the amount of neointima produced. Kornowski et al. (1998) showed in a porcine model that the amount of inflammation (measured by an inflammation score) correlated with both injury (through an injury score) and neointimal area, a finding later found in humans (Farb et al., 2002). Welt et al. (2003) found that MCP-1, a key marker of inflammation, measured in the bloodstream of patients, was significantly elevated

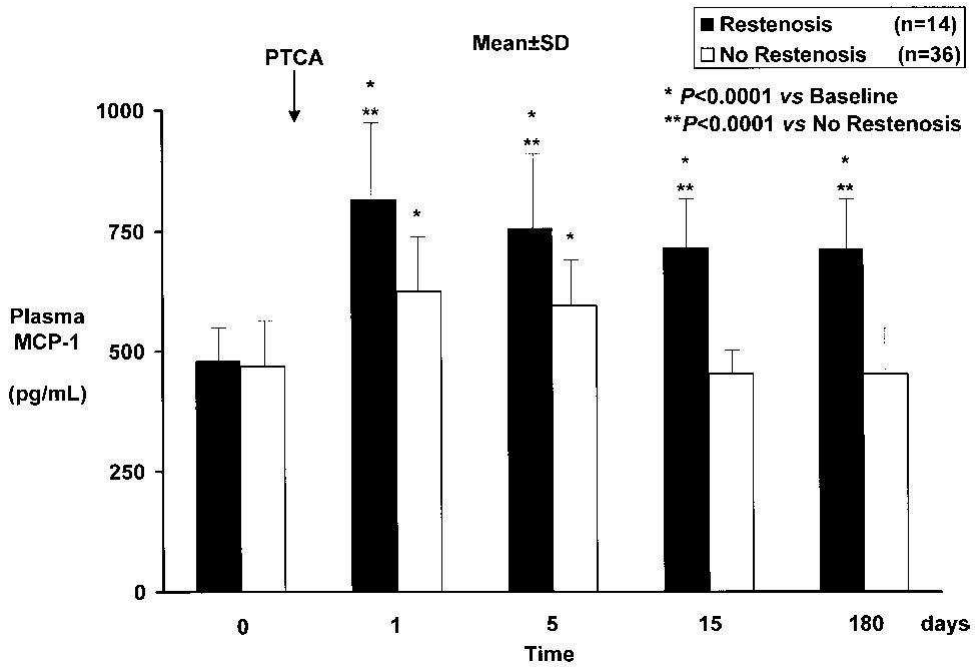

Figure 2.2: Measurement of plasma MCP-1 concentrations in patients before (control) and after balloon angioplasty. The data is split into patients who developed restenosis, and those who did not. From Cipollone et al. (2001)

immediately after injury in both balloon angioplasty and stent patients, while MCP-1 levels remained present long-term only in the stent model. Cipollone et al. (2001) further showed that stent patients who went on to develop restenosis had significantly higher levels of MCP-1, both at the initial time of stenting and longer-term (Fig. 2.2). Finally, Kuhel (2002) showed evidence from a murine model that suggested a genetic determinant to injury response, where specific genotypes produced very different amounts of neointima formation to the same injury, demonstrating the importance of accounting for genetic variability in inflammatory response when making predictions.

2.1.5 SMC behaviour

The smooth muscle cell (SMC) is the sole cell type to occur in the healthy medial layer of adult mammalian arteries (Thyberg, 1996). During development, SMCs are proliferative and secretory, helping to form the developing vessels while, in the healthy adult, SMCs express a contractile phenotype (Thyberg, 1996). This phenotype is characterised by the presence of smooth muscle alpha actin filaments, the ability to actively contract, and a minimal amount of synthesis. Upon injury, and in restenotic lesions, cells revert to a more synthetic phenotype, characterised by a large volume of endoplasmic reticulum and Golgi complex (Thyberg, 1996). In this phenotype, cells do not contract, and express increased amounts of extracellular components such as collagen, elastin and proteoglycans, which constitute much of the non-cell volume of neointima.

SMCs *in vitro* have been shown to express a contractile phenotype when seeded on a laminin substrate, while expressing a synthetic phenotype on fibronectin (Hedin et al., 1988; Hayward et al., 1995; Hirst et al., 2000). These studies lead to the theory that extracellular matrix constituents plays a major role in regulating SMC phenotype. This was further corroborated *in vivo*, where Thyberg et al. (1997) found a correlation between the phenotypes in various parts of the arterial wall before and after injury, and the extracellular constituents.

SMC proliferation is an important component of neointima development. While phenotype modulation is important for this process, it is not sufficient to induce SMC proliferation (Chamley-Campbell et al., 1981).

This requires exogeneous growth factors from a diverse array of sources such as the dysfunctional endothelium, dead SMCs, platelets, macrophages, leukocytes and other active SMCs (see Thyberg et al. (1990); Welt and Rogers (2002) and the references therein). These growth stimuli are expressed locally at the sites of damage/injury, and are short-lived so that cellular proliferation is regulated by the level of inflammatory activity.

Cell migration is a critical step in neointimal formation, allowing cells to populate new regions, and grow the tissue boundary (Casscells, 1992). The amount of tissue degradation may effect the motility of cells; (Zempo et al., 1996) and Bendeck et al. (1994) showed that medial SMC migration was reduced in a balloon-injured rat carotid artery when MMP synthesis was inhibited. DiMilla et al. (1993) showed that SMC migration was dependent on the surface density of extracellular proteins (fibronectin and collagen), and that an intermediate concentration induced maximal migration rates. These studies show the importance of modelling SMC migration, and in modelling the effects of the extracellular environment on migration behaviour.

2.1.6 Role of the endothelium

The healthy endothelium acts as an anti-thrombogenic barrier between the blood flow and the underlying vascular tissue (Esper et al., 2006). The ECs regulate the behaviour of SMCs by altering the amount of infiltration of inflammatory cells, and by directly expressing growth-promoting or growth-inhibiting factors. The dysfunction of endothelium may be brought

about by mechanical injury or alteration in blood flow. The endothelium may also become completely or partially denuded during stent implantations (Kipshidze et al., 2004). The level of endothelial dysfunction has been shown to correlate with the amount of restenosis produced (Kipshidze et al., 2004; Thanyasiri et al., 2007).

2.2 Stent Design Considerations

Revascularisation is a procedure to restore the patency of occluded vessels by forcing the blockage open. Stents are devices designed to be implanted within the occluded artery to maintain the patency of the artery after revascularisation. The first stent to be regularly used in practice was the Palmaz, which was a mesh of interconnected struts made by cutting rectangular cells in a stainless steel tube. The stent was mounted on a balloon and catheter and positioned in the occluded artery. The balloon was expanded under high pressure, expanding the stent, which underwent plastic deformation and remained expanded after the balloon has been deflated. Over the last two decades, many diverse stent designs have been accepted into clinical practice. These designs differ in their manufacturing technique (laser cut from a tube, wire, etched), their strut configurations (open-cell, with less strut links than closed-cell), and expansion methods (balloon expansion, self-expanding nitinol stents) (Lally et al., 2006). The main aim in stent design is to achieve adequate patency, while minimising the restenotic response. This requires a stent with good radial strength to resist recoil, flexibility to conform to tortuous arteries, and trackability and

a low crimped profile for ease of placement (Kandzari et al., 2002). Stent design has been improving (Blackledge and Squire, 2009), but restenosis remains a problem, and this problem will increase as stents are used to treat more high risk lesions.

2.3 Pre-clinical methods of stent evaluation

Animal experiments trials have explored the effects of geometric parameters such as stent length, strut configuration, and diameter, as well as material type and expansion method on the degree of restenosis produced (Morton et al., 2004; Garasic et al., 2000). Clinical trials have compared restenosis between stent designs, identifying the best performing stents relative to the original Palmaz stent (Hoffmann et al., 2002; Kastrati et al., 2001) (Fig. 2.3). However, it is difficult to extract general principles of device design from these specific comparisons because the link between stent design parameters and degree of restenosis is indirect and complex (Evans et al., 2008); it is a function of injury, inflammation and stochastic cell behaviour. The biological environment present in healthy, or even disease-model, animals may not provoke the same adaptive reactions as aged human patients, and the results of pre-clinical trials may be specific to that environment. Finite element analysis can quantify the mechanical perturbation imparted on the artery by stenting and has been used to compare stent designs in terms of tissue prolapse (Prendergast et al., 2003), vessel wall stresses (Migliavacca et al., 2002; Lally et al., 2005) and altered haemodynamics (Duraiswamy et al., 2007). However, these studies

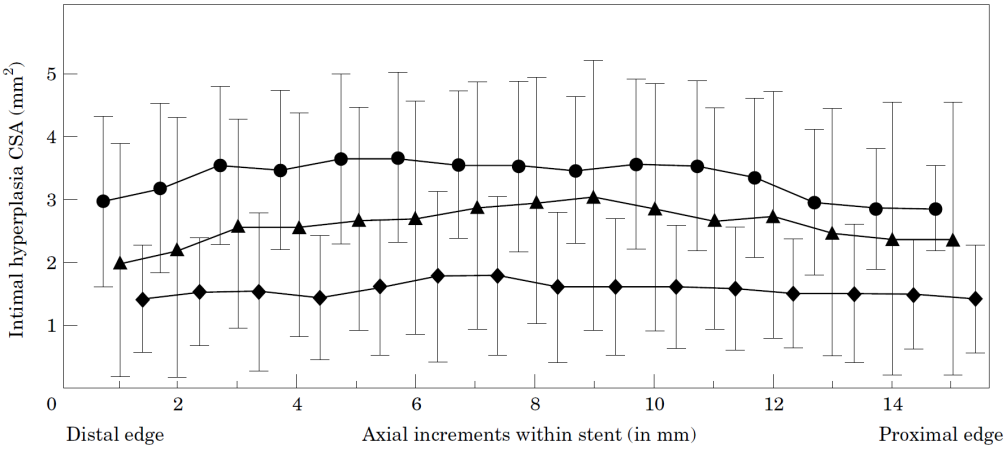

Figure 2.3: Neointima cross-sectional area along the axis of three stents measured six months after stent placement in a clinical trial (Hoffmann et al., 2001). The trial showed that the open cell design ('MultiLink', diamonds) outperformed the slotted-tube ('Palmaz', triangles), which outperformed the closed-cell design ('InFlow', circles) on average. The variation was large in all stent types.

only supply the initial (i.e. the direct post-intervention) conditions to any adaptive response. In order to accurately predict the long-term efficacy of mechanical treatments, we need a model of the relationship between biophysical stimuli and neointimal growth.

2.4 Mechanobiological models of restenosis

Rachev et al. (2000) took the first steps in modelling the link between stent induced deformations and tissue growth, relating the amount of neointimal growth directly to the vessel wall stresses induced by the stent. The growth of neointima, modelled as an increase in the thickness of the vessel wall, was then regulated by the deviation from the homeostatic stress state. This model could not be applied to short-duration procedures, such as bal-

loon angioplasty, and was phenomenological. An attempt was not made to corroborate this model with experimental data. Lally and Prendergast (2006) associated the mechanical stress with injury using fatigue damage curves, and related this to tissue in-growth via diffusion. Although these approaches constituted the first steps, the complex dynamics of lesion formation could not be adequately included in either method, limiting their applicability.

One method to account for cellular behaviour is to use a lattice-based modelling approach, where lattice points represent possible positions for individual cells. Lattice-based modelling provides a technique to model tissue-level phenomena based on the behaviour of individual cells (Merks and Glazier, 2005; Simpson et al., 2007). Rules governing cell behaviour are formulated based on experimental observation, providing a descriptive model of an individual cell. Tissue-level behaviour may then be modelled by simulating many of these single-cell models simultaneously. Preliminary results from the COAST project (www.complex-automata.org) have shown the potential power of a multi-scale, multi-physics model of restenosis development (Caiazzo et al., 2009). In that study, blood flow, structural stress and diffusion from a stent were simulated and combined with an agent-based model of smooth muscle cell behaviour in 2D. This model assumed that SMC proliferation was governed by local fluid flow, structural stress and drug concentration.

2.5 Agent-based cell-centred modelling

The agent based modelling paradigm aims to represent a complex system as a network of interacting agents, each of which can be represented with a simpler model. Merks and Glazier (2005) describes the steps to take in designing biological simulations using this technique:

1. *Infer biological behaviours from experimental studies.* Build up a description of the behaviour of cells under a range of external conditions, and try to infer the general behaviour of cells, for example: is the proliferation nutrient-limited or exponential? Do the cells reach senescence after a certain number of mitoses? This method can be seen as the traditional reductionist paradigm of breaking up the system into simpler components, but the cell is selected as the key level of activity.

2. *Obtain data on key cell behaviours.* Once the behaviours are identified, attempt to quantify the relationships/thresholds and responses of the cells. Identify the behaviours thought to be essential to the response, and accumulate data on these.

3. *Develop a single cell model.* Based on the behaviours found, and the quantified data, develop a model of a single cell which behaves according to these experimentally observed situations.

4. *Combine cells to produce a multi-cellular simulation.* It is only at this time that the model has any predictive potential. At this stage, simulations mimicking real experiments can be developed.

5. *Compare the predictions of the models to experimental observations*, applying them to a variety of situations.

If the model does not match up to experimental observation:

1. Return to experiments which informed the model, try to find some missing information (as in the traditional iterative approach to model building), or,

2. Study the effects of other parameter combinations in a high-throughput parameter study to find if the model behaves realistically under any parameter values, and if so, what this means for predictions

If the model does match up to experimental observation:

1. Make further predictions in new applications

2. Find out what happens when specific components are suppressed, particularly if there exists a method to knock-out the behaviour *in vivo*. This would not be possible using a phenomenological model.

There have been many different methods used to simulate biological systems at the cell level. Cellular automata models use a regular, orthogonal lattice at which state variables are defined, which represent cells. The automaton updates according to rules based on the environment around the cell, and all positions are updated simultaneously. Cellular Potts Models are also lattice based, and were originally developed for annealing phenomena in metals (Alber et al., 2002). In this case, the cells occupy several lattice points, and the model progresses stochastically towards some energy

minimisation. Off-lattice methods represent cells using some positional and morphology function, such as a sphere, while defining mechanical and biophysical interactions between bodies. These agent based models share some common characteristics, as has been summarised by Moreira and Deutsch (2002):

1. Spatial representation: In traditional engineering approaches, a continuum assumption is used to describe space, where a variable (such as cell concetration) is assumed to be defined at every point in space; cell morphology or the structure of cell aggregates are not represented. In the cellular automata approach, a representation of discrete cells is introduced, whereby one cell only can occupy a lattice site, thereby introducing an excluded volume (Drasdo, 2005), that is, a maximum concentration of cells in a region. In the cellular potts method (Glazier and Graner, 1993), cell morphology is represented by a collection of lattice points, allowing size and shape fluctuations to be modelled. Off-lattice methods have used spheroidal cell shapes (Drasdo, 2005), where the cell centre and radius defines the morphology. This allows more interaction behaviours, such as adhesion and physical growth stresses to be included.

2. States: The state variables such as cell phenotype, can be discrete, as is the case for strict cellular automata, or a continuous function based on mathematical rules (Moreira and Deutsch, 2002). Pérez and Prendergast (2007) used discrete cell states to represent cell phenotype in skeletal development, where mesenchymal stem cells commit

to diverse lineages, with no de-differentiation (return to stem cell phenotype) or trans-differentiation (change to another lineage). In other cases, here in particular for smooth muscle cells, cell phenotype exists on a continuum between extremes (e.g. from contractile to synthetic).

3. Dynamics: (or updating procedure). In strict cellular automata, the updating is synchronous, i.e. all sites are updated in every increment. The Monte-Carlo method of simulation may also be used, where only one lattice point, chosen at random, is updated per increment (Drasdo, 2005). In off-lattice methods, each cell is operated upon either sequentially (asynchronous) or in parallel.

4. Rules and behavioural models: These rules/models dictate the updating procedure of the simulation. All agent-based models have the property that rules are local, i.e. based on stimuli in the locality of the cells, but rules may be either homogeneous (in which case rules are the same at every point - as in a strict cellular automaton), or heterogeneous (as, for example in some early tumour growth models (Moreira and Deutsch, 2002)). Rules can be implemented as discrete, Boolean statements (Pérez and Prendergast, 2007; Moreira and Deutsch, 2002), where cells change discrete states based on Boolean rule sets, or can be implemented as an energy function which tends towards an equilibrium value stochastically in a Monte Carlo simulation (Glazier and Graner, 1993).

2.6 Cell Behaviour Algorithms

The modelling of tissue mechanobiology can be performed by producing simulations composed of independent algorithms for cellular behaviour. In this way, the simulations represent a surrogate for the natural system, and do not have a predefined start or finish. The initial state of the simulation domain is prescribed, and the algorithms are performed in an iterative process until a pre-defined end time-point is reached. Each of the algorithms can be seen as isolated modules, and are procedures for directing cellular behaviours (Proliferate, Migrate, Modulate Phenotype, etc.) based on external stimuli (growth factors, extracellular matrix, mechanical stimuli). Algorithms differ from simulations in that they have a well defined beginning (inputs) and end (outputs). They are strictly deterministic, although stochastic behaviour can be modelled by providing a random number as an input. The effects of algorithms are changes in cell states (e.g. cell phenotype, age, new cells, cell death and cell position). The inputs of cell algorithms include the number of cell neighbours, growth stimulus concentration, mechanical stimuli, etc. The algorithm can change between discrete cell states, using stimuli thresholds or Boolean statements, or can be based on continuous mathematical functions. These individual algorithms may be then isolated and validated against experiments independently of the simulation level.

Proliferation

The flux of the number of cells within a region of adapting tissue is a key component of many biological phenomena, such as tumour growth, tissue differentiation and neointima development in arteries. At the cell level, cells are created when existing cells double in size, and split into two daughter cells. Assuming a constant proliferation rate, this would produce the reaction: $[N] \xrightarrow{k} 2[N]$, where N is the number of cells, and k is the proliferation rate, producing the equation

$$\frac{\mathrm{d}N}{\mathrm{d}t} = kN \tag{2.1}$$

This produces exponential growth, $N = N_0 e^{kt}$, which is unrealistic as there is a limit to cellular proliferation imposed due to space constraint, senescence and nutrient scarcity. The logistic growth model postulates a carrying capacity, which limits the density of cells to a constant K. In this case, the growth can be modelled using the Fisher equation (Simpson et al., 2007),

$$\frac{\mathrm{d}N}{\mathrm{d}t} = \lambda N \left(1 - \frac{N}{K}\right) \tag{2.2}$$

This limits the concentration of cells to a prescribed quantity. A similar phenomenological relationship (the Gompertz curve) was explored in a cellular automaton model of tumour growth (Kansal et al., 2000). In this case, the rules governing proliferation were altered depending on the position within the tumour, i.e. inhomogeneous, and the approach is therefore of limited use for predicting growth of realistic cell populations. The

lattice-based strict cellular automaton method (Pérez and Prendergast, 2007) allows for a type of proliferation control, as each lattice point can occupy only one cell. This produces an 'excluded volume', whereby cells themselves produce a barrier to cellular proliferation (Drasdo, 2005), thus simulating contact inhibition, where the presence of neighbours leads to cellular quiescence. This type of modelling has helped show the importance of modelling cells when considering pattern formation and the effect of cell density (Zygourakis et al., 1991). However, when simulating dense aggregates of cells, this model implies that only the outer cells of an aggregate can proliferate, i.e. a proliferating layer which is one cell thick. Drasdo (2005) developed a method for allowing a deeper proliferation depth by allowing cells to proliferate into a vacant site within a specified radius greater than the nearest neighbours. This modelled the end-result of a cell proliferating and displacing neighbours. Galle et al. (2005) studied the effects of introducing contact inhibition and cell-substrate interaction on cellular proliferation, showing that confluent monolayers could be simulated by requiring cells to have contact with a substrate in order to proliferate.

These models, however, tend towards a saturated lattice of cells. This is an accurate representation of some forms of multi-cellular growth, such as the initial population of granulation tissue with stem cells (Pérez and Prendergast, 2007), or tumour growth (see, for example Moreira and Deutsch (2002)). However, some cell types and cell phenotypes only proliferate in response to exogeneous or endogeneous stimuli. Smooth muscle cells are such a cell type; they proliferate in response to an array of growth factors (see section 2.1.5). Dormann and Deutsch (2002) modelled growth based

on a diffusible stimulus from necrotic cells, and nutrients which could be consumed. The proliferation rate of cells was linked to the diffusible stimulus, and this was decreased at a constant rate in the presence of cells.

The cell cycle can be explicitly modelled, with triggers and thresholds regulating whether or not cells enter the next cell cycle phase (Walker et al., 2002). Cell proliferation may also be directly linked to mechanical variables (Caiazzo et al., 2009).

Migration

Cells move through crawling, whereby the cytoskeleton remodels over time, making and breaking bonds with its extracellular environment. In many cases, this motility can be modelled as a random walk process, whereby cells migrate at a constant rate in random directions. This migration may be completely isotropic, or biased towards a direction or gradient (Codling et al., 2008; Pérez and Prendergast, 2007). Isotropic random walk results in the diffusion partial differential equation at the continuum level (Murray, 2002).

Application of Agent-based models

The cell-centred technique is extremely versatile, and has been used to simulate a wide variety of biological systems. Developmental processes, cell sorting and tumour growth have been simulated using the Cellular Potts Method (CPM), (see the review by Merks and Glazier (2005)). Dermal wound healing has been simulated in three dimensions and wound healing

assays have been simulated using agent-based techniques (Mi et al., 2007; Simpson et al., 2007; Walker et al., 2002). The lattice-based approach has been used in a wide variety of mechanobiological models. Pérez and Prendergast (2007), were the first to use the random walk approach for cell proliferation and migration in a simulation of tissue differentiation. In this model, the migration and proliferation of mesenchymal stem cells were simulated in a lattice. Finite element analysis was performed at regular intervals to determine the mechanical stimuli of fluid flow and shear stress, which regulated the differentiation of these cells into osteoblasts, chondrocytes or fibroblasts, following the theory proposed by Prendergast et al. (1997). These differentiated cells produced their characteristic tissues, which then altered the mechanical properties of the tissue, and hence the stimulus. In this way, the time-course of tissue differentiation could be captured in a simulation. This was later applied to idealised bone scaffolds (Byrne et al., 2007), fracture healing (Byrne, 2008), tissue differentiation in a bone chamber (Khayyeri et al., 2009), and tissue differentiation with angiogenesis (Checa and Prendergast, 2009). In the latter study, angiogenesis was included by modelling the capillaries as sprouts of adjacent endothelial cells. These then influenced tissue differentiation, as bone formation was assumed to only occur within a specified distance of an oxygen source (capillary). The CPM has been used to simulate osteon formation, and bone remodelling through the explicit modelling of osteoclast behaviour (van Oers et al., 2008).

It is clear from the above literature that injury to the vessel correlates

with the amount of subsequent restenosis. The injury-based paradigm for restenosis after angioplasty and stent implantation has gained wide acceptance among clinicians. However, a computational technique capable of predicting the injury response has not been produced. As injury and tissue disruption is a necessary part of revascularisation, it is necessary to understand, and to be able to predict, the relationship between injury and the amount of re-blockage. While current Finite Element models offer a method to predict injury through stress calculation, a mechanobiological model for restenosis capable of predicting the long-term restenotic response of arteries has not been produced. Previous models have not included the external environment or inflammation explicitly. The agent-based modelling technique has been successfully applied to skeletal, wound healing and tumour growth applications, so it provides an ideal method to represent arterial mechanobiology.

Chapter 3

Lattice-Based Simulation of Restenosis in Stents: The Influence of Inflammation Intensity on Stent Performance[1]

[1]This chapter is based on the paper 'Computational simulation methodologies for mechanobiological modelling: a cell-centred approach to neointima development in stents' by Colin J. Boyle, Alexander B. Lennon, Michael Early, Daniel J. Kelly, Caitriona Lally and Patrick J. Prendergast in Philosophical Transactions of the Royal Society A (2010), 368, pp 2919–2935. All technical work described in this chapter was performed by the author.

3.1 Introduction

Percutaneous coronary intervention (PCI) involves the restoration of blood flow to arteries blocked as a result of cardiovascular disease. It involves expanding a mesh structure within the vessel, which acts as a scaffold to hold open the artery. It is a minimally invasive therapy, and is associated with high success rates (Bennett and O'Sullivan, 2001). A significant limitation to the technique is the persistent rate of failure due to re-blockage of the artery, termed restenosis, which is a tissue adaptation response to the implant. Engineering optimal treatments for cardiovascular diseases requires a model capable of predicting arterial tissue's response to mechanical stimuli.

Finite element analysis (FEA) has been used to predict the vessel geometry upon stenting (Prendergast et al., 2003), which can be used to optimise stent design towards maximising lumen area or minimising tissue prolapse. The vessel wall stresses upon stent expansion represent an important biophysical stimulus for vessel wall growth, and FEA may be used to compare alternative stent designs (Lally et al., 2005), and to optimise stent geometry with respect to arterial wall stress (Bedoya et al., 2006; Timmins et al., 2007). These techniques can rank stents based on mechanical variables, but cannot offer information on the response to these stimuli. To do this, a mechanobiological theory for tissue growth and mechanically-induced alterations is required.

Upon stent implantation, injury can induce tissue rupture, exposing underlying tissue to blood flow, inducing smooth muscle cell death, and inducing an injury response. The neointima formation in response to injury can be simplified into distinct, overlapping phases (Drasdo et al., 1995; Evans et al., 2008). An exudative phase occurs when macrophages and other inflammatory cells from the blood aggregate around and within the injury site. They initiate a resorptive phase where debris, tissue and dead cells are decomposed by inflammatory cells. These cells, together with the dead SMCs and endothelial cells (ECs) produce growth stimuli, which initiate the proliferation phase. In this phase, SMCs proliferate and infiltrate the injured region, initiating a repair phase that consists of deposition of collagen-based tissue in place of the granulation tissue. The endothelium is influential in providing a mechano-sensitive barrier between the smooth muscle and the blood, and can also actively regulate SMC behaviour. This

layer is damaged (often removed completely) during stent deployment and its growth-inhibitory effects are only restored when the layer re-heals.

The relationship between mechanical stimuli and tissue injury has been investigated for skeletal muscle tissue. Linder-Ganz et al. (2006) determined a threshold-type relationship between pressure applied to rat skeletal muscle and muscle cell death using indentation tests. Kornowski et al. (1998) and Gunn et al. (2002) showed a link between stretch and deep tissue injury and subsequent restenosis. These studies provide evidence for the mechanism of injury-induced restenosis. Garasic et al. (2000) found a large effect of stent design on restenosis in the iliac arteries of rabbits, and this model provides a test for the predictive model described here.

Many of the structural changes that biological systems undergo are complex, and are a result of many biological components interacting. It has been argued that producing mathematical laws governing such a complex system is difficult: 'to do so would be like expecting to discern the fundamental laws of electromagnetism in the output of a personal computer' (Lander, 2004). An alternative is to break-up the system, until the components begin to behave according to simple models. The extreme of this path is to reduce down to the molecular level, where chemical reactions and molecular dynamics govern. Even if this were possible for any relevant model size, it may not be useful, as the model system would be just as complicated as the reality (Merks and Glazier, 2005). The cell is a natural level of abstraction, as cells are discrete entities and their behaviour can be reduced to a simple set of rules. They process inputs such as extracellular environment, mechanical stimuli and chemical stimuli, and regulate

their behaviour accordingly to migrate, proliferate, secrete extracellular components, produce force, apoptose, etc. The aim of the modeller is then to develop a sufficiently accurate model of individual cell behaviour that, when many cells are combined in a simulation, a robust, and accurate, tissue-level model is produced.

In this paper, we test whether or not an injury-based simulation would show the relative efficacies (i.e. the differences in performance between stents) of stents similar to *in vivo* experiments, and what effect the inflammation level has on the response. In particular, we will test whether or not the amount of inflammation induced in response to injury can have an effect on restenosis predictions between stent devices.

3.2 Methods

The simulations were designed to correspond to the experimental setup of Garasic et al. (2000). In that study, two corrugated ring stents with different strut configurations were implanted into the iliac arteries of rabbits.

3.2.1 Finite element analysis

Finite element models of the two stents used were built using Rhino, meshed using Cubit, and developed into an ABAQUS finite element model. Stent A was built as a four-crowned design, where the number of crowns indicate the number of corrugated points in the circumferential direction[2]

[2]In the stents modelled here, this means that the number of struts in the middle of a circumferential unit is double the number of crowns.

Table 3.1: Artery wall Mooney-Rivlin material model parameters, from Gervaso et al. (2008)

Parameter	a_{10}	a_{20}	a_{30}	a_{40}	a_{50}	a_{60}
(kPa)	6.52	48.9	9.26	760	-430	86.9

Stent B was designed to have the same diameter as stent A, and had six crowns. (Fig. 3.1). Stent A consisted of three cells connected axially, while stent B consisted of four, ensuring that both stents had the same axial length (see Fig. 3.1). The artery wall was modelled as a hollow cylindrical tube with a homogeneous, isotropic constitutive model. The inner diameter was 2.75 mm and the vessel wall had a thickness of 0.5 mm, which is representative of a rabbit iliac artery (Garasic et al., 2000). A sixth-order Mooney-Rivlin strain-energy function was used:

$$\psi = a_{10}\left(I_1 - 3\right) + a_{20}(I_1 - 3)^2 + a_{30}(I_1 - 3)^3 \tag{3.1}$$

$$+a_{40}(I_1 - 3)^4 + a_{50}(I_1 - 3)^5 + a_{60}(I_1 - 3)^6 \tag{3.2}$$

The solution was calculated using ABAQUS/Standard (SIMULIA) v6.8. The constants for the material model were taken from Gervaso et al. (2008), who fitted the model to the experimental data reported by Holzapfel et al. (2005) (see table 3.1), in which circumferential sections of tissue were tested in uniaxial tension. The tissue was assumed to be isotropic and homogeneous, and the medial tissue layer was assumed to dominate the loading, hence the artery was modelled as one layer.

The stent material was modelled as an elasto-plastic material with the properties of stainless steel, as reported by Early et al. (2009) (see table

Table 3.2: Stent material model parameters

Parameter	E	σ_y	E_T	ν
(MPa)	188×10^3	240	513×10^3	0.27

3.2).

Physiological conditions in the artery were simulated by applying an axial pre-stretch of 1.2 and a blood pressure of 13.3 kPa to the lumen surface prior to stent expansion. A radial displacement was applied to all nodes of a cylinder positioned within the stent, expanding it from an initial diameter of 1.15 mm to 3.3 mm. This achieved an expansion ratio of 1.2 between the artery and the stent. The cylinder was then retracted allowing recoil of the stents. To reduce the simulation times, symmetry was used to reduce to a 1/8th model circumferentially for the 4 crown stent, and a 1/24th model for the 6 crown (see Fig 3.1). Appropriate boundary conditions were applied along the planes of symmetry.

Minimum principal stress was used as the injury stimulus, based on experimental findings which showed the effects of pressure stresses on cell viability in skeletal muscle (Linder-Ganz et al., 2006). It was assumed that this represented a threshold in the tissue, such that above this value, cells died and initiated an inflammatory response. Before translating the FEA results to the lattice model, a full artery model was built from the symmetric models by mirroring about the planes of symmetry.

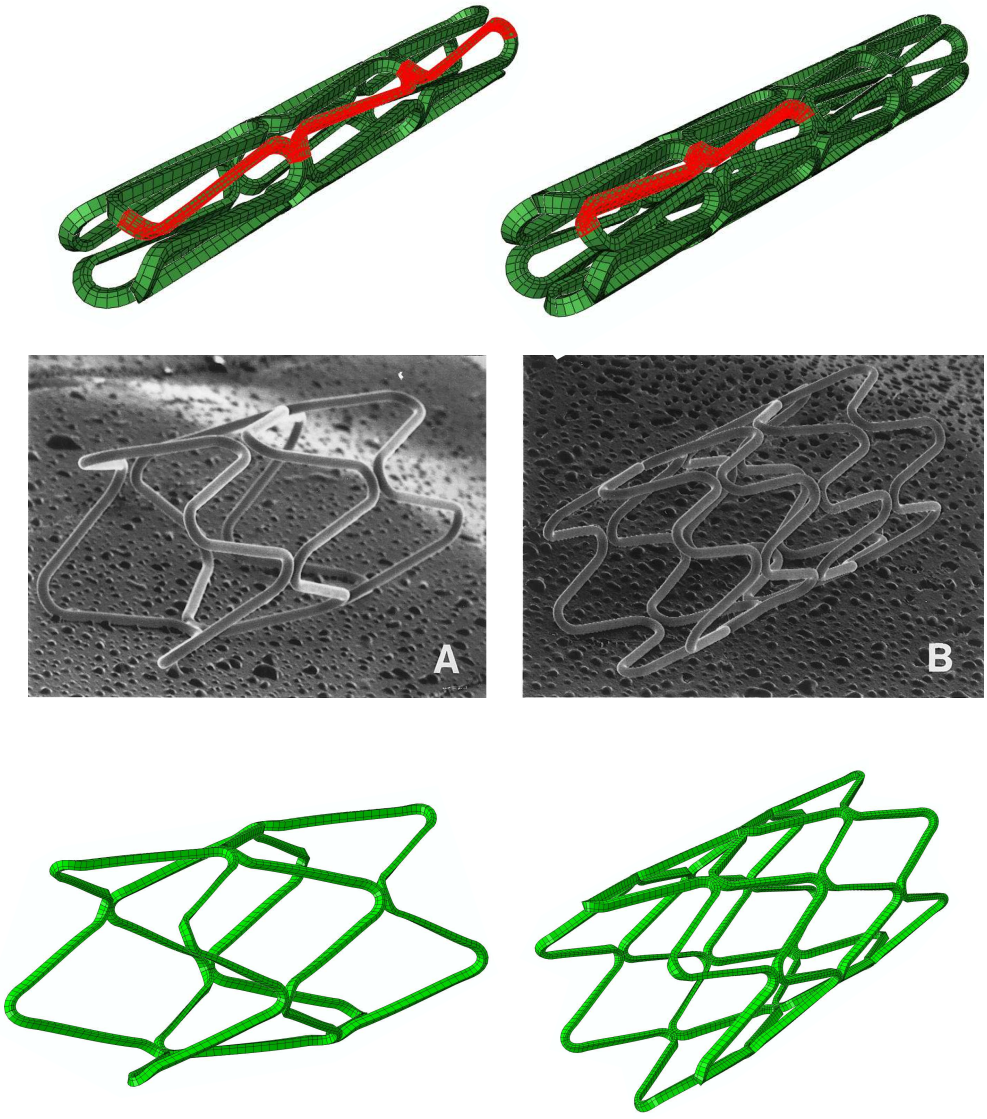

4 Crown 6 Crown

Figure 3.1: Finite element representations of the two stents simulated, the 4 and 6 crown types. Top, the unexpanded configuration. The region shown in red indicates the actual simulated region, due to symmetry. Centre, scanning elecron microscope images of the stents used in the experiments of Garasic et al. (2000). Bottom, the stents at full expansion.

3.2.2 Lattice Model

Three cell types (contractile smooth muscle cells (cSMCs), synthetic smooth muscle cells (sSMCs) and endothelial cells (ECs)), and three extracellular components (extracellular matrix (e), matrix degrading factors (m), and growth stimuli (g)) were modelled (Fig. 3.2). A regular, orthogonal, 3D lattice was defined, representing the spatial domain in which tissue adaptation occurs. The cell algorithms require positional information about the cell, and the local environmental stimuli. The proliferation and migration algorithms use an algorithm for assessing the suitability of a neighbouring lattice site based on cell presence and extracellular matrix (Algorithm 3.1). This algorithm ensures that each lattice point is occupied by a maximum of one cell, and that only points suitable for cell attachment are available for cell movement. In the case of SMCs, this means there must be an average ECM in the local region greater than the critical value[3]. For ECs, there is a further stipulation that the lattice point itself must contain no ECM, so that cells only proliferate over the lumen surface[4].

Initialisation

In order to map stress from the FE mesh onto the lattice, the lattice bounds were initialised to encompass the entire FE mesh. The spacing of the lattice points (Δx) was equal in each orthogonal direction. For each

[3] $e_{\text{avg}} \geq e_{\text{min}}$, where e_{avg} is the average ECM in the Moore Neighbourhood (see section 4.2.3, page 76), and e_{min} is the minimum amount of ECM to support cell migration

[4] the lattice point which contain no ECM, but are adjacent to lattice points that do.

[5] for a description of local neighbourhoods in lattice-based models, see section 4.2.3, page 76

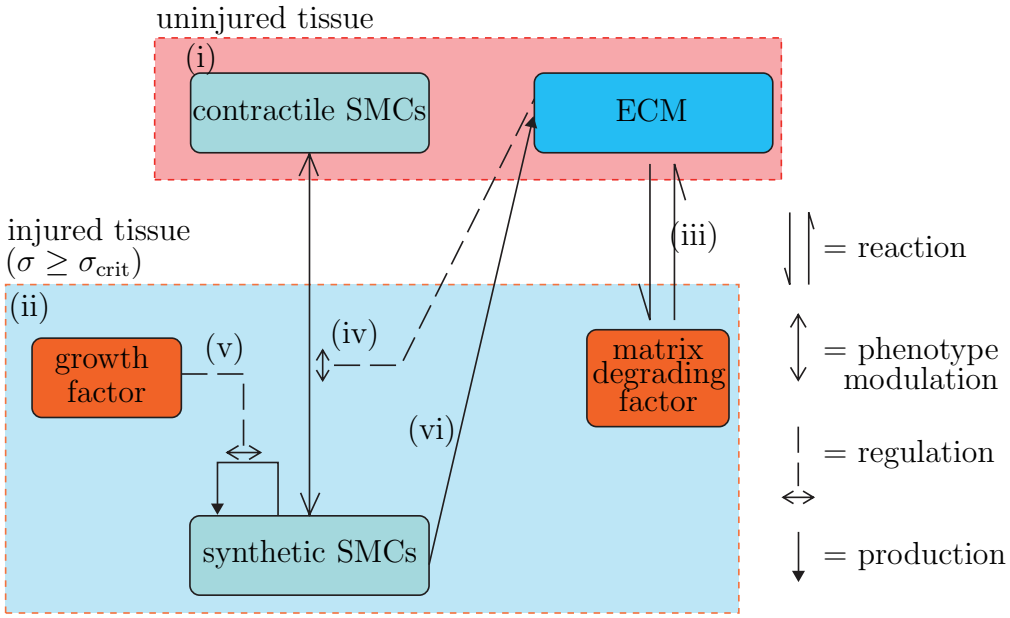

Figure 3.2: A system diagram of the components (in boxes) and processes (arrows) involved in the model of smooth muscle cell behaviour. (i) The uninjured artery wall is quiescent and contains contractile smooth muscle cells (cSMCs) and extracellular matrix (ECM). Injury induces cell death and tissue damage/rupture. (ii) In response, inflammatory cells infiltrate the injured region and produce matrix degrading factors and growth factors. (iii) Matrix degradation of ECM induces (iv) SMCs to modulate their phenotype from contractile to synthetic (sSMC). These sSMCs proliferate in response to growth factors (v) and express ECM (vi). SMCs can resort back to the contractile phenotype if the ECM is fully restored.

Algorithm 3.1 Get Free Cell Neighbours

```
1: Inputs: Cell Phenotype, cell position
2: for VonNeumann neighbourhood[5] (N, S, E, W, Up, Down) do
3:   if No SMC or EC present then
4:     if e_avg > e_min then
5:       if Phenotype = EC then
6:         if e < e_min then
7:           Add Position to List of Available Positions
8:         end if
9:       else
10:        Add Position to List of Available Positions
11:      end if
12:    end if
13:  end if
14: end for
```

element in the FE mesh, the lattice points within that element were found following the method of Byrne (2008). Briefly, a bounding box was formed around each element, with each lattice point within this box tested to check if it fell within all six faces of the element. These points were initialised as 'artery lattice points' by assigning the stress value of the element and by initialising them with $e = 1$. cSMCs were randomly distributed within a certain fraction of the arterial lattice-points (c_{SMC}). At lattice points with a minimum principal stress value above σ_{crit}, cells were removed and initial conditions for growth factor (G) and matrix degrading factor (MDF) were introduced. These represent an acute source of injurious factors, and encompass production from SMCs, EC, platelets and inflammatory cells. ECs were initialised to cover the lumen surface proximal and distal to the stent ends, simulating total denudation within the stented region, as has been found for balloon-expanded stents (Harnek et al., 1999).

Inflammation

In lattice points containing both ECM and MDF, both of these components were reduced at a constant rate of degradation, k_{deg}, over the course of the simulation. In this respect, inflammation response was modelled as a constant ECM removal term (m_{init}), and an initial amount of growth stimulus for cellular proliferation (g_{init}). This initial amount then decreases linearly over time, until ECM and/or MDF are removed. The inflammation parameters were altered by $\pm 50\%$ to investigate the effect of different inflammation responses on restenosis prediction.

SMC Phenotype

The SMC phenotype was governed by the local ECM concentration: it was contractile if the ECM was present and not degraded ($e = 1$) and the local concentration of cells was below a critical value $c_{\text{SMC,crit}}$, and synthetic otherwise (Algorithm 3.2). This ensured that a region would return to quiescence when the ratio between cells and ECM was appropriate. Differentiation was assumed to be reversible.

Algorithm 3.2 Modulate SMC Phenotype

```
Inputs: e, c_SMC
if e ≥ 1 then
    if c_SMC < c_SMC,crit then
        Phenotype = Contractile
    else
        Phenotype = Synthetic
    end if
else
    Phenotype = Synthetic
end if
```

SMC Proliferation

sSMCs proliferated if the local growth stimulus was above a critical level (g_{crit}), and occurred at a constant rate (p_{SMC}) (Algorithm 3.3). A successful proliferation reduced the local growth stimulus by (g_{crit}), modelling an external limiting factor to growth.

Algorithm 3.3 SMC Mitosis

```
1: Inputs: g
2: if g ≥ g_crit then
3:    Get Free Neighbours (SMC, Cell Position) (A3.1)
4:    if Free Neighbours > 0 then
5:       Randomly Select from Free Positions
6:       Add new SMC to selected position
7:       g = g − g_crit
8:    end if
9: end if
```

SMC Migration and ECM production

Migration of sSMCs occurred in random directions at a constant rate (v_{SMC}) through lattice points which either had or were adjacent to points with ECM present (Algorithm 3.4). sSMCs produced ECM at a constant rate (k_e) at their lattice position (Algorithm 3.5).

Algorithm 3.4 SMC Migration

```
1: Get Free Neighbours (SMC, Cell Position) (A3.1)
2: if Free Neighbours > 0 then
3:    Randomly Select from Free Positions
4:    Move cell to selected position
5: end if
```

Algorithm 3.5 SMC ECM expression

```
for Each neighbouring lattice point do
    if e < 1 then
        Increase ECM in each neighbouring position by k_e/(no. of neighbours)
    end if
end for
```

EC Proliferation

The model assumes endothelium heals through proliferation of healthy endothelial cells in neighbouring regions to the stent. Endothelial cells were only allowed to occupy lattice points which fulfilled the following conditions: they did not contain ECM, and they were adjacent to a lattice point with ECM, i.e. ECs could only proliferate along the lumen surface (Algorithm 3.6). Proliferation occurred at a constant proliferation rate, p_{EC}. SMCs cannot occupy a lattice point containing another cell, so a position occupied by an endothelial cell represents an immovable and impenetrable barrier to SMCs.

Algorithm 3.6 EC Mitosis

```
Get Free Neighbours (SMC, Cell Position)
if Free Neighbours > 0 then
    Randomly Select from Free Positions
    Add new EC to selected position
end if
```

3.2.3 Simulations

The neointimal area at an axial position within the stent was calculated as the total area of lattice points containing extracellular matrix minus the

initial cross-sectional area of the artery. The volume of the lesion was the sum of these areas over the length of the artery. The simulation was then run for an equivalent of 180 days post-stenting.

At each time increment, all cells were operated upon based on their phenotype. Random walk migration and proliferation were performed on each active cell a number of times per increment based on the migration and proliferation rates respectively. Differentiation of SMCs and ECM production were performed every increment, with the increment corresponding to one day.

The pseudocode for the simulation technique is given in procedure 3.7, and represented schematically in figure 3.3.

3.2.4 Parameters

The model parameters were selected based on experimental values, calibrated against experiments or selected based on the descriptions of the time-course of neointima development. DiMilla et al. (1993) measured the migration speed of individual human SMCs on various substrates *in vitro* and found migration speed to be on the order of $10 - 20$ μm/h. The proliferation dynamics of SMCs in the artery are controlled by the proliferation rate and amount of initial growth stimulus. These parameters were selected to produce a similar proliferation profile to human smooth muscle cells (Schwartz et al., 1996) in respect to the time to peak proliferation, and duration of proliferative response[5]. Matrix degradation was

[5]In that study, the time to peak proliferation was calculated to be approximately 15 days, and the proliferation rate dropped to below 1 % of the peak value after 120 days.

Procedure 3.7 Pseudocode representation of the steps involved in the simulation. t_f is the final simulation time.

```
Compute Minimum Principal Stress in the artery during stenting
Initialize Lattice Variables
for t = 0 to t_f do
  for each lattice point do
    if m > 0 and e > 0 then
      e = e − k_deg
      m = m − k_deg... matrix degradation
    end if
    if SMC present then
      Modulate SMC Phenotype (A3.2)
    end if
  end for
  for number of EC proliferations per timestep do
    Randomize list of ECs
    for each EC do
      Proliferate EC (A3.6)
    end for
  end for
  for number of SMC proliferations per timestep do
    Randomize list of SMCs
    for each SMC do
      Proliferate SMC (A3.3)
    end for
  end for
  for number of SMC migrations per timestep do
    Randomize list of SMCs
    for each SMC do
      Migrate SMC (A3.4)
    end for
  end for
  for each SMC do
    Express ECM (A3.5)
  end for
end for
```

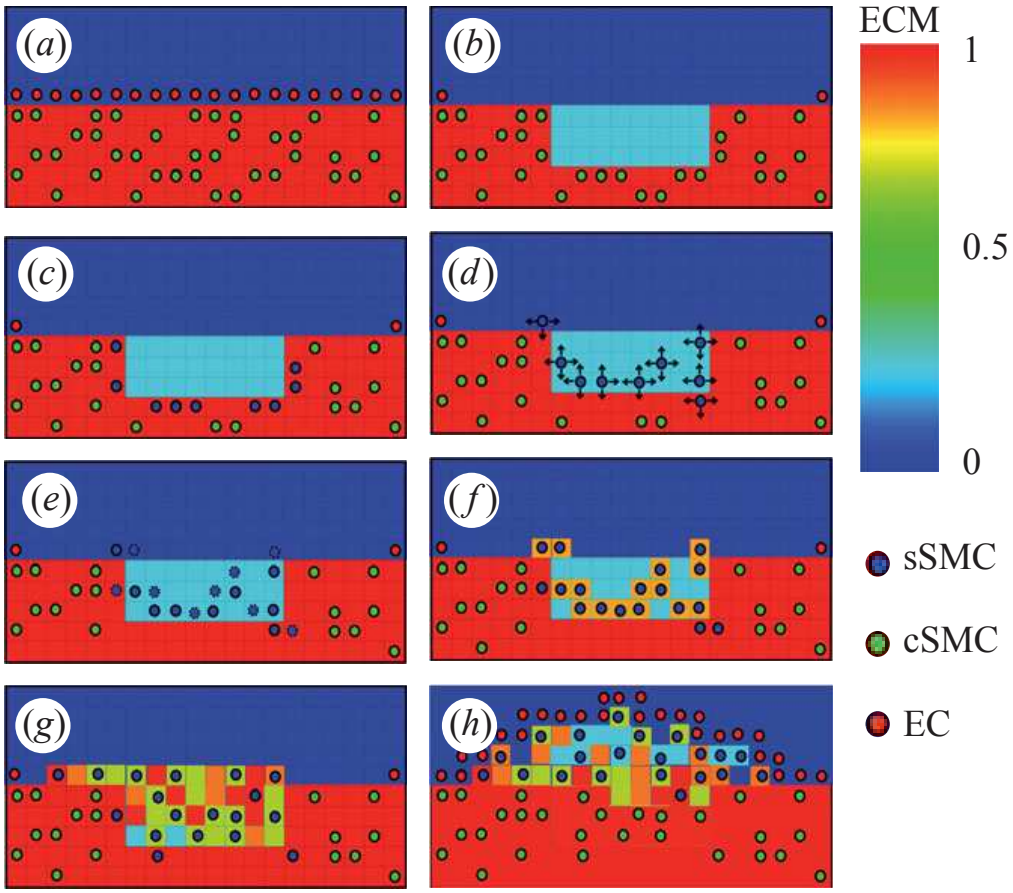

Figure 3.3: Schematic diagrams of the rules governing cell activity in the lattice model. (a) SMCs surrounded by ECM and with an intact endothelium express a contractile phenotype, (b) ECM is reduced in injured areas, simulating the degradation of ECM by MDFs, and SMCs are removed (c). cSMCs neighbouring the reduced ECM region modulate to the synthetic phenotype, (d) sSMCs migrate by random walk (arrows indicate possible movements) and (e) proliferate (dashed lines indicate daughter cells), (f) ECM is produced by cells as they move, and (g) over time a lesion forms until (h) the endothelium has healed. A video of this process in action is included as the electronic supplementary material, video S1 (green circles, cSMC; blue circles, sSMC; red circles, EC).

Table 3.3: Parameters for the initial baseline runs

Parameter	Unit	Value
Δx	mm	.01825
σ_{crit}	kPa	35
c_{SMC}	$cells/mm^2$	3.16×10^4
v_{SMC}	$\mu m/day$	.24
p_{SMC}	$doublings/day$	.24
m_{init}		1
g_{init}		3
k_{deg}		.2
k_{e}		.1
p_{EC}	$doublings/day$	2

assumed to completely resorb damaged tissue (in the absence of matrix producing cells) after 20 days. The endothelial healing rate was selected to achieve re-endothelialisation of an 8 mm denuded artery after 180 days (giving p_{EC} =2). Due to the large variation in this parameter, it was varied over a wide range (proliferation attempt rate of 0 - 4 per cell per day). The lattice density represents the maximum cell density possible. This was set to 1.64×10^5 cells/mm^3, based on human cell concentrations in neointima (Schwartz et al., 1996). The initial concentration of SMCs was based on cell concentrations in human artery tissue (Tracy, 1997), and set to 3.16×10^4 cells/mm^3. Experiments on skeletal muscle have shown that the threshold for skeletal muscle cell viability is between 35 kPa and 70 kPa (Linder-Ganz et al., 2006), and the lower limit of 35 kPa was used as the injury threshold (σ_{crit}) for arterial smooth muscle in the simulations presented here. Parameters are summarised in table 3.3.

3.3 Results

The finite element analyses predicted injury primarily beneath the stent struts (Fig. 3.4). The four-crown stent produced much larger regions of stress than that of the 6 crown stent. The amount of injury beneath the struts increased as the number of scaffolding points decreased. The volume of injured tissue predicted was found to be insensitive to the precise value of the injury threshold (Fig. 3.4). A qualitative analysis of the lattice state over the simulation shows the dynamics of the restenosis progression (Figs. 3.5 and 3.6). Initially, SMCs are removed from the injured regions beneath the stent struts, and ECM begins to be removed. SMCs from the surrounding regions modulate to the synthetic phenotype and proliferate. These cells produce extracellular matrix, and migrate randomly, moving the tissue boundary as new ECM is laid down. Endothelial cells proliferate from the proximal and distal ends of the artery to eventually completely reform over the neointimal surface, at which point the lesion stops growing. The depth of neointima is larger at the stent strut locations, and the amount of neointima produced increases as the number of struts decreases.

In the case where a low amount of initial growth and matrix-degrading stimuli is prescribed (the low inflammation case), there is a significant difference in the amount of restenosis produced in the 4 crown stent compared to the 6 crown (Fig. 3.7), with a two-fold increase in average neointimal area. In this case, there is also a significantly higher neointima produced at the stent ends than in the centre. For the high inflammation case, the differences between the stents is markedly less pronounced, and there is

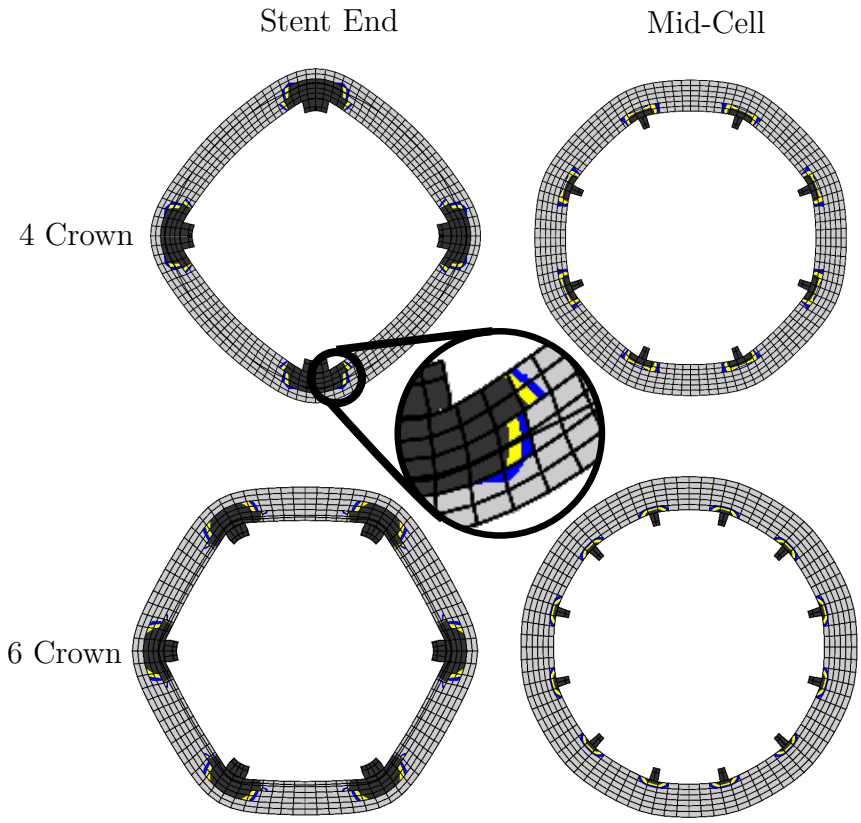

Figure 3.4: Cross-sections of the finite element model showing the injury predicted. The injured region is shown for three different stress thresholds (black = 17.5 kPa, yellow = 35 kPa, blue = 52.5 kPa, while the uninjured is in light grey. The injured regions correspond to the areas under the stent struts and are greatest at the stent crowns (left column) compared to the centre of the cells (right column). The blue and yellow indicate the effect of varying the injury threshold by ±50% , indicating a minimal effect on the predicted volume.

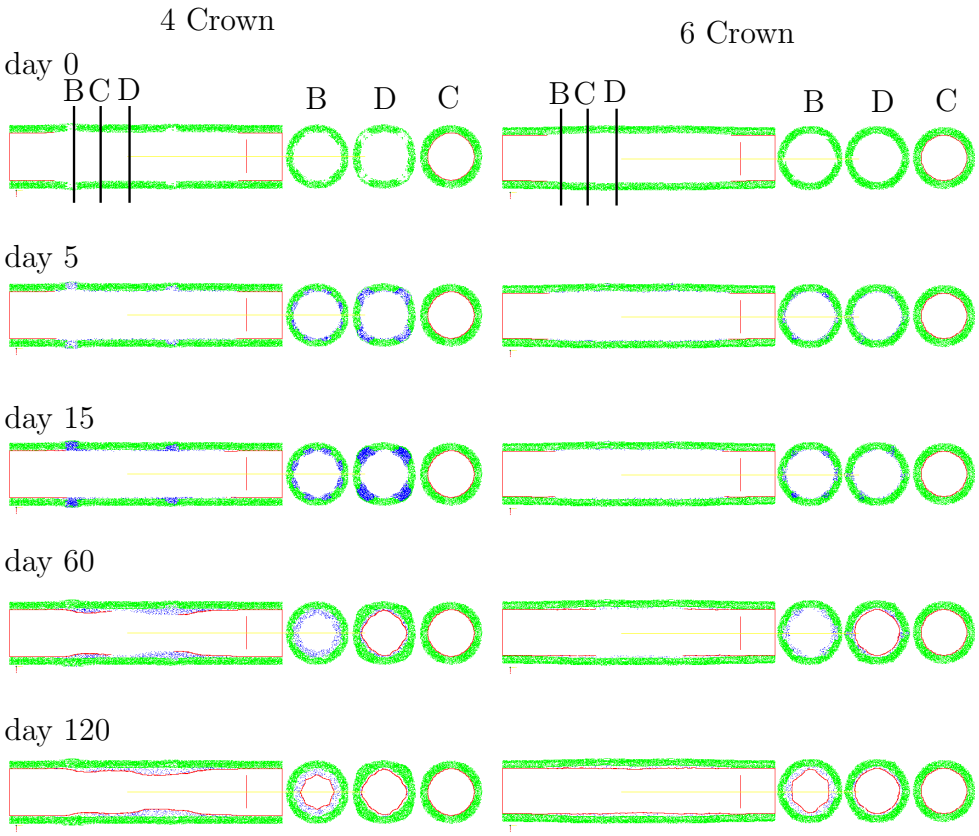

Figure 3.5: Simulation plot of the lattice over time in the simulation of both stents. This plot shows the distribution and phenotype of cells. Green points indicate cSMCs, blue points indicate sSMCs, and red points indicate ECs.

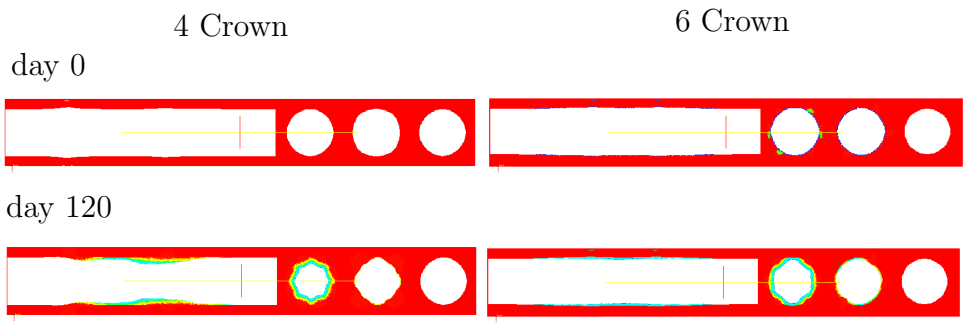

Figure 3.6: Simulation plot of the lattice over time in the simulation of both stents. This plot shows the ECM in the model over time. Red indicates ECM = 1, while blue indicates ECM = 0.

little difference in the peak neointimal area (Fig. 3.8). There is also a change in the distribution of restenosis within the 4 crown stent; neointimal area peaks in three places corresponding to the cell intersections. The 6 crown stent still produces more neointima at the stent ends. The relative volume of restenosis within the stents is not constant over time (Fig. 3.9). In the low inflammation case, the difference gradually increases over time, and eventually reaches a constant value of 1.6, while in the high and intermediate simulations, the difference peaks at 20 days, then reduces coming to a steady value of 0.4.

The rate of endothelial healing had a significant effect on the amount of restenosis formed, and its distribution within the stent (Fig. 3.10).

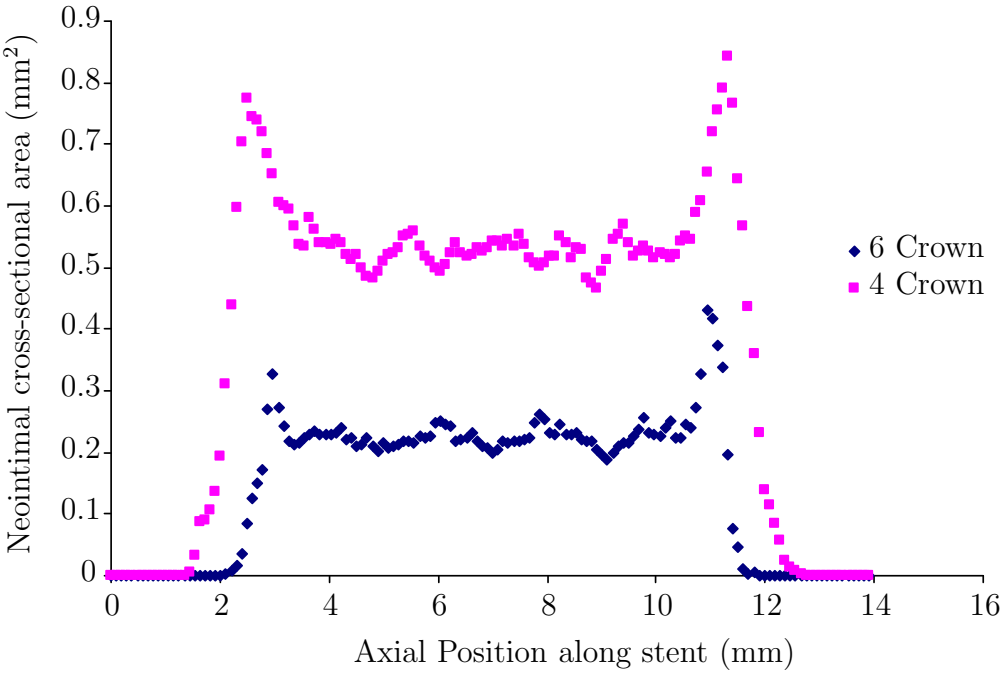

Figure 3.7: The axial distribution of restenosis in the two stents for the low inflammation case. The lesion volume is significantly lower in the 6 crown stent than in the 4 crown stent.

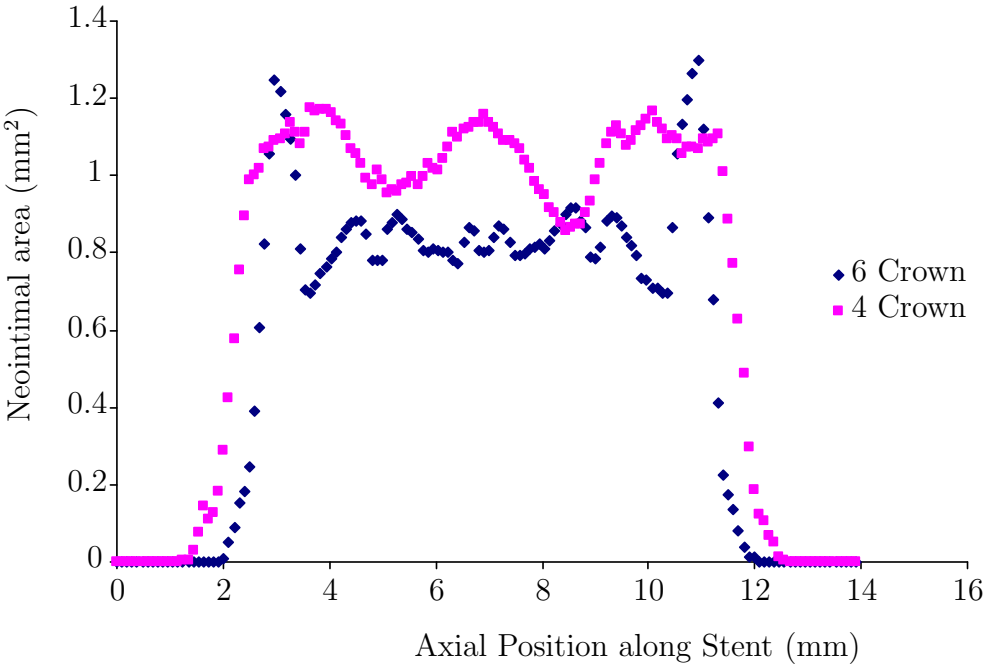

Figure 3.8: The axial distribution of restenosis in the two stents for the high inflammation case.

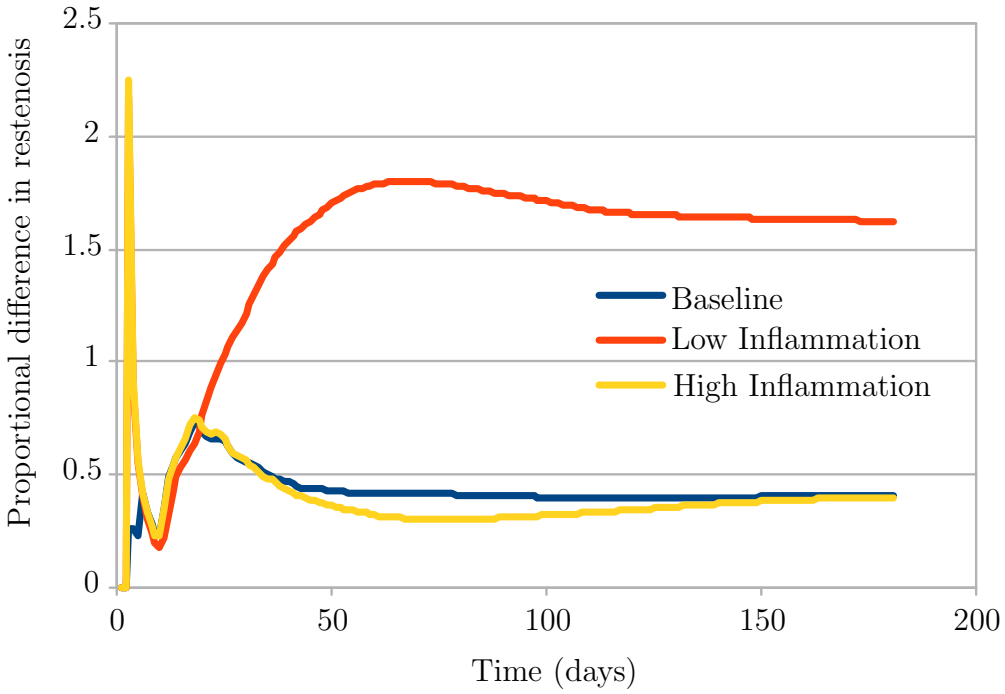

Figure 3.9: Relative difference in lesion volume between the 4 and 6 crown stent (as a function of time). The relative difference is calculated as: (Lesion volume in 4 Crown - Lesion volume in 6 crown)/ Lesion volume in 6 crown. This means that a value of 0 indicates no difference, and a positive value indicates the 4 crown stent induces more restenosis. Increasing the inflammation response intensity constants (i.e. the amount of MDF and G produced) does not significantly alter the prediction, but decreasing the inflammation does. In the low inflammation case, the differences between stents is predicted to be much higher than in the baseline simulations.

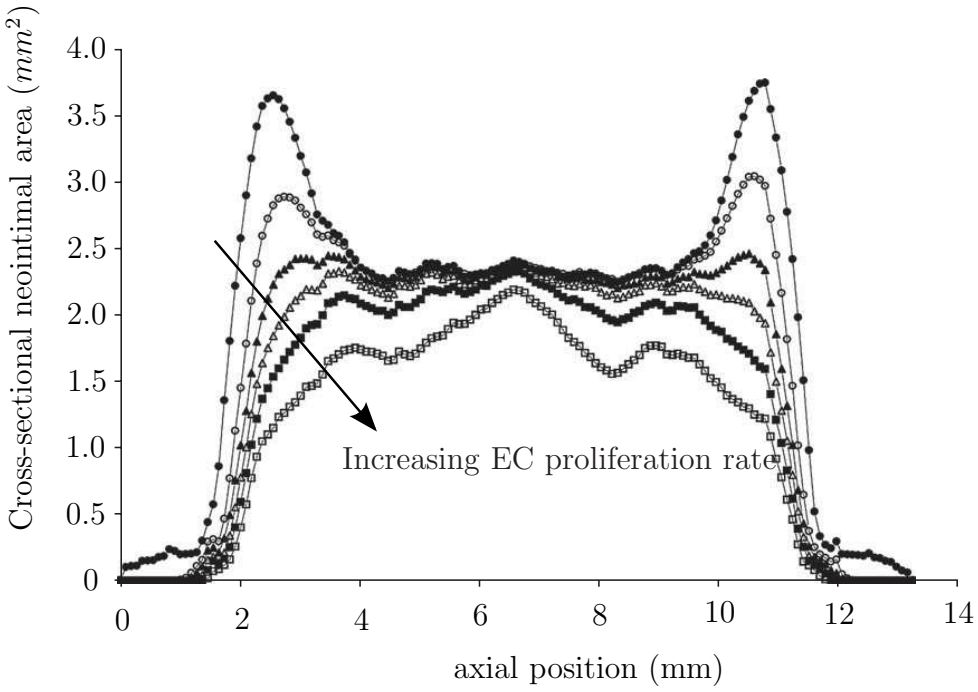

Figure 3.10: Effect of changing the rate of endothelial cell proliferation on restenosis predicted. With higher proliferation rates, the restenosis decreases, and the effect is most pronounced in the ends of the stent.

3.4 Discussion

A simulation technique was developed and tested, which was based on mechanically induced injury, inflammation and smooth muscle cell behaviour. It was found that for the case when the inflammation response was low, a large difference between two stent designs was found, similar to the results of Garasic et al. (2000) *in vivo*. The differences reduced as the amount inflammation prescribed increased, and was not constant over time. The results corroborate the hypothesis that injury induces restenosis, and that this can provide the basis of a predictive model of stent performance. The study highlights the importance of the inflammation response not just on the amount of restenosis produced, but also on the relative performance of stents.

The example described here has some limitations. The geometry of the problem was simplified to a cylinder, whereas in patients, a significant stenosis with heterogeneous properties would affect the calculations of stress (and therefore injury) in the artery (Gijsen et al., 2008). Compressive stress was chosen as the stimulus causing tissue injury; however other variables such as strain, tensile stress or strain energy density may better predict injury. The inflammatory response was modelled only as an initial condition of matrix degrading factors and growth factors. In reality this is a complex response, which occurs as monocytes, macrophages and platelets gradually invade the injured zones from the lumen and act locally to remove debris and stimulate SMCs. In particular, a delay between the injury and the peak of the subsequent inflammation response is not

present in the current model, which may be essential to accurately model the capacity for regulation between injury and inflammation. For example, if the inflammatory response is slower to respond, the injury persists, and could prevent the tissue returning to quiescence. The parameters for the behaviours of the cells in the system have been taken from *in vitro* and *in vivo* data from various species. These parameters have an effect on the outcome of the simulations, and will need to be defined experimentally and for humans. The endothelium healing rate was found to have a large effect on the amount of restenosis. Endothelial proliferation rate varies considerably, and the healing rate is dependant on the injury of the underlying tissue (Kipshidze et al., 2004), underlying substrate strain (Moretti et al., 2004), and fluid flow-induced shear stress (Resnick et al., 2003; Wentzel et al., 2003; White et al., 2001; Zarins et al., 1987). The endothelium model implemented here represented a healed endothelium as a rigid, physical barrier to growth. In reality, the endothelium inhibits growth by acting as a barrier to growth stimuli; underlying tissue can continue to grow. However, even with such simplifications, the simulation could capture important characteristics of lesion growth found *in vivo* in the following ways: lesion development was found to be non-linear in time; unevenly distributed within the stent; and the endothelial healing rate was found to have a large effect on the progression of restenosis. In the future, a method for allowing sub-endothelial growth could be implemented by allowing displacement of ECs by smooth muscle cells. The physical barrier of the stent struts was not included in this model, which could affect the pattern of SMC migration.

The stents tested were based on an *in vivo* study in rabbit iliac arteries (Garasic et al., 2000). In that study, a two fold difference in neointimal area was found 28 days after stent implantation between the 4 crown and 6 crown stents. This provides evidence of the importance of stent design on restenosis. When considering the results shown in this paper, a few important points must be made. Firstly, young, healthy rabbits may be expected to have a less pathologically high inflammatory response to injury. As the simulations here indicate, the level of inflammation response to injury could affect not only the amount of neointima developed, but also the differences between stents. The time-point of comparison may also be important, as the simulations shown here indicate that the differences between stents may not be constant over time. This dependence on the response to injury when comparing device design means that it may be necessary to specify the inflammatory phenotype of test subjects, as this may be expected to vary between patients, lesion types, patient ages, etc.

This is very much a physiomic modelling approach, allowing the synthesis of a diverse range of information. Components may be studied in relative isolation, allowing the implementation of *in vitro* work, and the cell models should be generic enough to apply to a range of applications. The cell models underlying the cell-centred techniques must be based on sound rules, extracted from experimental observation, as the model behaviour is controlled by these rules.

One current limitation of the cell-centred technique when applied to restenosis is the paucity of quantitative information on the dynamics of the system. However, if the loop between experimentation and theory

is to be followed, more data is needed on key behaviours of cells within their natural environments rather than *in vitro*. This would require a benchmark experiment which is controlled to the highest degree possible, such as the bone chamber, which informed skeletal tissue differentiation models (Khayyeri et al., 2009). Until such data is available, the simulation methodology is useful in exploring the possible behaviours of the system (Peck, 2004).

A key benefit of including more biological processes in a model of tissue adaptation is the ability to make predictions about what happens when these processes are altered by the presence of an implant. As biomedical devices become more biologically active (such as drug-eluting prostheses or tissue-engineered implants), predictions from traditional models become more difficult. Also, biological parameters can be highly variable between patients, meaning a pure mechanical analysis may not accurately predict a device's behaviour in a population, as each patient's reaction to an identical stimulus will be different. Including biology allows the effect of this source of variation on the system to be studied. The COAST project aims to include growth-inhibiting drug diffusion in a multi-scale, multi-science model of restenosis development (Evans et al., 2008; Caiazzo et al., 2009). Their preliminary work assumes smooth muscle cell proliferation is induced in response to high structural stress, or low wall shear stress, providing contact inhibition and drug concentration are acceptable. In contrast, the model described here includes explicitly the extracellular matrix (which constitutes a large proportion of restenotic tissue), growth factors (which control SMC proliferation, are diffusible, locally expressed, often short lived) and

endothelium (which is influential in regulating smooth muscle tissue activity). The inclusion of these complexities provides a cell-centred model whose rules are based on the known biological mechanisms of restenotic tissue development. The regulatory effects of mechanical stimuli can in future be implemented through a known/postulated link, such as wall shear stress regulating the production of growth factors at the lumen surface, or tissue stress inducing cell death and subsequent inflammation.

The gold standard for preclinical testing is currently still animals. However, their limitations in many key applications have been increasing. Their biological and mechanical systems are not accurate in predicting performances in many cases (see, for example a review of animal models on drug-eluting stents (Schwartz et al., 2004)). Provided that methodologies are adopted which can synthesise the independent islands of knowledge, computational models will overtake animal models in prediction of tissue adaptation. In this study we have shown that it is possible to predict differences found *in vivo* using an injury-driven model.

This study highlighted two key processes influencing the prediciton of restenosis: the healing of the endothelium, and the inflammatory response of the artery. The inflammation parameters, in particular, were shown to have a large effect on the stent comparison. In the next chapter, the model introduced here will be further refined in order to: provide an inflammation model which can be fully calibrated to in vivo data; include a mechanical, damage-based model of injury; and refine the smooth muscle cell model. In this way, the predicitons of the simulation technique can be made more specific and useful, and more clinically-relevant problems can be addressed.

Chapter 4

In silico Prediction of the Mechanobiological Response of Arterial Tissue: Application to Angioplasty and Stenting[1]

[1]This chapter is based on the paper 'In silico Prediction of the Mechanobiological Response of Arterial Tissue: Application to Angioplasty and Stenting' by Colin J. Boyle, Alexander B. Lennon and Patrick J. Prendergast in Transactions of the ASME, Journal of Biomechanical Engineering (2011), 133, pp 081001. All technical work described in this chapter was performed by the author.

4.1 Introduction

The restriction of blood flow characterises many cardiovascular diseases including stroke and myocardial infarction. Revascularisation generally involves inserting a catheter into the vasculature and navigating the end

of the catheter to the restricted region, where a balloon on the end of the catheter is inflated to force material outward. This process is called balloon angioplasty, and its most significant limitation has been the re-occlusion of the vessel either by elastic recoil of the tissue or by growth of new tissue (neointimal hyperplasia), a process termed restenosis. Stents have become a most successful device for preventing elastic recoil, and are used in increasingly complex lesions. These devices are deployed in the occluded region and are designed to prop open the lumen; however they do no prevent restenosis. There are a wide range of stent designs available and stent designs have been shown to induce varying rates of restenosis (Hoffmann et al., 2001, 2002; Morton et al., 2004). Despite many generations of coronary stents, up to 10% of stenting procedures require revision due to restenosis, a rate that increases to 50% in some high-risk lesions (Bennett and O'Sullivan, 2001; Lally and Prendergast, 2006). It can be argued that successful engineering of stents requires a design tool or model that can predict the tissue hyperplasia induced as a function of stent design.

The key determinant of long-term success after revascularisation is whether the lumen area reaches an equilibrium value that provides sufficient patency for blood flow. The first event to occur upon expansion of the stent is that the endothelium becomes denuded within the stent region, exposing the underlying tissue to blood flow and producing a thrombogenic surface. The stresses within the arterial wall are also increased: tissue is stretched circumferentially between the struts, and compressed radially beneath them. Damage to the laminae and the media can occur

(Gunn et al., 2002; Kornowski et al., 1998). Smooth muscle cells (SMCs) within the media may become necrotic / apoptotic. These combined alterations trigger an inflammatory response (Scott, 2006; Welt and Rogers, 2002). The first phase of the tissue response is characterised by thrombus formation, platelet deposition, and monocyte infiltration into the injured areas. Matrix degrading enzymes and growth factors are expressed by the invading inflammatory cells, platelets and necrotic/apoptotic SMCs (Thyberg et al., 1990). Matrix degradation encourages surrounding contractile SMCs to express a synthetic phenotype (Thyberg et al., 1997); reduction of MMPs (matrix metalloproteinases - a family of matrix degrading enzymes) by inhibitors have been shown to reduce subsequent restenosis (Zempo et al., 1996). The SMCs migrate into injured regions, and proliferate in response to growth stimuli, characterising the proliferation phase. The synthetic SMCs produce extracellular matrix components such as collagen, elastin, proteoglycans, laminin and fibronectin, which constitute the neointimal lesion. Provided the source of injurious factors recedes, and the lumen does not occlude, the cells in the lesion can resort back to quiescence and the lumen area equilibrates. If, however, the cell proliferation and matrix synthesis is too intense, the neointima can restrict the artery, requiring further revascularisation steps. A schematic of restenosis development is shown in Fig. 4.1.

Advances in arterial tissue modelling, and computational fluid dynamics allow the mechanical stimuli imparted by a stenting procedure to be calculated. Significant advances have been made over the last twenty years to the precision and accuracy of these models, including improved consti-

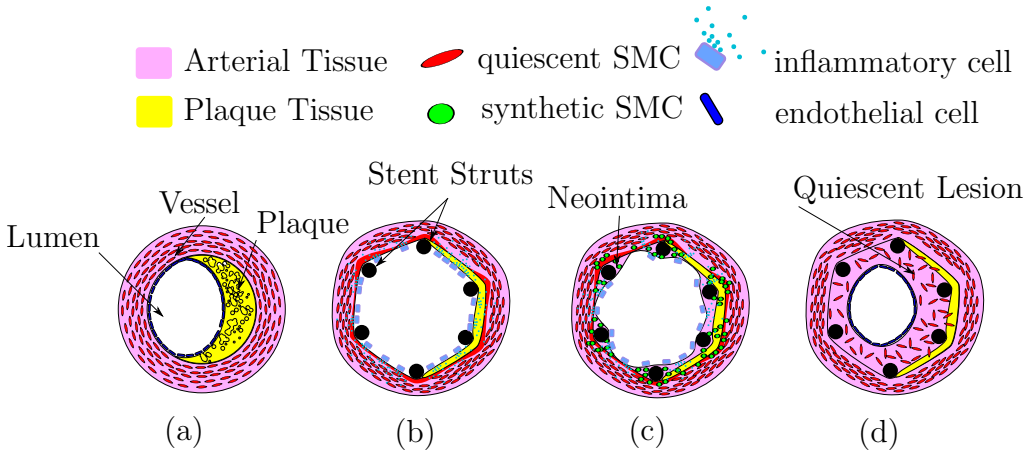

Figure 4.1: Schematic representation of restenosis development. Initially, quiescent SMCs occupy the vessel wall and an intact endothelium exists (a). Upon stenting, the plaque is plastically deformed, endothelium is denuded, vascular tissue is stretched and inflammation is initiated (b). In response, SMCs become synthetic, migratory and proliferative, producing neointima (c), which may achieve homeostasis, provided the inflammation stimulus recedes and a layer of endothelial cells is re-established (d). Neointimal area is measured as the difference between the lumen area immediately post-stenting and the lumen area upon follow-up.

tutive modelling of tissues (Holzapfel et al., 2005), more realistic models of stent deployment (De Beule et al., 2008; Gervaso et al., 2008) and the use of patient-specific geometries (Gijsen et al., 2008; Holzapfel et al., 2002). These provide detailed information on the stresses induced in the arterial wall due to stenting, and allow comparisons between stent designs, in terms of tissue prolapse (Prendergast et al., 2003) or induced stresses (Lally et al., 2005; Migliavacca et al., 2004). These models may then be used to optimise stent design with respect to mechanical stress (Bedoya et al., 2006; Timmins et al., 2007), and to investigate the effect of structural differences between coronary and peripheral vessels (Early and Kelly, 2010). These studies provide methods to determine the initial stimuli or triggers for restenosis. The reaction to a stent by the arterial tissue, however, is a complex biological process (Evans et al., 2008), which is difficult (if not impossible) to predict from the initial stimuli described by the mechanical environment post-stenting. It is unclear, for example, which, if any, mechanical stimulus correlates with subsequent restenosis volume. One path forward is to develop mechanobiological models that relate mechanics to biological response (i.e. injury, inflammation and SMC behaviour) in order to simulate the process over time.

Mechanobiological models offer a method for predicting the long-term effects of perturbing the mechanical environment. These models have been successfully applied to bone remodelling (García, 2002) and skeletal tissue differentiation (Prendergast, 2009), and have been investigated for cardiovascular applications (Evans et al., 2008; Lally and Prendergast, 2006; Rachev et al., 2000). The modelling approach where cell activities are

modelled using a regular lattice has been of particular utility in modelling processes that are the result of complex cell activities (Pérez and Prendergast, 2007). In these models, individual cells act at a local level based on the local environment; and tissue-level changes occur as a result of the net effect of local cell activity. This allows a wide range of information and complexity to be included through prescribing algorithmic rules for cell behaviour, and is particularly suitable to modelling the relationships between cell activity and mechanobiological stimuli (Boyle et al., 2010; Merks and Glazier, 2005).

In this paper we ask the question whether or not a mechanobiological model for restenosis in arteries can be developed using the lattice-modelling approach to describe local cell activities. Specifically we aim to set the model parameters using the clinical results of balloon angioplasty presented by Schwartz et al. (1996) and information on the levels of inflammation in patients after angioplasty described by Cipollone et al. (2001). We then test the model by using the same parameters to simulate restenosis in an artery in response to the injury caused by cardiovascular stenting. If the model can predict reasonable results in these simple cases then it opens up the opportunity to apply mechanobiological modelling in three dimensional complex environments for the design of cardiovascular stents.

4.2 Methods

The growth of new tissue into the lumen of arteries in response to stenting is assumed to be appositional; i.e. due to the deposition of extracellular

matrix by smooth muscle cells (SMCs) on the lumen surface. Volume addition is brought about by migration into, and matrix deposition at, a previously unoccupied region of space such that the boundary of the tissue is extended. The number of cells available to produce matrix in a region is not constant over time; it is a function of net migration into the region, proliferation, apoptosis and the phenotype of the present cells. SMC migration can be modelled as a random-walk process (Pérez and Prendergast, 2007) — with the constraint that cells only migrate within, or on the surface of, tissue. SMCs proliferate in response to growth factors. The rates of proliferation and migration depend on the individual smooth muscle cell phenotype, which is modulated according to the constituents of the extracellular space around the cell: in particular the amount of intact extracellular matrix — the greater the volume fraction of extracellular matrix, the more likely SMCs are to express a quiescent phenotype. Matrix degrading factors (MDFs) such as matrix metalloproteinases, and growth factors (for example platelet derived growth factor, PDGF) are produced by inflammatory cells, apoptotic cells, SMCs and ECs. Mechanical stimuli induce inflammation through injury / damage — introducing a *mechano*-biological link. An outline of the simulation technique is given in Fig. 4.2.

The spatial domain in which cell activities occur is represented as a regular, orthogonal lattice with dimensions $\{X, Y, Z\}$, and a lattice-point spacing, denoted Δx, which is identical in all three directions. At each lattice point, Boolean and continuous variables are defined representing the model constituents. Cells are represented by a Boolean variable such that

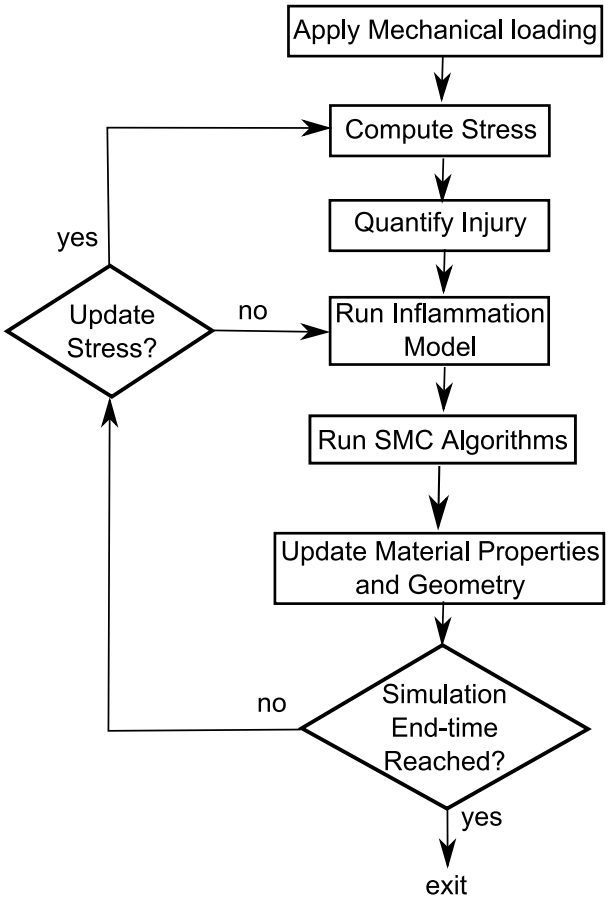

Figure 4.2: Flow chart outlining the computational method for the simulation of restenosis. The stress may be updated, depending on whether or not the new geometry significantly effects the structural behaviour of the artery; and whether the injury stimulus is assumed to occur once in the initial expansion procedure, or chronic.

a lattice point is either occupied by one cell, or the lattice point is vacant. The variables at each lattice point are then explicitly updated over time based on algorithms for each cell activity, as described below. A boundary condition describes the migration behaviour of cells at the edge of a symmetric boundary, such as that found when simulating a circumferential segment of an artery (see section 4.2.8 below). At these boundaries, a cell in reality ought to be able to move into surrounding tissue, just as a cell from the surrounding tissue ought to be able to migrate into the simulation domain. To simulate this, a cell moving across a boundary is transported to the equivalent point inside the corresponding surface. If the domain is rectangular, this means a cell migrating off the top of the lattice will move to the bottom, i.e. the simulation domain becomes a torus and cells are conserved within the lattice. In an artery segment model, the boundaries are at an angle to each other, dictated by the angle of the segment. In this case, the equivalent point to each boundary point is found by rotating the point by the angle between the boundary lines, and about the point of intersection of the lines (Fig. 4.3). For a regular orthogonal lattice, the angle between boundaries may mean that the equivalent position may not correspond to a lattice point, in which case the nearest point is chosen.

4.2.1 Stimulus computation

The finite element method was used to compute the arterial wall stresses during loading. Arterial tissue was modelled as an isotropic, hyperelastic

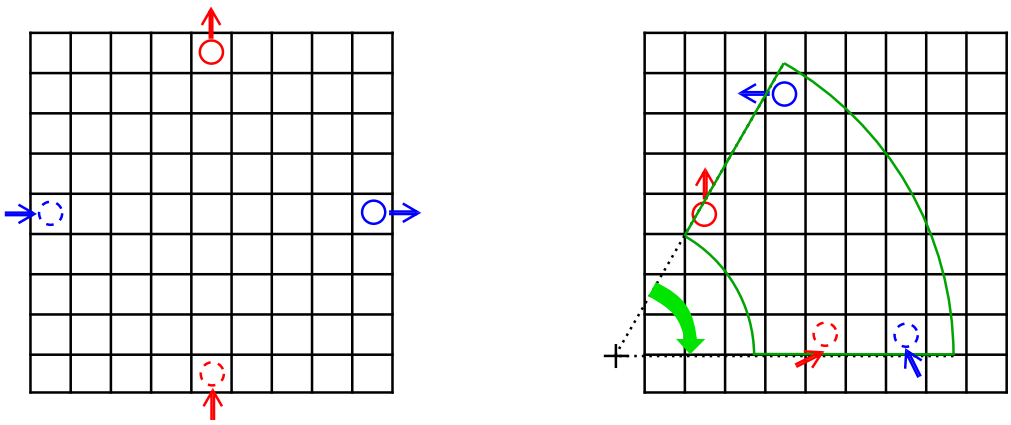

Figure 4.3: The boundary conditions for cell activity in the lattice model. In a rectangular domain (left), a cell seeking to move off the top of the domain (red circle) is transported to the bottom of the domain. A cell moving off one side of the lattice is transported to the other side (blue circle). In the case of a segment of a circle (right), a cell which leaves the tissue domain (green lines) in the circumferential direction is transported to the nearest lattice point to the equivalent position at the corresponding boundary. This is found by rotating the point about the intersection between the two boundaries (green arrow). Cells are not restrained from moving in the radial direction.

material using a second-order Mooney-Rivlin strain-energy function:

$$\begin{aligned}\psi = a_{10}\left(I_1 - 3\right) + a_{01}\left(I_2 - 3\right) \\ + a_{11}\left(I_1 - 3\right)\left(I_2 - 3\right) + a_{20}(I_2 - 3)^2\end{aligned} \tag{4.1}$$

Finite element analysis was performed using ABAQUS (SIMULIA) v6.8. Von Mises stress was used to compute damage accumulation using a log-linear relationship for fatigue-induced damage:

$$\sigma = \alpha \log N_{\mathrm{f}} + \sigma_{\mathrm{f}} \tag{4.2}$$

where N_f is the number of cycles to failure, σ_{f} is the failure strength (i.e. when $N_{\mathrm{f}} = 1$) and α is a constant. We define a fatigue strength, σ_0, below which the damage accumulation rate is assumed to be zero. Rearranging, and taking that the rate of damage formation denoted $\dot{D}$ is given by $\dot{D} = \frac{1}{N_{\mathrm{f}}}$ (Miner's rule (Lee et al., 2005)), we get:

$$\begin{aligned}\dot{D} &= 10^{-\frac{\sigma_{\mathrm{f}} - \sigma}{\alpha}} && \sigma_0 < \sigma \leq \sigma_{\mathrm{f}} \\ &= 0 && \sigma \leq \sigma_0 \\ &= 1 && \sigma > \sigma_{\mathrm{f}}\end{aligned} \tag{4.3}$$

4.2.2 Modelling inflammation

The production of, and reactions between, three biological species – growth stimulus (g), matrix degrading factor (m) and extracellular matrix (e) in

response to damage (D) is simulated using a mathematical model. The variables are updated at each lattice point based on their rate equations. The reaction between e and m is approximated as first-order, with the extracellular matrix degrading at a rate proportional to the amount of matrix degrading factor,

$$\frac{\mathrm{d}e}{\mathrm{d}t} = -k_{\mathrm{deg}} m \tag{4.4}$$

and the amount of matrix degrading factor (m) reducing correspondingly, but being replenished in proportion to the injury present,

$$\frac{\mathrm{d}m}{\mathrm{d}t} = -k_{\mathrm{deg}} m + k_m D \tag{4.5}$$

In equations (4.4) and (4.5), k_{deg} is the rate of reaction between the species, and k_m is a constant relating the production of matrix degrading factor (m) to damage, D. Growth stimulus production is assumed to be linearly related to damage (via constant k_g), and is assumed to decay exponentially at a rate d_g

$$\frac{\mathrm{d}g}{\mathrm{d}t} = k_g D - d_g g \tag{4.6}$$

Damage removal is assumed to be equal to the removal rate of the extracellular matrix (e), so the damage evolution equation is,

$$\frac{\mathrm{d}D}{\mathrm{d}t} = N \cdot \dot{D} - k_{\mathrm{deg}} m \tag{4.7}$$

where N is the number of cycles at a given stress and $\dot{D}$ is the damage accumulation rate (see section 4.2.1 above).

4.2.3 Modelling Smooth Muscle Cell Activity

Each smooth muscle cell occupies a single lattice point. Migration is modelled as the movement of a cell from one lattice point to a neighbouring, vacant lattice point. The local neighbourhood of a cell is defined as the lattice points within a surrounding sphere of radius Δx centred around the lattice point, i.e. a von Neumann neighbourhood (Chopard and Droz, 1998), which includes the orthogonally adjacent lattice points (in a 2D lattice, there are four such neighbours, see Fig. 4.4). Proliferation is modelled as the creation of a new cell at a vacant lattice point in the von Neumann neighbourhood. If a cell has no vacant neighbours, it cannot proliferate, introducing a contact-inhibition effect. The direction of migration and proliferation is random, implemented by selecting from the vacant neighbours of an active cell randomly. These processes could, in principle, be dependant on a chemical gradient; in this study, however, isotropic migration and proliferation are used.

Phenotype Modulation

The SMC phenotype (ϕ) is assumed to vary continuously between fully contractile ($\phi = 0$) and fully synthetic ($\phi = 1$), and is modulated by extracellular matrix concentration, e. The ideal or homeostatic phenotype is assumed to be given by $\phi^* = 1 - \bar{e}$, where $\bar{e} = \frac{\sum_{i=1}^{n} e}{n}$ is the average of

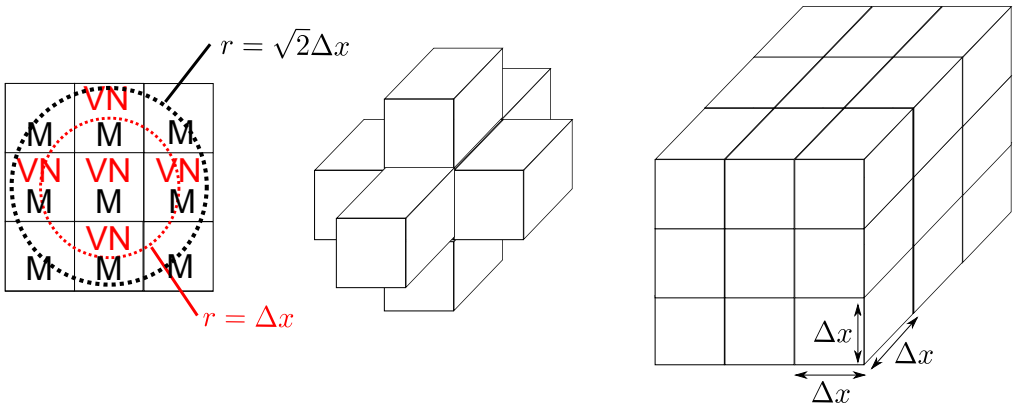

Figure 4.4: The neighbouring points around a cell in an orthogonal lattice. In the left-most diagram, VN indicates the von Neumann neighbourhood (shown in 3D in the central diagram), and M indicates the Moore neighbourhood (shown in 3D in the right-most diagram).

e within a sphere of radius $\sqrt{2}\Delta x$ (n number of points); i.e. the 'Moore' neighbourhood (Chopard and Droz, 1998), which includes both orthogonally and diagonally adjacent lattice points (Fig. 4.4). The rate of change of phenotype is described by:

$$\frac{\mathrm{d}\phi}{\mathrm{d}t} = k_\mathrm{d}\left(\phi^* - \phi\right) \tag{4.8}$$

where k_d is a constant, such that the phenotype of a cell approaches the homeostatic phenotype of its environment at a rate proportional to the deviation of its phenotype from homeostasis.

Proliferation

Cells are assumed to have an intrinsic maximum proliferation rate (p_smc) such that exponential proliferation would occur if there was no contact-inhibition; however the lattice modelling approach explicitly provides for

contact-inhibition behaviour because, as the lattice fills, the number of vacant lattice sites for cells to occupy are reduced. The mitosis rate of a given cell is assumed to depend linearly on the local amount of growth stimulus (g), and the phenotype of the SMC (ϕ). We therefore write an expression for the probability of cell division when it has been ascertained that there is a vacant neighbouring lattice, within a timestep Δt, as:

$$\mathrm{P}^{\mathrm{proliferation}} = p_{\mathrm{smc}} \cdot g \cdot \phi \cdot \Delta t \tag{4.9}$$

Algorithm 4.1 SMC Mitosis

```
Inputs: g, p_SMC, φ, , r = RAND ∈ (0, 1)
if g · p_SMC · φ ≤ r then
    Get Free Neighbours (SMC, Cell Position)
    if Free Neighbours > 0 then
        Randomly Select from Free Positions
        Add new SMC to selected position
    end if
end if
```

Migration

SMCs are assumed to have an intrinsic maximum migration speed v_{smc}. The actual migration speed is linearly related to phenotype, so the probability of a cell moving to a vacant lattice point, within a timestep Δt, is:

$$\mathrm{P}^{\mathrm{migration}} = \frac{v_{\mathrm{smc}}}{\Delta x}\phi \cdot \Delta t \tag{4.10}$$

A lattice site is only acceptable for migration if no cell is present and the extracellular matrix is greater than a critical value $e_{\min}$. This means cells will only migrate into a region if there is sufficient matrix to provide a scaffold for cell attachment.

Algorithm 4.2 SMC Migration

```
Inputs: v_SMC, φ, , r = RAND ∈ (0, 1)
if v_SMC/Δx · φ ≤ r then
    Get Free Neighbours (SMC, Cell Position)
    if Free Neighbours > 0 then
        Randomly Select from Free Positions
        Move SMC to selected position
    end if
end if
```

Extracellular matrix synthesis

Cells are assumed to produce extracellular molecules which assemble around the cell to form extracellular matrix. Material is deposited within a radius $r_{\max}$ of the cell (here $r_{\max}$ is assumed to be $\sqrt{2}\Delta x$), i.e. to each lattice point in the Moore neighbourhood. The rate of change of e at a point is given as $k_e\left(\frac{r-\delta}{r}\right)$, where δ is the distance from the centre of the cell and k_e is a constant. The rate of change of e at a point within r of a cell is

$$\frac{\mathrm{d}e}{\mathrm{d}t} = k_{\mathrm{e}}\phi\left(\frac{r-\delta}{r}\right) \qquad 0 \leq \delta \leq r \tag{4.11}$$

Due to these equations and the geometry of the lattice, there are three expression rates around a cell: $\delta = \Delta x$ for von Neumann neighbours, $\delta = \sqrt{2}\Delta x$ for diagonally adjacent neighbours and $\delta = 0$ for the cell position itself.

4.2.4 Computational implementation in a lattice

The simulation time is divided into equal timesteps, Δt. During each timestep, each cell expresses extracellular matrix and modulates its phenotype. It also selects its behaviour from the set {proliferate, migrate, no change}. To ensure that each cell can perform only one of these behaviours per timestep, the timestep must satisfy:

$$\left(\mathrm{P}_{\max}^{\text{proliferation}} + \mathrm{P}_{\max}^{\text{migration}}\right) \leq 1, \tag{4.12}$$

and so from from Eqns. 4.9 and 4.10:

$$\Delta t_{\max} = \frac{1}{p_{\text{smc}} + v_{\text{smc}}/\Delta x}. \tag{4.13}$$

To search for a vacant neighbouring lattice point, a neighbouring point is chosen at random using a random number generator. If the selected position is not vacant, another position is randomly chosen, and this is repeated until a vacant position has been found, or all positions have been searched.

These algorithms were implemented using the Visualization Toolkit (VTK) code and custom-build classes and methods in C++ (called the MechanoBiology ToolKit, MBTK; see Lennon et al. (2011)). This allows representation of the finite element mesh (an unstructured grid in VTK) and the lattice (image data set in VTK). The interpolation algorithms from VTK were used in mapping variables between the spatial representations, and the algorithms described above were implemented. A pseudocode

representation of the simulation technique is given in algorithm 4.3.

Procedure 4.3 Pseudocode representation of the steps involved in the simulation

```
Compute maximum stresses in the artery
for t = 0 to t_f do
  if t mod Δt_σ = 0 then
    Update Stress State
  end if
  if t mod Δt_inflam = 0 then
    Run Inflammation Model
  end if
  if t mod Δt_smc = 0 then
    for every cell do
      Generate a Random Number r = RAND ∈ (0, 1)
      if r < P(prolif) then
        Proliferate
      else if r < P(prolif) + P(migrat) then
        Migrate
      else if r < P(prolif) + P(migrat) + P(apop) then
        Apoptose
      end if
    end for
  end if
  if t mod Δt_out = 0 then
    Output Lattice variables
  end if
end for
```

4.2.5 Inflammation model testing

The inflammation model was isolated for study by assuming no SMC activity occurs, reducing the system to a set of coupled ordinary differential equations for e, D, m and g. We examined the behaviour of the model when an initially uninjured tissue is loaded in uniaxial tension. Four cases were analysed: (i) an instantaneous stress (σ_0) is applied and removed im-

mediately, (ii) a stress (σ) is held constant, (iii) a stress (σ) decays linearly with time, and (iv) a constant stretch ratio (λ) is applied. These give rise to the prescribed conditions:

$$(i) \qquad \sigma(t) = \sigma_0 \qquad 0 < t < t_1$$
$$= 0 \qquad t \geq t_1 \tag{4.14}$$
$$(ii) \qquad \sigma(t) = \sigma_0 \qquad \forall t \tag{4.15}$$
$$(iii) \qquad \sigma(t) = \sigma_0 - kt, \qquad \sigma \geq 0 \tag{4.16}$$
$$(iv) \qquad \lambda(t) = \lambda_0 \qquad \forall t \tag{4.17}$$

4.2.6 Parameter estimation

Material properties were chosen based on porcine coronary artery uniaxial tension tests (Lally et al., 2005). The fatigue parameters (Eqn. 4.2) were determined using the data of McLoughlin (McLoughlin, 2008), as shown in Fig. 4.5. In these experiments, circumferential porcine coronary artery segments were fatigue tested in tension. The samples were subjected to cyclic tensile loading at three mean stress magnitudes (200 kPa, 500 kPa and 1 MPa), and the number of cycles to failure was recorded. A log-linear model was fitted to this data (σ vs $\log N_f$). Assuming damage would not accumulate in the healthy artery, the lower limit for the fatigue strength of the material is the maximum stress magnitude induced under physiological loading. To compute this, a finite element model of a healthy artery (with inner radius of 1.5 mm and wall thickness of 0.5 mm) was pressurised to 13.3 kPa (mean physiological blood pressure), and the maximum stress

induced was taken as the fatigue limit. The mechanical parameters are summarised in Table 4.1.

Cell migration was set based on in vitro measurements of human SMC migration (DiMilla et al., 1993). The lattice size was set such that $\Delta x = 0.018$ mm, allowing a maximum cell concentration of 3000 cells/mm^2. The initial concentration, c_{smc}, was set to a density of 1620 cells/mm^2, based on the data of Tracy (1997) for SMC densities in healthy human arteries. In practise this was achieved by assigning 50 % of all lattice points a smooth muscle cell randomly; all cells were assigned a contractile phenotype initially ($\phi = 0$). Cell model parameters are summarised in Table 4.2.

The inflammation parameters (k_m and k_{deg}) were calibrated to achieve similar inflammation time-courses as found in the study of angioplasty in humans by Cipollone et al. (2001). In this study, a key marker for inflammation (monocyte chemoattractant protein 1 (MCP-1)) was measured in angioplasty patients. It was found that in patients who did not develop restenosis, MPC-1 reduced much quicker than in the restenosis-prone group. For this reason, three inflammation responses were simulated in our computational models: a prolonged (high) and shortened (low) source of inflammation corresponding to the restenosis and no restenosis groups in the above study respectively, and an intermediate response, which lay halfway between both responses, as tabulated in Table 4.3.

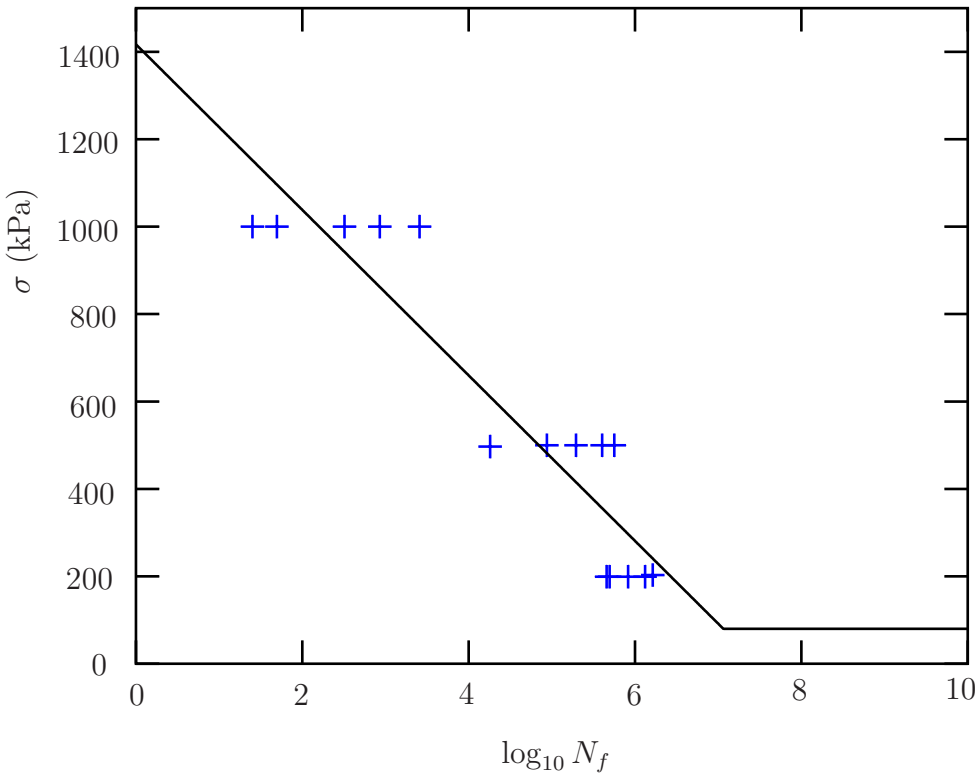

Figure 4.5: Stress versus remaining life (number of cycles to failure, N_f) for porcine coronary artery. Crosses indicate experimental data from McLoughlin (McLoughlin, 2008), The solid lines show the fitted bilinear model; the horizontal line indicates the fatigue strength, $\sigma_0 = 90$ kPa, the y-intercept is the failure strength, $\sigma_f = 1417$ kPa, and the slope, α, is -187.

4.2.7 Balloon expansion calibration

A simulation of balloon expansion was used to estimate matrix production and cell proliferation parameters by comparing the response to human data (Schwartz et al., 1996). In that paper, the number of cells over time post-angioplasty was estimated from the restenosis area measurements and the known concentration of SMCs in restenotic tissue. In the analogous simulation, a 2D cylindrical, isotropic hyperelastic artery with inner radius 1 mm and outer radius 2 mm was expanded by applying a displacement to the inner lumen surface to achieve an expansion ratio (maximum dilated diameter/initial lumen diameter) of 1.4. The parameters which control cell proliferation (k_g, d_g) as well as the matrix production and migration parameters (k_e and $e_{\min}$) were calibrated to achieve an accurate model match for cell numbers and neointimal area (Table 4.4). To calculate the mean response of the model, ten simulations were run at each parameter combination, and the mean of the results was calculated.

4.2.8 Stent expansion

To simulate stent expansion, an analytical rigid body representing a stent strut with circular cross-section was displaced radially into the wall of the artery (Fig. 4.6). The stent strut was assumed to have a circular cross-section and a diameter of 150 μm. To analyse the effect of increasing the extent of stent expansion on the degree of restenosis induced, the stent radial deployment was varied between 0.17 mm and 0.88 mm. This was performed for the three different inflammatory responses described in sec-

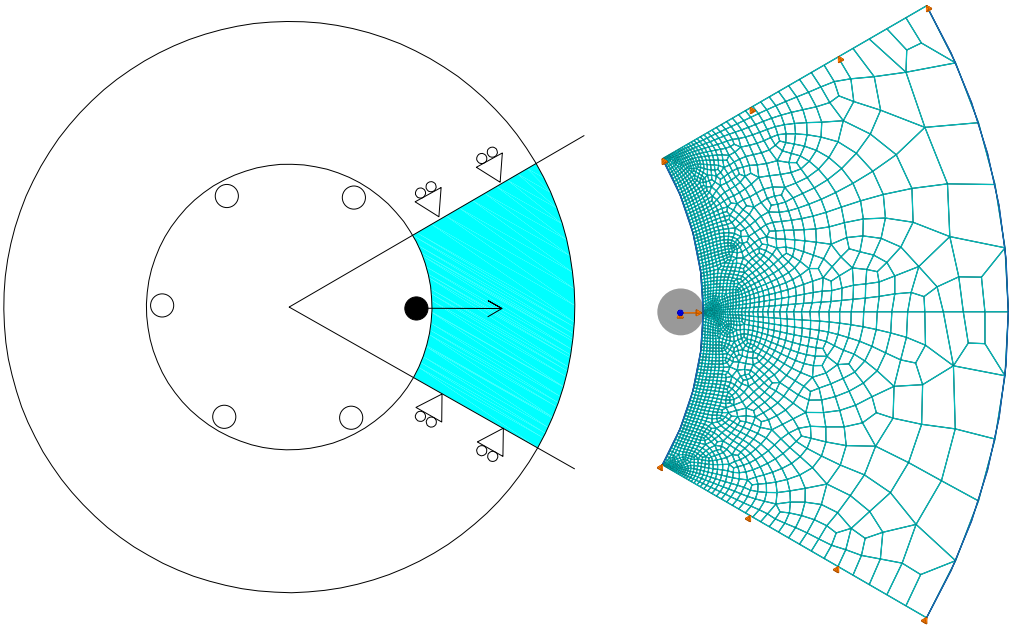

Figure 4.6: The geometry of the idealised artery and stent (left). A cross-section of a symmetrically stenosed artery is shown with six stent struts. A 1/6 segment is considered due to symmetry, and this model is meshed as shown on the right. A displacement is applied to the strut, and the upper and lower surfaces of the mesh are restrained circumferentially.

tion 4.2.6 above.

Table 4.1: Mechanical and fatigue parameters

Parameter	Unit	Value
α	kPa	-187
σ_{f}	kPa	1417
σ_0	kPa	90
N	day^{-1}	1

Table 4.2: Cell parameters

Parameter	Unit	Value
c_{smc}	%	50
p_{smc}	day^{-1}	.24
v_{smc}	$\mu m.day^{-1}$	.48
k_d	day^{-1}	0.2
$r_{\max}$	μm	.0255

Table 4.3: Inflammation parameters, showing high, intermediate and low responses

Parameter	Unit	Value
k_m	day^{-1}	(H: 0.0043, I: .04, L: 0.2)
k_{deg}	day^{-1}	(H: 0.98, I: 0.4, L: 0.9)

Table 4.4: Balloon angioplasty-derived parameters

Parameter	Unit	Value
k_g	day^{-1}	.04
d_g	day^{-1}	.011
k_e	day^{-1}	0.025
$e_{\min}$		0.11

4.3 Results

4.3.1 Inflammation model

In case (i), where an initial stress is applied and removed, damage decayed exponentially to zero, while extracellular matrix reduced exponentially to a final value of $e(t = 0) - D(t = 0)$ (Fig. 4.7). Therefore D, in this case, is a measure of the quantity of injury in the artery which must be removed. In case (ii), when a constant stress is applied, damage never stabilises and accumulates eventually to 1; the rate of accumulation is higher for higher stress magnitudes (Fig. 4.7). At low stresses, the extracellular matrix is not significantly altered, whereas at high stresses all the material is removed rapidly. Case (iii) is in between cases (i) and (ii) depending on the stress relaxation prescribed (Fig. 4.7); the damage accumulates with prolonged stress, whereas with less-prolonged stress, damage can be removed. In case (iv), the stretch to which the artery is exposed determines whether damage accumulates or decays, and by how much (Fig. 4.7). A long-term stress-relaxation-type response is found, where the stress reduces to a homeostatic stress state at a rate which depends on the initial magnitude of the stretch.

4.3.2 Balloon expansion calibration

The calibration gave a reasonable match to the experimental data of Schwartz et al. (1996) in terms of the number of SMCs found over a 350 day period (Fig. 4.8). In particular, an initial rapid proliferation rate gradually

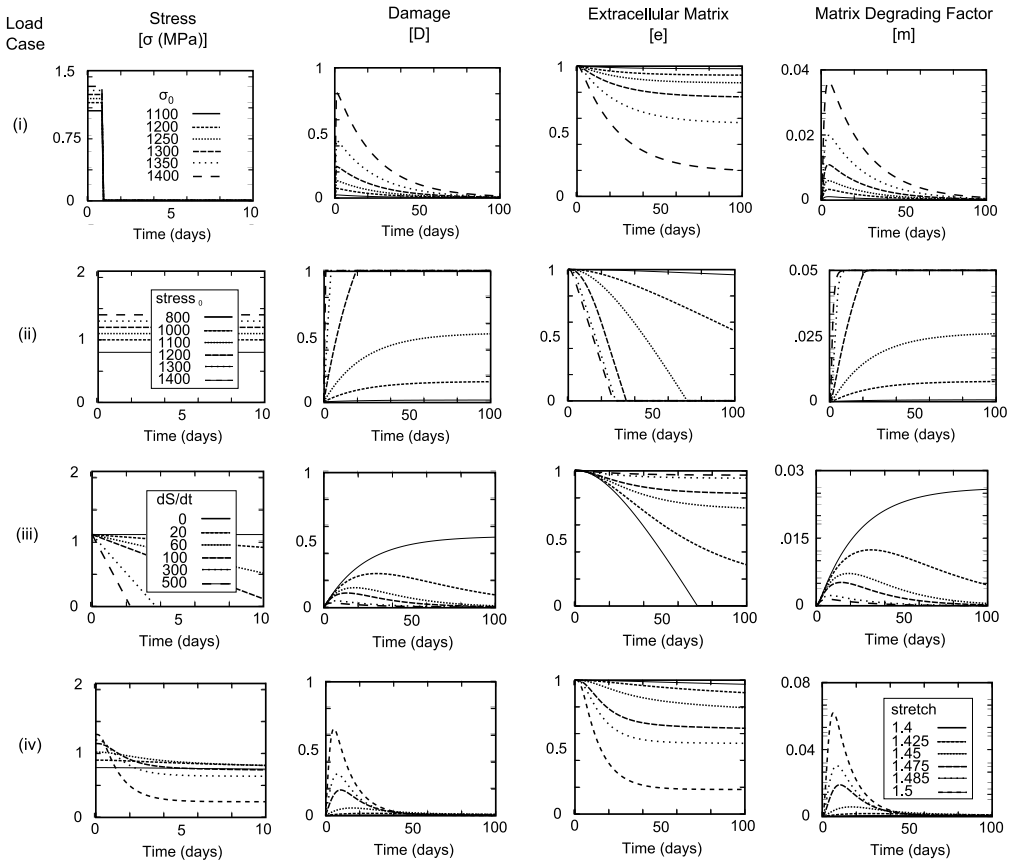

Figure 4.7: **Case (i)**: An initial stress is applied and removed. Damage is initiated abruptly, and decays exponentially to zero, while extracellular matrix decays exponentially to $e = e|_{t=0} - D|_{t=0}$. **Case (ii)**: A constant stress is prescribed, leading to complete ECM removal at a rate dependant on the stress applied. **Case (iii)**: A decaying stress is prescribed. **Case (iv)**: A constant stretch is prescribed, which leads to stress-relaxation.

decreased to zero over the course of the simulation. The smooth muscle cells in the injured region modulated their phenotype after approximately 5 days, and began migrating, proliferating and producing extracellular matrix. The maximum proliferation rate achieved was most affected by the parameter p_{smc}, while the final cell number and time to peak proliferation rate (approximately 10 days in the baseline simulations) were most affected by the parameters affecting growth factor kinetics (d_g and k_g).

The simulations produced a final cell distribution in which there was a gradient of cell concentration through the thickness of the neointima, with the injured media having the most cells, and the surface of the neointima having less (Fig. 4.9).

4.3.3 Analysis of stent expansion

The model predicted a nonlinear relationship between neointimal area and initial lumen gain. Below a lumen area of 6 mm^2, restenosis was minimal, but for gains greater than that, neointimal hyperplasia and restenosis increased with initial lumen gain (Fig. 4.10).

The simulations results were not deterministic, allowing a prediction of the variability in the restenosis developed (Fig. 4.10). The level of inflammation affected the relationship between restenosis and stent area, with high inflammation inducing more restenosis and a greater dependency on stent area with high inflammation, as can be seen from the final slope of the curves (Fig. 4.10).

Lattice variables are plotted in Fig. 4.11 for the high inflammation

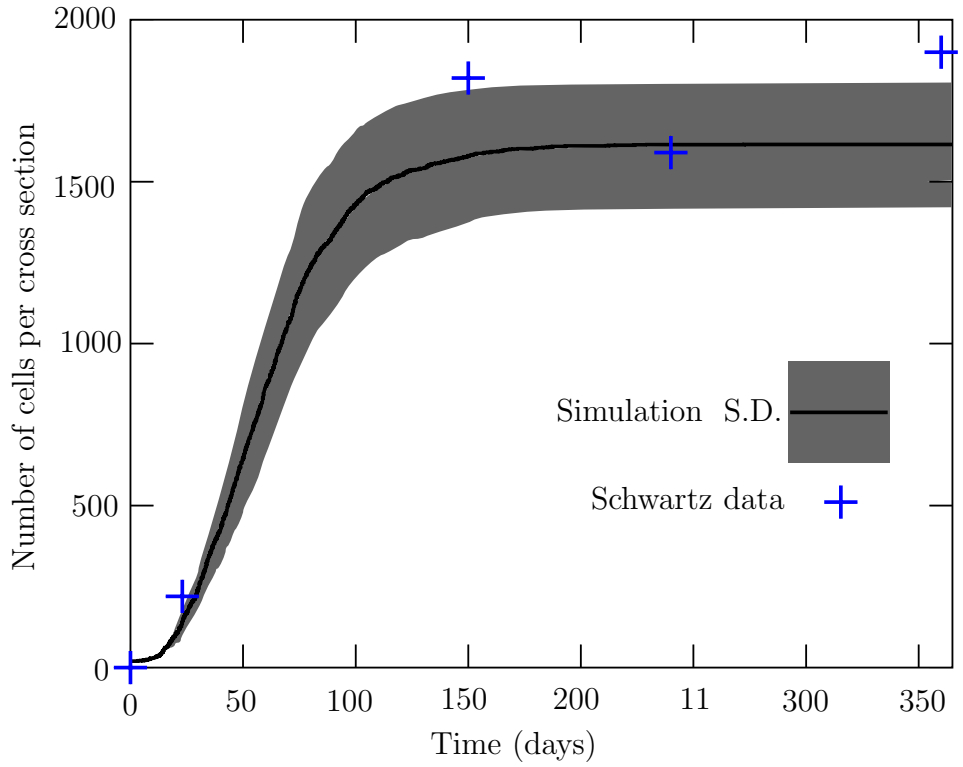

Figure 4.8: The best-fit approximation to the data of Schwartz et al. (1996), found by systematically testing variable values. The solid line indicates the average cell number over ten simulations, with the grey region indicating the variation between runs (±1 standard deviation). The experimental data (shown as crosses) indicate cell numbers calculated from human PTCA patients.

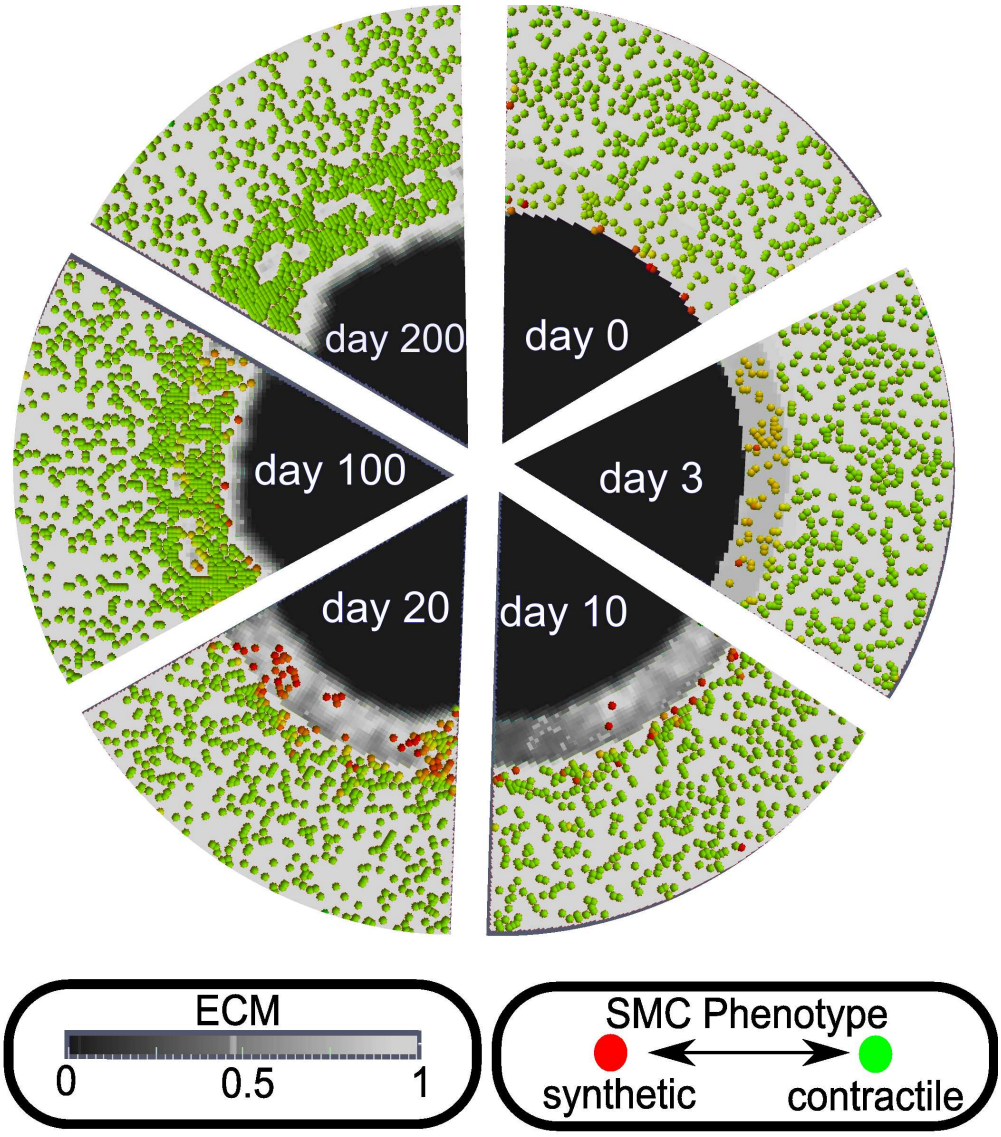

Figure 4.9: Diagrams of lattice state over time after balloon angioplasty (i.e. no stent). The background colour indicates concentration of extracellular matrix (e). The spheres indicate the positions of cells, while the colour indicates phenotype (green contractile to red synthetic). A band of injury forms at the lumen surface due to balloon expansion, from which cells proliferate and migrate into the lumen over time.

case, indicating lumen narrowing within the stent.

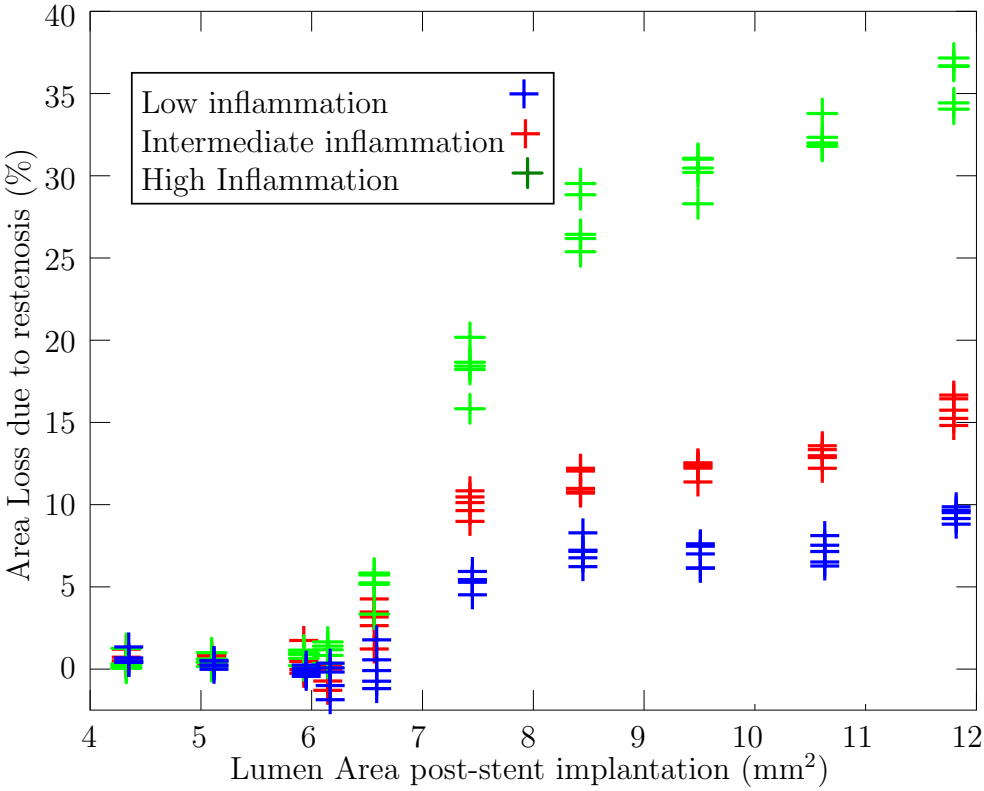

Figure 4.10: The amount of restenosis (neointimal area/initial lumen area*100%) as a function of initial lumen area (i.e. the area within the expanded stent). Five simulations were conducted at each point with variation occurring due to the stochastic cell activity model. In the high inflammation case, parameters controlling inflammation were calibrated to produce long-term inflammation, while in the low inflammation case, these were selected to produce a removal of damage within 15 days.

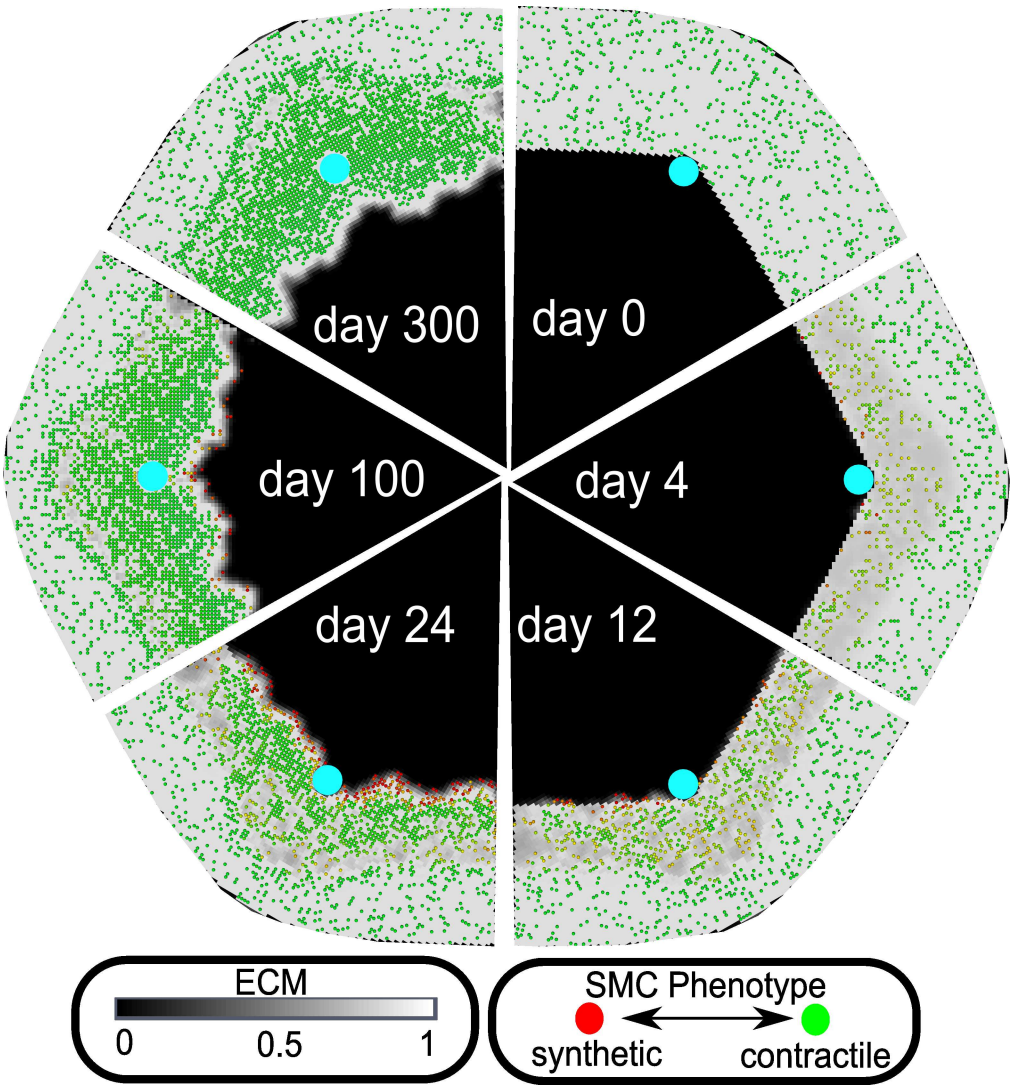

Figure 4.11: Diagrams of lattice state over time after stent expansion, showing SMC activation and proliferation leading to lesion formation and restenosis over time. The background colour indicates concentration of extracellular matrix. The spheres indicate the positions of cells, while the colour indicates phenotype (green contractile phenotype to red synthetic phenotype).

4.4 Discussion

A computational simulation methodology has been described which captures key characteristics of lesion growth within arteries subjected to non-physiological mechanical forces. It can predict outcomes with respect to how stent expansion affects the final restenosis within an artery. The model produced rapid neointima formation and cell proliferation in the first few weeks post-implantation, approaching a steady state after 6 months in an artery after balloon expansion. The model could be calibrated against the neointimal area and cell quantity data measured after PTCA. With this calibration done, the model was then applied to stenting.

In the analysis of stenting, a nonlinear relationship between lumen gain due to stenting and subsequent restenosis was predicted. In a clinical study of the effect of stent expansion on restenosis, a more linear trend was found (Farb et al., 2002). The differences between the simulation setup and the clinical environment may explain this discrepancy. In the clinical study, several stent types were used, the targeted lesions were highly variable in structure, and the individual patients may have had varying inflammation responses, all of which contribute to the high amount of variability in outcome. These sources of variability have not been included in the simulations described here. Our study was an attempt at a mechanistic model of the biological processes involved in restenosis; using as few parameters as possible, while remaining physically relevant. The simulation is made up of modular algorithms for key biological processes, which can, in principal, be independently validated.

Previous models have not accounted for cell activity explicitly; instead volume change is related phenomenologically (e.g. directly) to stress (e.g (Rachev et al., 2000)). However, the complex interactions between stress, cells and their environment is important. In other cell-based models (Caiazzo et al., 2009; Evans et al., 2008; Lally and Prendergast, 2006), the cells are represented (either as discrete bodies, or a diffusible species), but the extracellular environment is not; the behaviour of these cells is directly linked to their mechanical environment, which assumes a mechanotransduction mechanism. The importance of extracellular species (modelled here as e, g, and m) can be seen from the drugs that target them, such as anti-proliferative drugs, MMP inhibitors, extracellular matrix production inhibitors, etc. If we are to capture these processes *in silico*, the explicit modelling of extracellular species is a crucial first step. For example, an antiproliferative drug could be simulated as a substance produced at the surface of the stent, and which diffuses through the tissue. This drug could inhibit the proliferative activity of cells (adding a new term in Eqn. 4.9) in a dose-dependant way, and decay over time.

There are limitations with the present modelling approach. The FEA described here idealises the artery to a single-layered, atherosclerosis free, isotropic hyperelastic cylindrical vessel. This could be improved with better material models and patient-specific geometries (Holzapfel et al., 2002). Another limitation is that the fatigue data is based on tests performed at three test levels in the circumferential direction. More comprehensive data relating the stress/strain in the tissue to injury would allow more accurate predictions. Other damage-mechanics models may prove more suitable to

the once-off injury source which is a characteristic of balloon expansion, and perhaps also stenting. For this reason, more work is needed to define the injury and damage behaviour of vascular tissues. Another limitation is that the inflammation model is based on an assumption that inflammatory factors are produced at a rate proportional to the injury. In reality, the inflammation is brought about by several cell types, each with their own specific proliferation, metabolic and migratory behaviours. As more is known about the activities of these cells, this information can easily be incorporated by adding a new cell type/types.

The algorithms governing smooth muscle cell behaviour are rudimentary, as there are many other stimuli for SMC behaviour, such as oxygen, Nitric Oxide, heparin and many others, as well as direct mechanical signalling through stretch (Moore et al., 2001). The extracellular matrix variable currently encompasses all extracellular species which, in reality, consists of a diverse array of constituents, and each component may affect cell behaviour differently. For example laminin and fibronectin are found to have opposite effects on cell phenotype, and the ratio of these species is shown to change throughout restenosis development (Thyberg et al., 1997). In the simulations presented here, extracellular matrix was considered a variable which sought to define the conduciveness of the environment to the contractile phenotype. Similarly, the growth stimulus term could be further subdivided into diverse chemical agents, as could the matrix degrading factor variable. Biomolecular species have previously been modelled as diffusible (e.g. (Bailón-Plaza and van der Meulen, 2001), see (Murray, 2002)), which has not been considered in this study. However,

when considering that many biomolecules have short half-lives, it may not be valid to model their dispersal using diffusion. Instead, the cells dictate where biomolecules are expressed, and the region in which the molecules are present can only be changed by cell migration, phenotype modulation or cell-to-cell signalling, all of which could be simulated in the lattice-based approach.

In this paper, we have not introduced the environmental and genetic variabilities which characterise many clinical trials. Lesion and artery structure can be expected to vary in a realistic population, and often differing amounts of inflation pressure are used by surgeons. Patients may also have differing responses to the same stimuli due to genetic variability in cell processes. These effects have been considered recently for skeletal tissue mechanobiology by Khayyeri et al. (2011).

The endothelium is not considered here. In a previous paper from our group, the endothelium was modelled as a cell type which constantly proliferated over the lumen surface (Boyle et al., 2010). In reality, endothelium is also mechanoregulated (Reneman et al., 2006), and this could be incorporated into the future simulations as a mechanically-regulated source of inflammatory factors at the lumen surface. For example, the production of g and m at the surface could be dependant on the presence of endothelium, (e.g. based on a surface migration model), and on the shear stress encountered at that position. This would require calculating fluid flow-induced biophysical stimuli (wall shear stress, oscillatory shear index, etc.). A previous model of restenosis uses fluid flow induced stimuli to directly affect the proliferative behaviour of smooth muscle cells (Evans et al., 2008), and

the inclusion of this mechanism in the model proposed here may be important for accurately modelling the restenotic response of arteries. However, fluid flow-induced alterations alone cannot predict restenosis, as it leads to homeostatic equilibrium when the growth lesion produces physiological stresses. The time-course of fluid-flow induced diseases, such as vascular remodelling and atherosclerosis is also typically longer than restenosis. Finally, arterial wall stress is not updated in the simulations applied to the stent, i.e. injury is assumed to occur immediately post-stenting, and assumes chronic injury build-up does not occur.

The lattice-based approach offers advantages over other modelling techniques. The simulation is built up of separate algorithms which perform specific tasks based on biological processes. Providing the inputs to these algorithms can be controlled experimentally, these algorithms can then be validated independently (Prendergast et al., 2010). The migration algorithm, for example, requires that we know the initial concentration and phenotypes of cells. These independent algorithms are then combined to provide a cell-centred model. The algorithms, although based on simple behaviour, when coupled together have been shown to produce much of the complex behaviour found *in vivo*. Having these biological processes, i.e. proliferation, phenotype modulation, etc. allows the technique to be applied to a range of problems involving cardiovascular injury and biology (Zahedmanesh, 2011). It may be useful to simulate stents, grafts, and (with more biological rules and the inclusion of fluid flow) even initial atherosclerotic development.

This paper has demonstrated the potential of the lattice-based mod-

elling approach to the simulation of the mechanobiological response of arterial tissue. It was shown that the model captures the key phenomena of inflammation, cell activity and tissue production, and that it could be calibrated against experimental results to simulate balloon angioplasty results in humans. The inclusion of key biological process opens the way for including inherent inter-patient variability in these processes, providing a prediction of the rates of success of a stent, rather than a deterministic answer. By applying the fundamental model described here to stenting procedures in 3D, we can optimise the stenting procedure to maximise long-term lumen gain. This represents a step forward from trying to infer what growth will occur from stress analyses, and has the potential to include the bioactive properties of drug-eluting stents. In conclusion, this method may be able to examine the interactions and trade-offs between design options (stent geometric design, expansion method and pharmaceutical action) and long-term lumen gain.

Chapter 5

Application of a Mechanobiological Simulation Technique to Stents used Clinically

5.1 Introduction

Many cardiovascular diseases are characterised by the occlusion of arteries due to plaque build-up, which restricts blood flow and can lead to myocardial infarction. Restoring patency to occluded vessels through mechanical means (such as implanting a cardiovascular stent, or removing plaque) is increasingly used as a treatment for cardiovascular disease. While accurate models for simulating the mechanical response of arteries to stent implantation have been developed, these models cannot capture the long-term adaptive response of arterial tissue to biophysical stimuli. This response can lead to restenosis, which is a re-blockage of the artery due to tissue ingrowth through the stent into the lumen of the vessel. In order to optimise stent designs with respect to long-term lumen gain using pre-clinical computational tools, a mechanobiological model of arterial tissue adaptation is necessary.

Restenosis has been correlated to injury and inflammation (Kornowski et al., 1998; Gunn et al., 2002), and a paradigm of wound-healing has been adopted to explain restenosis progression (Welt and Rogers, 2002; Farb et al., 2007; Geary et al., 1998). The restenotic response begins immediately upon stent expansion, when damage is imparted on the arterial tissue. The tissue is stretched circumferentially and compressed radially beneath the stent struts (Gunn et al., 2002). Cell death and tissue tearing may occur, and the endothelium is denuded through the shearing force

of the stent and expanding balloon. These injuries induce a healing response from the arterial tissue. Inflammatory cells, such as leukocytes and monocytes, attach to the injured regions from the blood, and infiltrate the damaged tissue. Matrix degrading proteins are expressed, which enzymatically degrade the collagen and other tissue constituents. Growth stimuli are released from the degrading tissue, from the inflammatory cells, from the blood, and from apoptotic/necrotic smooth muscle cells. The degradation of extracellular matrix has the effect of stimulating a phenotype modulation in the SMCs; this means that the SMCs alter their phenotype, losing their ability to contract, becoming synthetic, proliferative and matrix synthesising.

Optimising stent designs in relation to arterial wall mechanics has been done before. Bedoya et al. (2006) and Timmins et al. (2007) optimised stent designs by minimising the volume of tissue above critical stress thresholds. This approach attempts to capture restenosis by predicting the regions where adverse biological reactions are likely to occur. However, a mechanobiological model is necessary to predict the outcome of these adverse reactions, and the link between mechanics and tissue growth response was not accounted for. Lally and Prendergast (2006) were the first to attempt a predictive model of restenosis based on the damage induced by stent expansion. In that study, a finite element model was implemented in which the accumulation of damage was assumed to induce tissue in-growth into the arterial lumen. The model could not predict stabilization of the lesion; progression eventually lead to occlusion[1]. The mechanisms of ac-

[1]This is due to the modelling technique used, which was a diffusion model in which

tion linking the damage to tissue growth was also not included; in this respect, the model's predictive power was limited. The technique was also deterministic, and could not account for the intrinsic stochastic nature of biological processes, nor the variation in patient responses to injury.

In the first study (chapter 3), a simplified model could, under specific circumstances, produce differences between stents found *in vivo*. In the previous chapter, we developed, calibrated, and tested a cell-centred, lattice-based model, which modelled the injury, inflammation and biological response of arterial tissue to stent and angioplasty induced injury. In order to test the practicability of using an injury-driven mechanobiological model as an engineering design tool, the predictions of the model must be compared to clinical trial-based tests. Hoffmann et al. (2001) gave a detailed study of the clinical performance of three different stent designs, which included information on the stent types, and detailed data on the outcomes of these stents in terms of the neointimal areas produced (see Fig. 2.3 on page 19). Kastrati et al. (2001) also analysed clinical data for the same stent types, and ranked their performance based on a multivariate analysis of restenosis predictors. This was done by analysing a large number of patient statistics (grouped into clinical-, lesion-, and procedure-related variables). Any variables that were statistically significantly different between 'restenosis' and 'no restenosis' groups were used in a logistic regression model. This showed the MultiLink to perform better than the Palmaz-Schatz and the NIR, with no statistically significant difference between the Palmaz-Schatz and NIR.

the tissue boundary grew as a diffusible species entered new finite elements

In this study, we sought to test the hypothesis that mechanical injury stimulates restenosis, and specifically to test whether a model driven by injury, as developed and calibrated previously, could predict the long-term outcomes of stent design. We applied the simulation technique in 3D to three stents similar in design to the ones studied *in vivo* by Hoffmann et al. (2001), in an idealised analogue of the clinical situation. If the hypothesis is further corroborated, and the model can predict reasonable results, this methodology could be applied to future device design and treatment options. It may also prove useful in identifying patients who may be susceptible to restenosis with a given device design, allowing the patient-specific and lesion specific matching of stents or other treatment options.

5.2 Methods

The simulation technique used in this study was described in Chapter 4. The technique was adapted to 3D, and applied to three different stent designs. The artery was modelled as a cylindrical vessel, with isotropic, hyperelastic material properties and inner and outer radii of 1 mm and 2 mm respectively. A Mooney-Rivlin formulation was used and calibrated to the data of Lally et al. (2005), who measured the stretch response of porcine coronary artery to uniaxial tensile stress (Lally et al., 2005). The injury in the arterial tissue was calculated using the von Mises stress criterion and a remaining life approach, in which the damage is related to the number of cycles undertaken during a loading period versus the number of

cycles to failure from fatigue test. The inflammatory response was modelled as two variables: a matrix degrading factor (MDF), and a growth factor (G). Extracellular matrix (ECM) was explicitly modelled as a variable with a value from zero to one. The MDF simulates the removal of extracellular matrix within the injured region, and the growth stimulus controls the proliferation of SMCs. The production of MDF is assumed to be linearly related to the amount of injury present, and the MDF reacts with the ECM in a 1st order reaction depending on the amount of MDF present (see section 4.2.2). These variables are modelled on a regular orthogonal lattice, which also holds the SMCs. The phenotype of SMCs is assumed to be linearly related to the amount of ECM present in the region, with high ECM inducing a contractile phenotype. This phenotype governs the maximum proliferation and migration rates within the tissue. The actual probability of proliferation of a cell is dependent on the availability of suitable neighbour sites, and the amount of growth stimulus in the region. The growth stimulus decays exponentially over time.

Due to the size of the artery and the average size of SMCs used in the previous study, a coarse-graining approach was necessary in the 3D case, in order to achieve a practical solution time. The lattice used had a characteristic length (point spacing) of 0.05 mm, compared to 0.01825 mm in the previous model presented in Chapter 4. In this way, a scaling-up of the lattice was performed, whereby each lattice cell represented several biological cells, in a mesoscopic representation of the cells. The lattice cells remain independent random walking cells, and all parameters are conserved from the 2D model, but are scaled accordingly. In particular,

the migration rate of the cells is related to lattice spacing, as is the initial amount of lattice cells present[2].

5.2.1 Stent Geometries

Three stent types were modelled: an open cell-type design (similar to the commercially available MultiLink stent), a closed cell, corrugated ring-type design (similar to the NIR stent), and a slotted-tube design (similar to the Palmaz stent) (Fig. 5.1). These designs represent diverse stent geometries, and cover the three stent types studied by Hoffmann et al. (2001). The full stent can be described as a series or repeating rings, joined along the axial direction of the stent. In the open cell design (from here on described as MultiLink, or ML), neighbouring rings are only connected at every second crown, while for the closed cell design (from here on described as the NIR), each crown is connected, meaning a smaller unscaffolded region. The slotted tube design (from here on described as the Palmaz-Schatz, or PS) is made by cutting slots in a metallic tube. Each of the stent designs were produced by drawing the print of the stent in AutoCAD to produce a 2D sketch of the flattened stent inner surface. This was then imported into ABAQUS and meshed, and nodal coordinates were extracted. These coordinates were then manipulated from planar, Cartesian representation to a cylindrical geometry of the inner stent surface, at which time the model was re-imported into ABAQUS, and coincident points at the surface join were merged. The surface was then extruded in the radial direction to

[2] $v_{\mathrm{SMC,lattice}} = v_{\mathrm{SMC}} \cdot \Delta t / \Delta x$ lattice points per increment. For cell numbers, the fraction of occupied lattice points is kept constant.

produce the 3D stent. In this way, the stents had a quasi-rectangular cross section (consisting of two arcs from the inner and outer cylinders, and two straight radial lines). The material model used for the stent was an elasto-plastic model (see sec. 3.2.1). Each stent was expanded to a balloon:artery ratio of 1.2. Finite element simulations were solved with ABAQUS/Explicit, using a quasi-static analysis.

The simulations were performed on each of the three stents using parameters calibrated to high, low and intermediate inflammatory responses to injury. Each stent/inflammation combination was simulated with three replicates, producing 27 simulation runs overall.

To generate results, the cross-sectional area of lumen and neointima was measured at several axial sections along the axis of the artery. The total number of cells, and total volume of tissue was recorded during the simulation.

The simulations were implemented using the MechanoBiology ToolKit (MBTK), which is a library built upon VTK (the Visualization ToolKit) to produce mechanobiological models using lattice-based methods (Lennon et al., 2011).

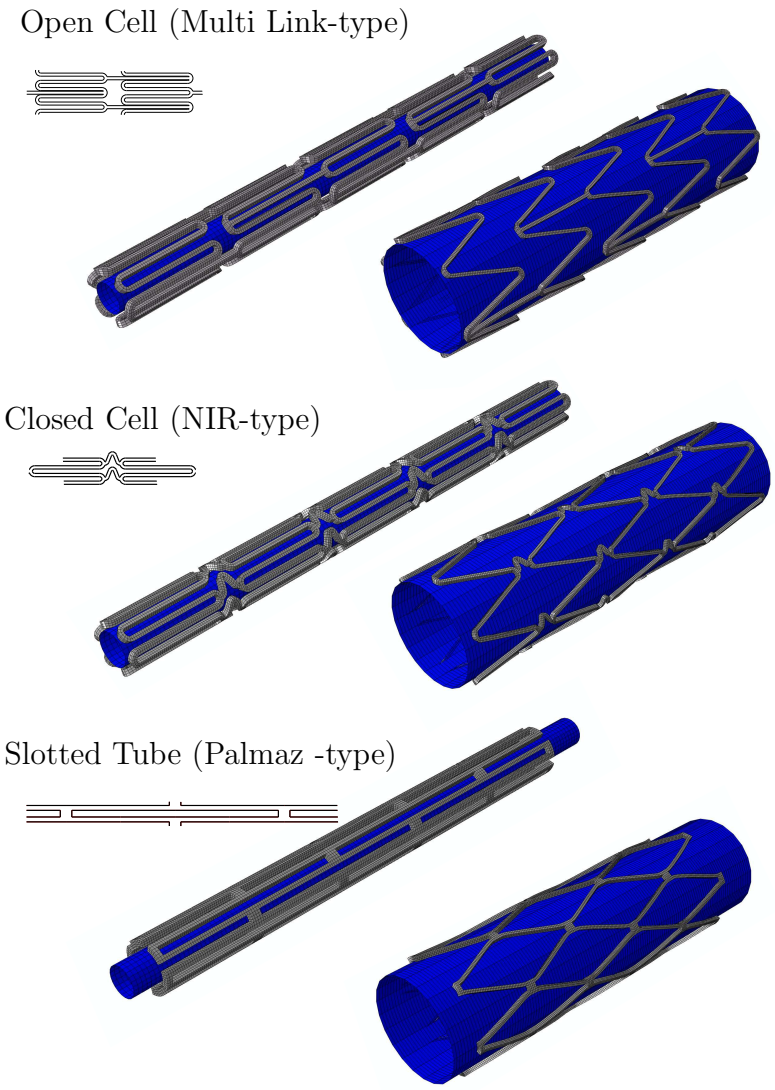

Figure 5.1: The three stents simulated. Each stent shows the unexpanded configuration and the stent at maximum expansion, as well as a 2D representation of the unexpanded stent cells.

5.3 Results

The finite element analysis showed that the NIR induced the highest peak von Mises stresses (4.00 MPa), followed by the PS (3.86 MPa) and the ML

(3.29 MPa), however, these differences are relatively small. Stresses were highest around the stent struts, and the highest of these were at stent crowns (Fig. 5.2). With the MultiLink, the highest stresses were induced at the stent ends.

The injury induced at 80% expansion shows a greater amount of injury present in the PS and NIR stents compared to the ML (Fig. 5.3), which persists at full expansion (Fig. 5.4). Peak stresses upon removal of the balloon and stent recoil were 1.30 MPa for the NIR stent, 0.33 MPa for the PS stent, and 0.30 MPa for the ML stent.

The simulation produced a large amount of restenosis in the three stents (Fig. 5.5). A gradual production of restenosis is predicted within the stent area, eventually covering the stent, and reducing lumen area (Fig. 5.6). The simulation predicts a gradual reduction in the amount of active cells in the neointimal area, and predicts a relatively acellular final neointimal area, whereas in the media and deep neointima, cells accumulated. Cell numbers in the model at the end-point of the simulations were higher for the NIR than the PS, and both were higher than the ML stent (Fig. 5.12).

The neointimal areas in the ML stent produced lower restenosis rates when simulation runs were analysed (Fig. 5.10); there was little difference found along the length of the stent between the PS and the NIR. The extent of the differences between stents was dependant on the inflammation present (Figs. 5.7, 5.8 and 5.9), with differences more pronounced in the low inflammation case. The lumen geometry (combining elastic recoil and restenosis) at the end point was substantially different between stents (Fig. 5.11).

The volume of tissue above several von Mises stress thresholds was calculated for each stent. The differences between stents was then evaluated as the ratio of tissue above the threshold for each stent (Fig. 5.12). For each stress criterion used, the PS and NIR stents achieved similar results (with the greatest difference occurring when the damage limit (1.417 MPa) was used). The difference between these two stents and the ML stent depended on the level of the stress criterion used, with the differences greater for higher stress thresholds (Fig. 5.12).

The neointimal volume within the stents depended on the level of inflammation (Fig. 5.13), with low and intermediate responses producing a higher growth rate at early time points than the high response. The final amount of restenosis was inversely related to the initial speed of lesion growth, and directly related to inflammation level. This data also shows that the rate at which quiescence (a low growth rate) was achieved was inflammation dependent; the ML, for example, becomes quiescent for low inflammation at approximately 150 days (Fig. 5.14). The predictions of the relative efficacies between stents were different depending on the amount of inflammation (Fig. 5.14). The relative efficacy, measured as the ratio of the numbers of cells produced between stents, showed that the relationship between stents altered over time, and was related to the inflammation level (Fig. 5.15). The inflammation level affected the relative performance between each of the stents, except for the relative performance between the PS and NIR, which converged to the same value (Fig. 5.15).

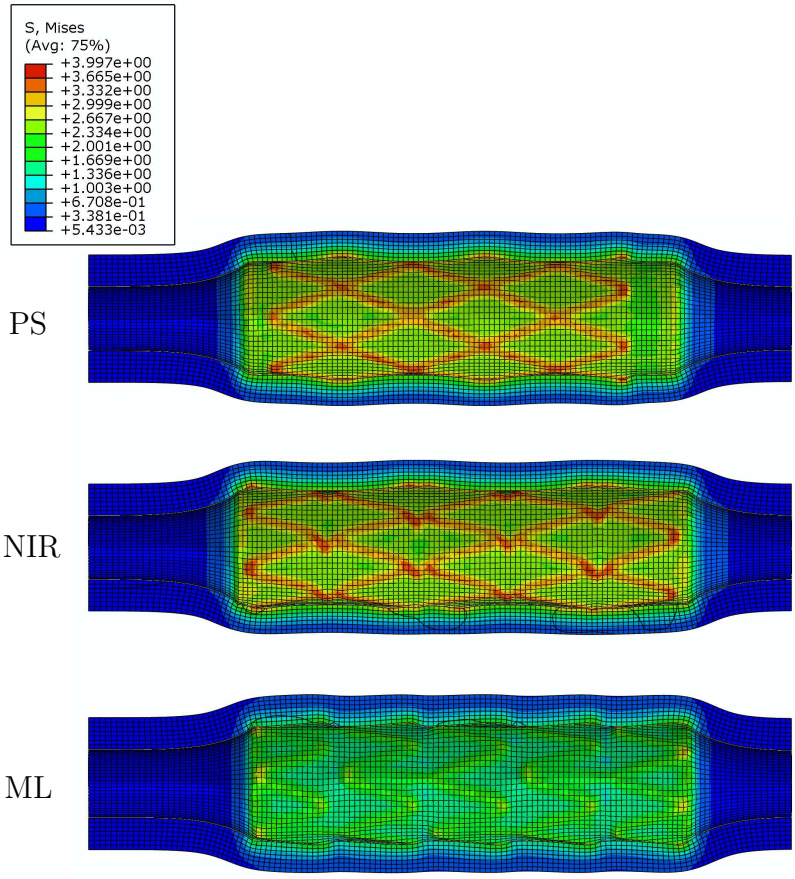

Figure 5.2: Contour plots of von Mises stress (in MPa) in the arterial tissue at maximum expansion for the three stent types.

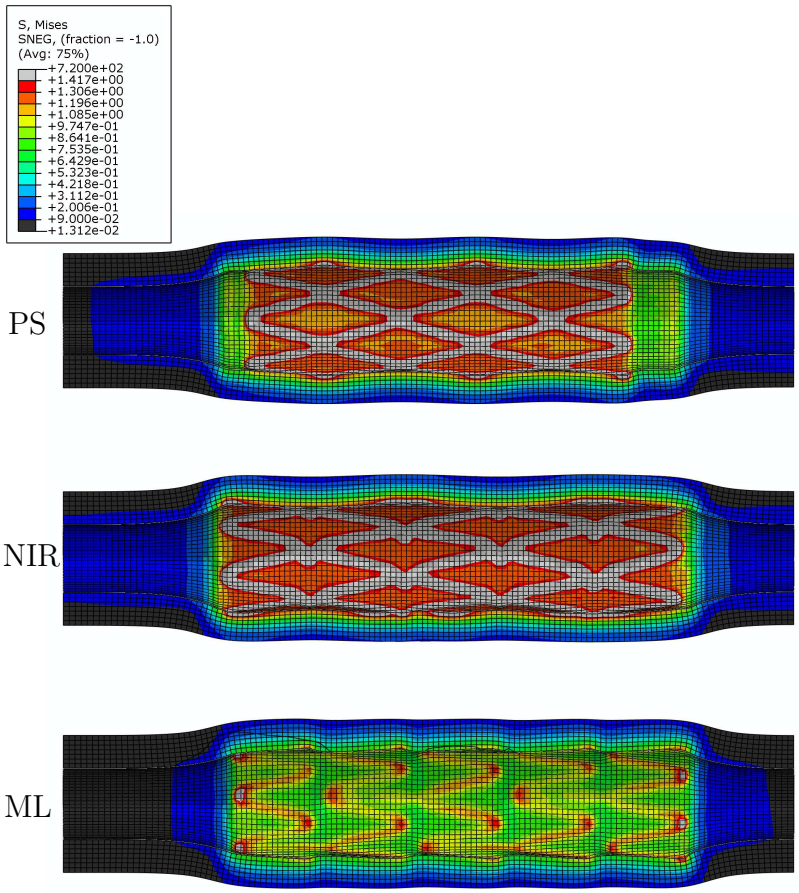

Figure 5.3: Contour plot of von Mises stress (in MPa) at 80 % expansion indicating the areas above the maximum injury, i.e. greater than failure strength (1.417 MPa) in light grey. The dark grey regions indicate regions of tissue below the fatigue strength of the tissue (0.09 MPa).

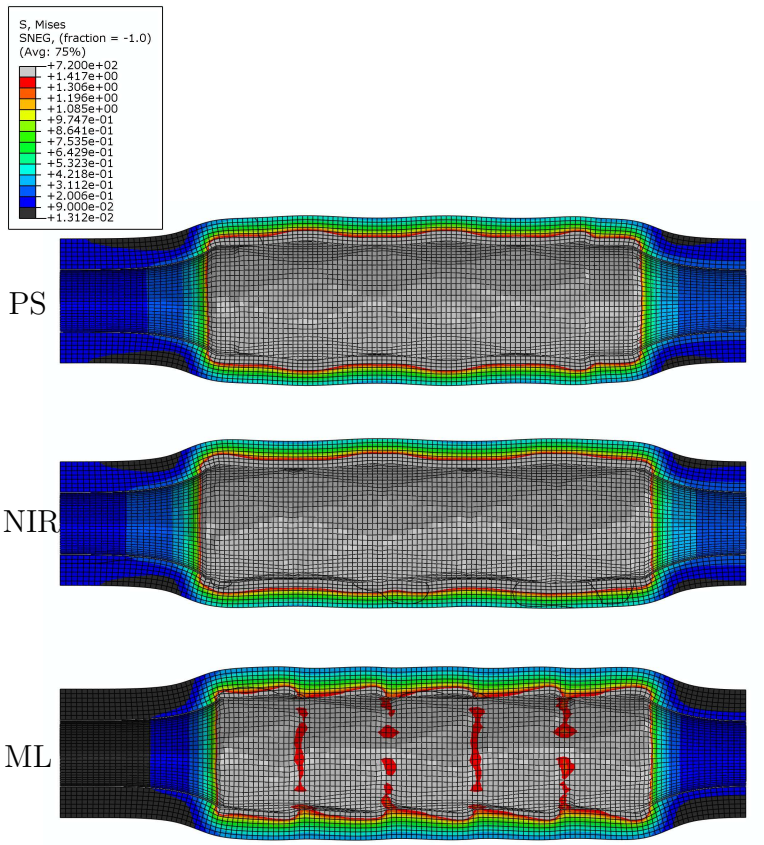

Figure 5.4: Contour plot of von Mises stress (in MPa) at full expansion indicating the areas above the maximum injury, i.e. greater than failure strength (the value at which number of cycles to failure is predicted to be one, i.e. 1.417MPa) in light grey. The dark grey regions indicate regions of tissue below the fatigue strength of the tissue (0.09MPa).

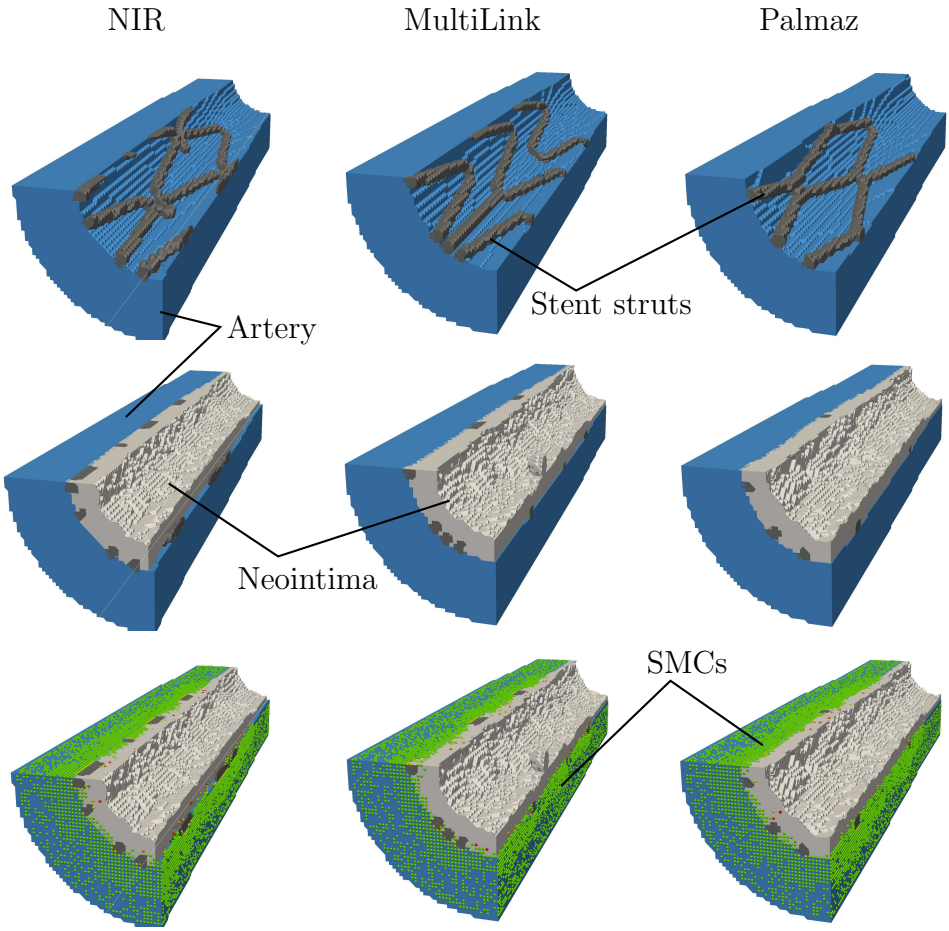

Figure 5.5: A plot of the lattice models showing 1/8 of the full model. Above, the lattice representation of the artery and stent immediately post-stenting. Centre, showing the neointimal volume superimposed on the original geometry. Bottom, the lattice with SMCs at the end point of the simulation.

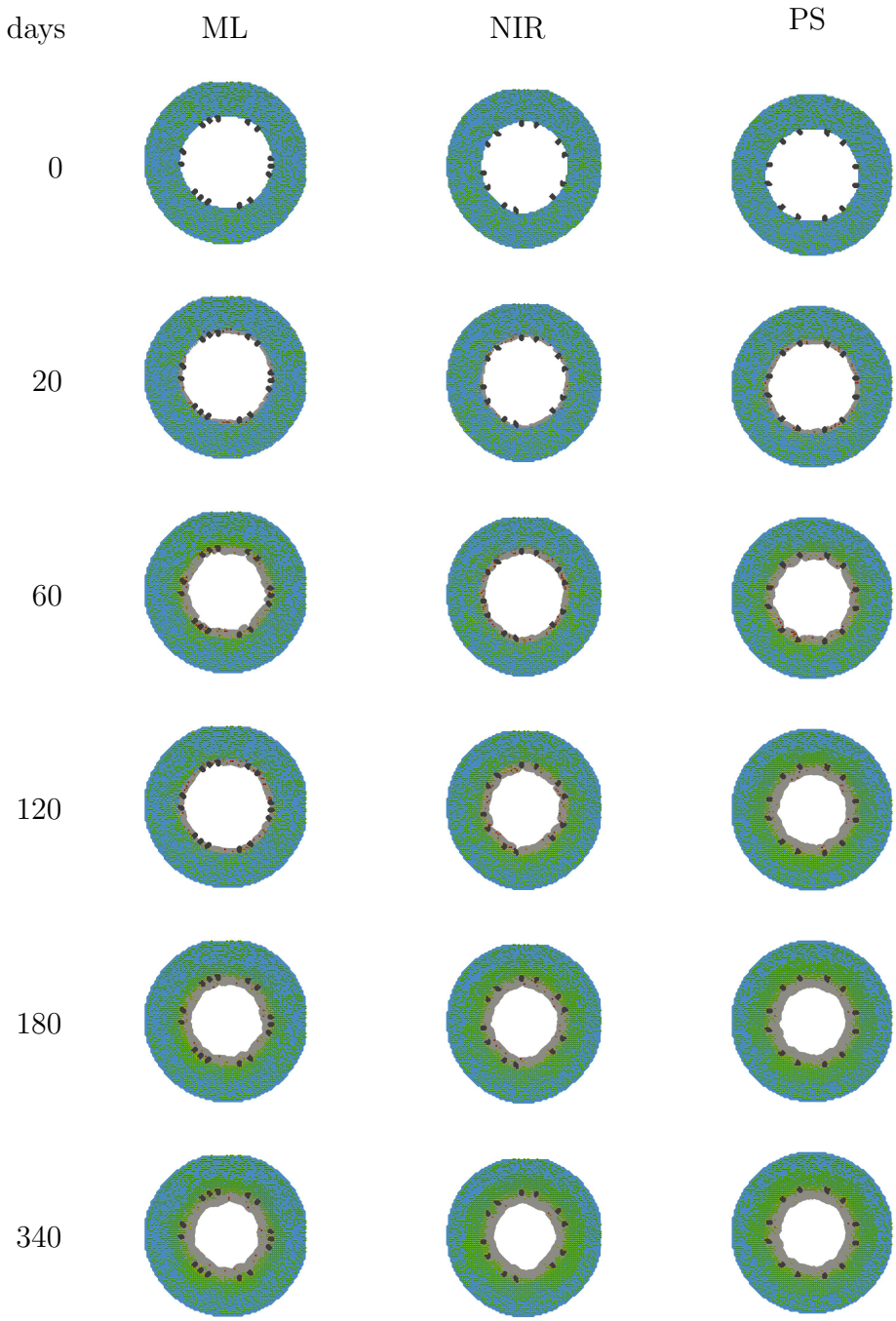

Figure 5.6: Simluation plot of the lattice over time in the simulation of all stents, a section of a z-normal plane at the midsection of the stent. This plot shows the distribution and phenotype of cells. Neointima is in grey.

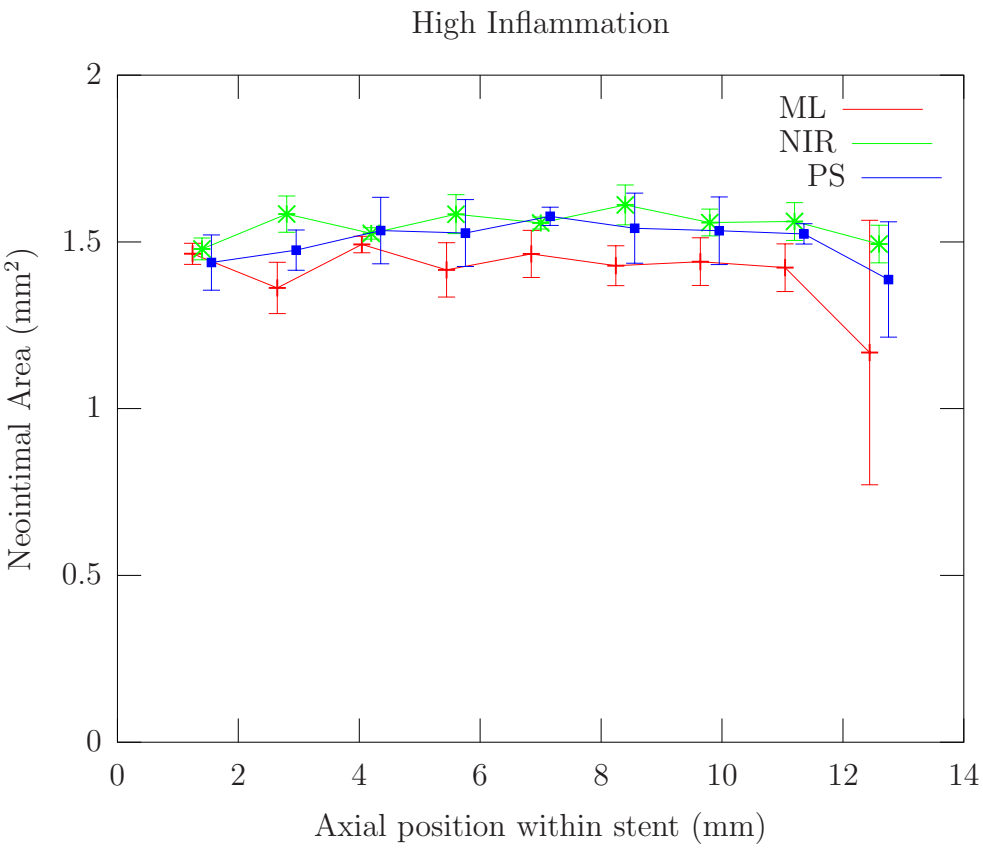

Figure 5.7: The cross sectional area of restenosis within the stents along the axial direction. This figure is for the high inflammation case.

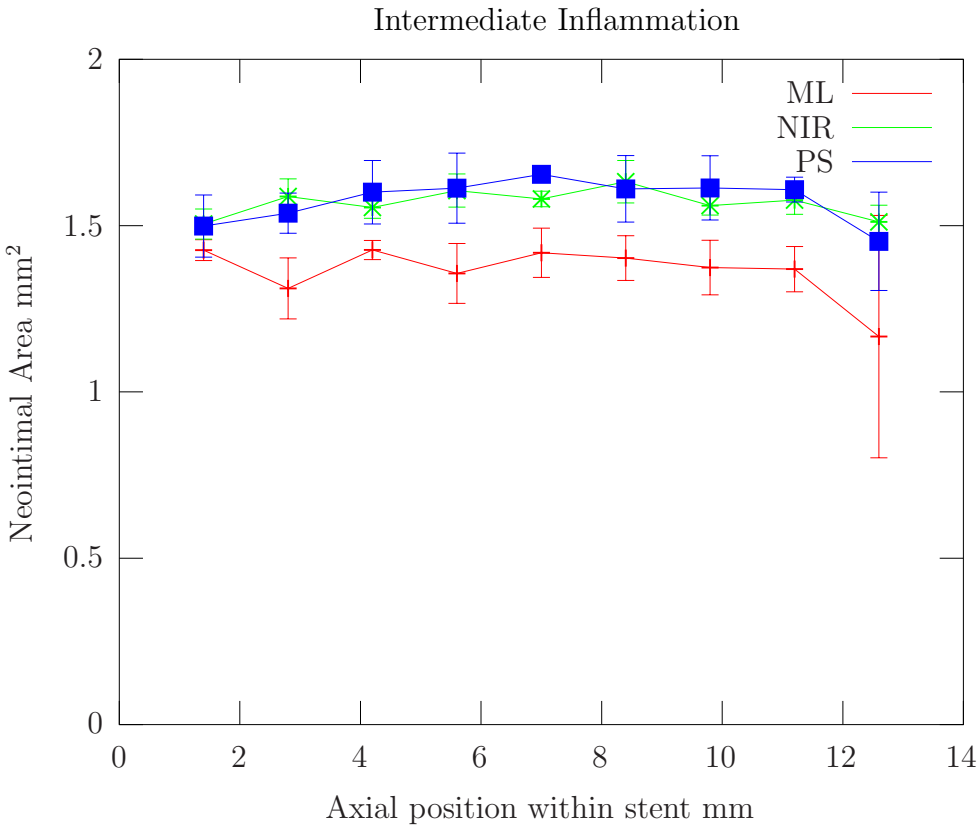

Figure 5.8: The cross sectional area of restenosis within the stents along the axial direction. This figure is for the intermediate inflammation case.

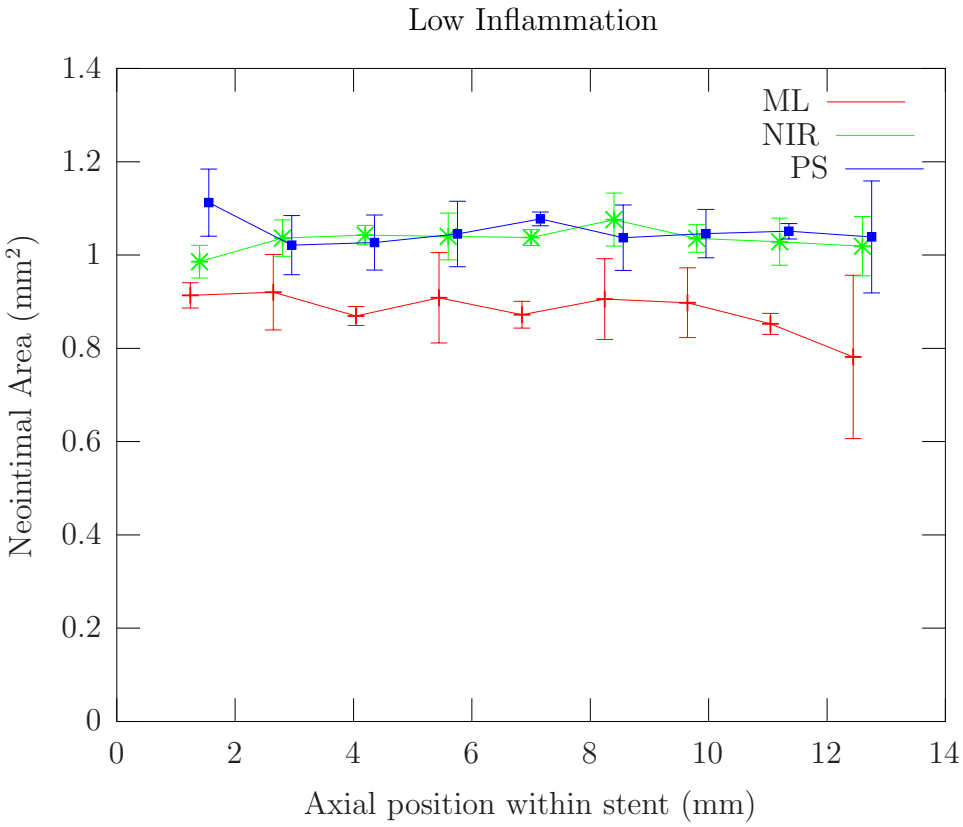

Figure 5.9: The cross sectional area of restenosis within the stents along the axial direction. This figure is for the low inflammation case.

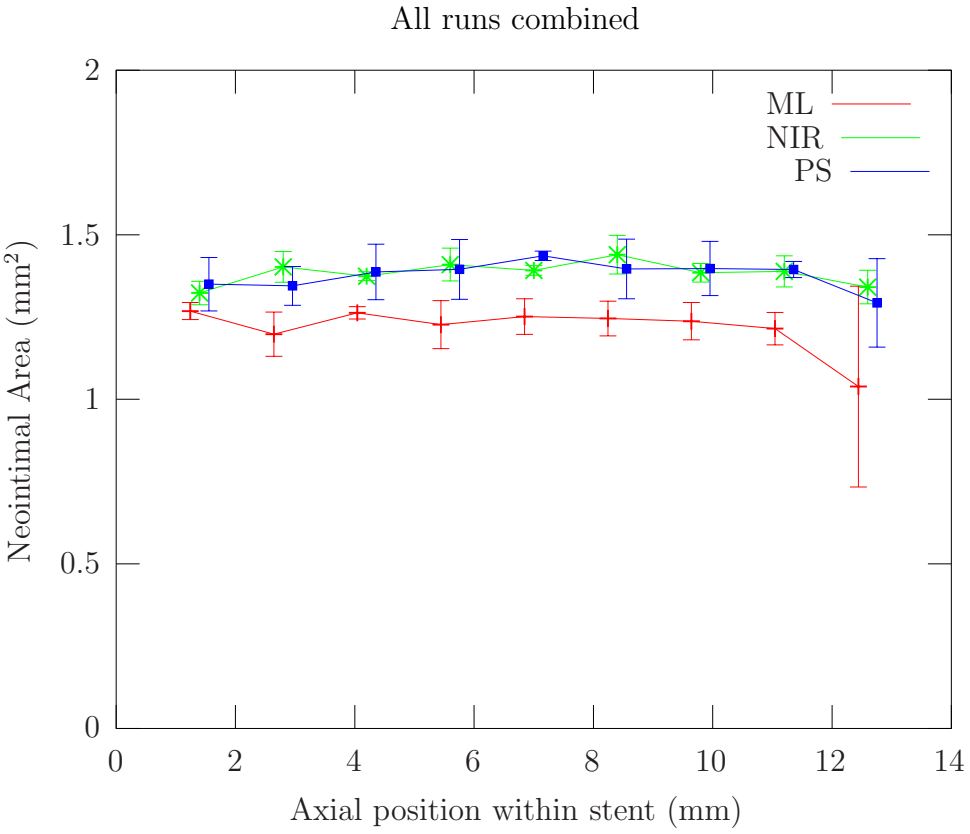

Figure 5.10: The cross sectional area of restenosis within the stents along the axial direction. This diagram combines all data from high, low and intermediate inflammation for each stent.

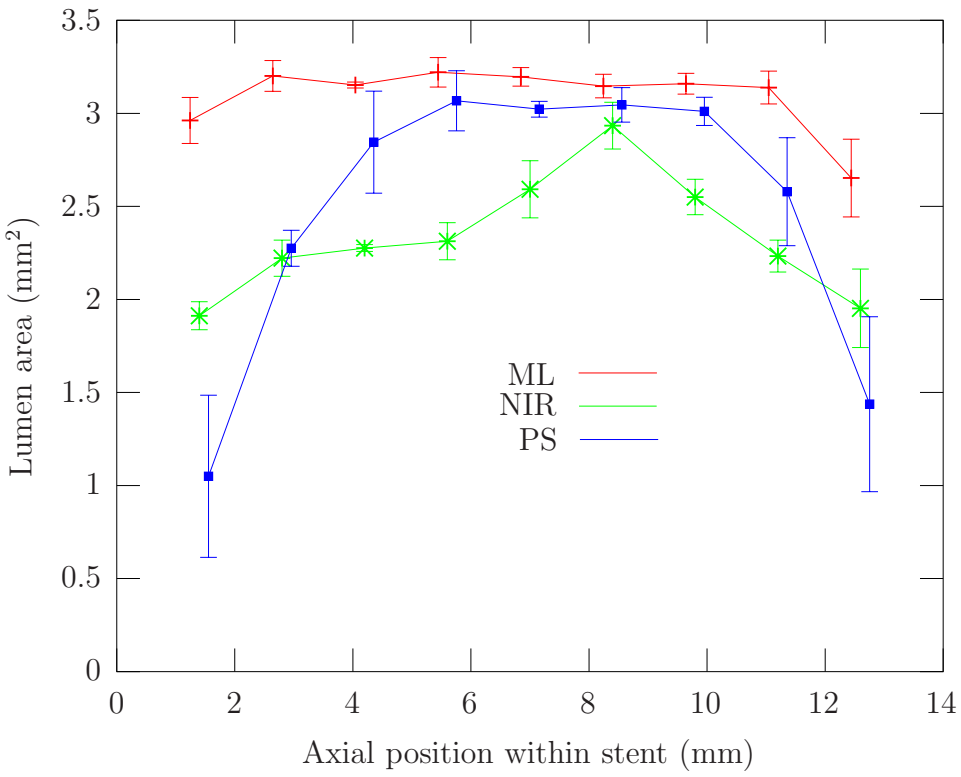

Figure 5.11: The lumen cross sectional area at the end of the simluations for each stent, with all data from each inflammation level included.

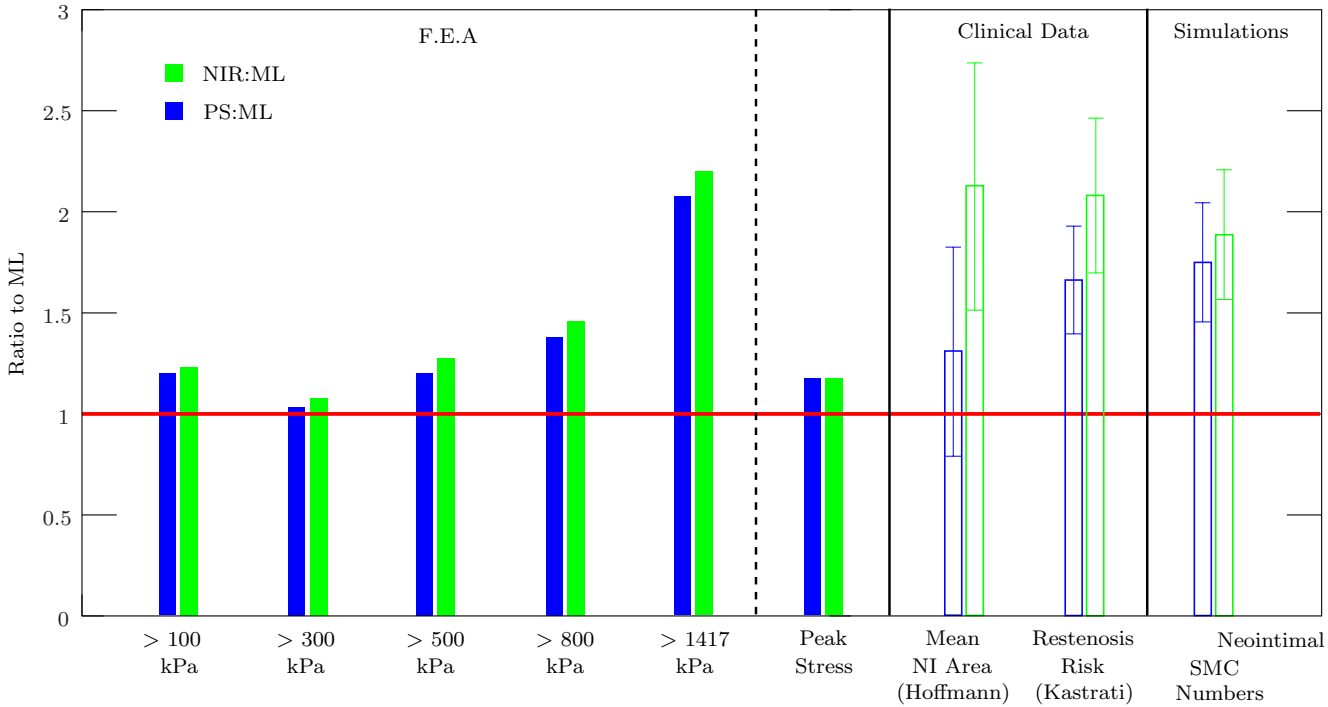

Figure 5.12: The relative performance of the three stents based on several different criteria. The PS and NIR stents are given as ratios to the best performing (ML) stent. The first five are the volume of arterial tissue above a critical stress. The sixth criterion is the peak stress induced in the artery. The seventh criterion is the mean neointimal area measured by Hoffmann et al. (2001), including standard deviation. The eighth criterion is the risk of restenosis, judged through multivariate analysis of binary restenosis rates (Kastrati et al., 2001). The final criterion is based on the numbers of cells in the neointima measured in the simulations for all inflammation levels. Error bars are ± 1 S.D.

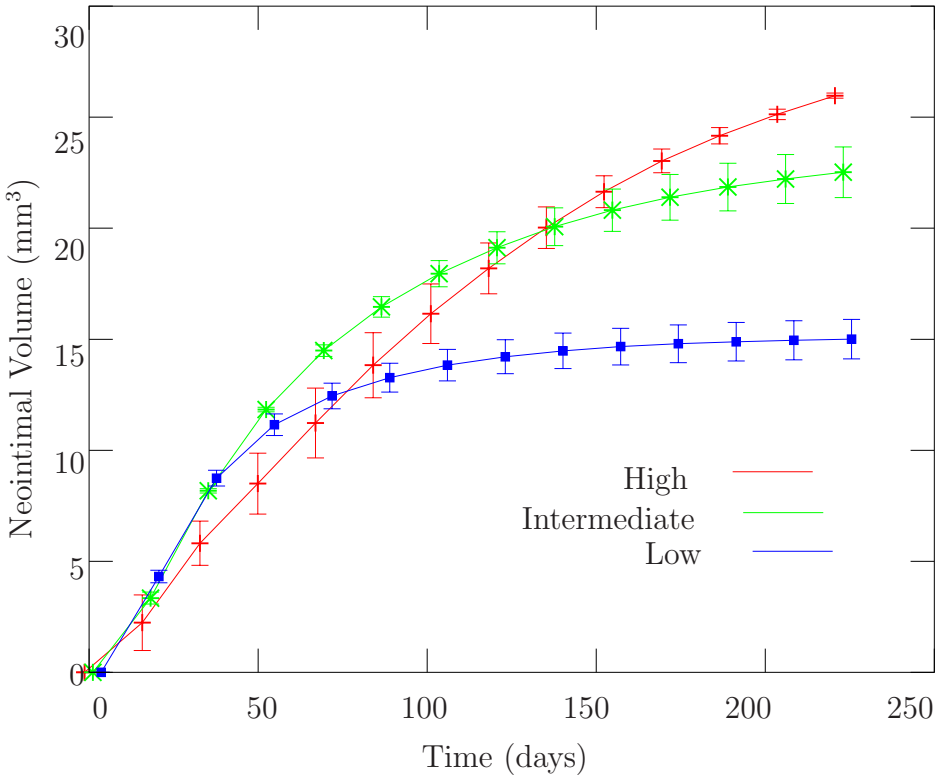

Figure 5.13: Volume of neointima within the MultiLink stent over time for the three inflammation rates. Similar trends were found for the Palmaz and NIR stents (not shown).

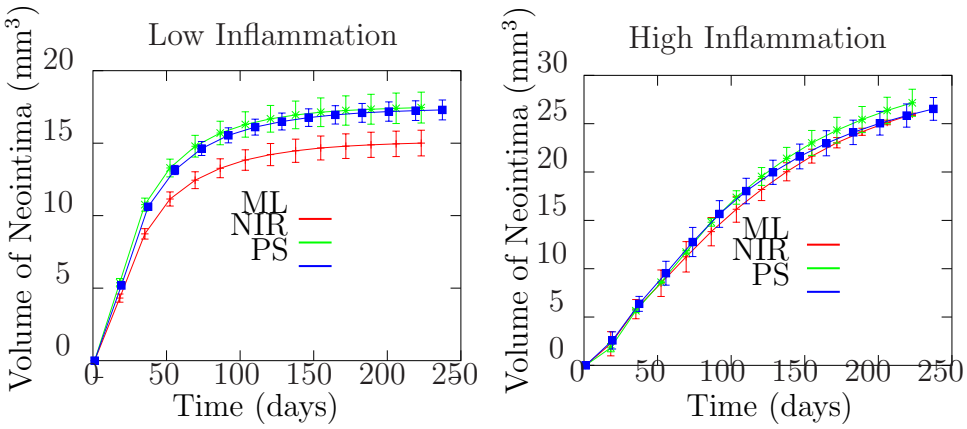

Figure 5.14: Volume of neointima within the three stents over time for both the low and high inflammation states.

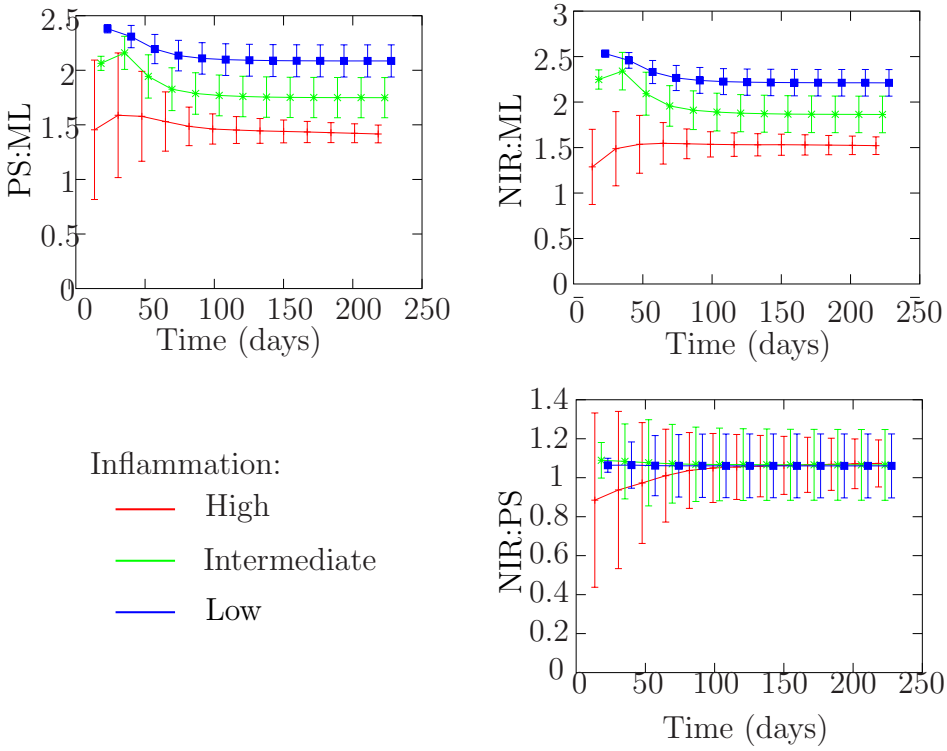

Figure 5.15: A plot of the ratio of the amounts of neointimal cells between the three stents. The numbers of neointimal SMCs in the model was calculated for each stent. The ratio of the numbers of cells produced between stents is plotted here for each of the stent combinations. A value of 1 indicated no difference between the stents.

5.4 Discussion

The hypothesis that vessel wall stress stimulates restenosis growth in stents through injury was tested using a computational mechanobiological model for the injury response. The technique predicted the same ranking of stents as two clinical studies (Hoffmann et al., 2001; Kastrati et al., 2001), with the open-cell, MultiLink-type stent outperforming the slotted-tube, Palmaz-type stent, which outperformed the closed-cell, NIR-type stent in terms of neointimal area (on average). The simulations predicted less of difference between the PS and NIR stent than between the ML and PS stent, in terms of both tissue volume/area and cell numbers. The magnitude of the differences between the stent designs was greater when considering cell numbers, and closely matched the spread of data of the clinical trial (Fig. 5.12).

The clinical study of Hoffmann et al. (2001) showed large variations in the neointima formed in the stents, so much so that a statistically significant difference in neointimal area along the axis of the stent was not obtained between the stents. This variability may come from the inherent variability between patients in terms of lesion size, biological response, procedural variability, etc., which were not included here. The simulations described here showed a similar trend to the clinical studies when the stents are compared using cell numbers produced (Fig. 5.12). However, the differences between the NIR and PS in the model was not as pronounced as between the InFlow and the PS in the Hoffmann study. The InFlow stent is similar to the NIR, but has a more complex geometry, which was not

accounted for in this study. The model described here may not account for some of the differences between stent designs. In particular, many corrugated ring stents can have a more rounded cross-section strut, while the Palmaz slotted tube stent is rectangular. This may have an important part to play in cell migration around the stent. The number of crowns in the stents was constant for all three stents modelled here, but this may not be the case for the stent designs considered.

Our simplified model in Chapter 3 predicted a large difference between the four and six crown stents, while this study shows a less pronounced difference when crown configurations are the same. The expansion ratio may have a large effect on predictions, as the injury pattern produced at 80 % expansion looked significantly different between stents (Figs. 5.3 and 5.4). The differences between the stents may be more pronounced when considering patient-specific, complex lesion geometries and material properties, differences which may not show up in the straight, idealised artery model used here. The relatively small differences in neointima predicted between stents may, however, be close to the clinical reality, as several papers on the relative performance have pointed out that significant differences between current stent designs have been difficult to identify (Edelman and Rogers, 1999; Windecker and Meier, 2001).

The study described here did not include some important characteristics of stent implantations in clinical practice. There was no variability in the geometry or material properties of the host vessel, which was idealised, isotropic and homogeneous. This is important for gaining an accurate prediction of injury, but also to be able to predict the initial biological

configuration of the artery. For example, the plaques of most arteries can have a-cellular regions, or regions with foam cells, and not SMCs. The distribution of SMCs was assumed to be constant in the arteries. The stent geometries and expansion methods could be adapted to be more realistic.

This study demonstrates the use of computational simulation techniques to predict the mechanobiological reaction of arteries to stent implantation. It offers a pre-clinical technique capable of including the patient's restenotic reaction to stenting, and offers scope for including inter-patient variability in the reaction to injury. The technique could be adapted, with more complex mechanical models, to patient-specific lesions.

Chapter 6

Discussion

A computational model of neointima formation based on injury was capable of predicting many of the important characteristics of restenosis formation after stent implantation. It predicted non-linear lesion growth with time, a dependency on the number of stent struts, and on stent expansion diameter. This work corroborates the hypothesis that injury is a major factor in restenosis development, and can be used to predict differences between stents. The model was calibrated to experimental findings,

and was applied to both angioplasty and stent implantation. The model could differentiate between stent designs and was corroborated with clinical performance data.

Inflammation was shown to have a large effect on the model predictions, and the hypothesis that the level of the inflammatory response affects the correlation between injury and restenosis was corroborated. This suggests that current stent design performance relative to other stent designs may be dependant on the inflammation response intensity.

6.1 The Stimulus for Restenosis

The amount of vessel wall stress has been linked in this thesis to tissue growth using the hypothesis that injury stimulates neointimal formation through inflammation induction. In contrast, it has also been hypothesised that mechanical stimuli imparted on the vessel wall may directly regulate SMC behaviour, and that stent-induced neointima is a functional response of the artery to restore homeostatic mechanical stimuli[1] (Glagov et al., 1993; Glagov, 1994). Rachev et al. (2000) later used this hypothesis as a basis for their mathematical model. A similar distinction can be seen in skeletal tissue, whereby bone can adapt to a mechanical stimulus by remodelling its internal structure over time (Huiskes et al., 1987). However, when a fracture occurs, callus growth and differentiation becomes the more dominant phenomenon (Frost, 1989). Experimental studies have shown that the vessel wall remodels in response to changes in blood pressure (Zhuang

[1]This is in the category of remodelling in response to mechanical load, as opposed to modelling, where new tissue is laid down.

et al., 1998). However, the tissue alters in a long-term, controlled, and remodelling-type process, where the structure of the vessel wall remains organised (Glagov, 1994). In comparison, the pathobiology of restenosis is far more analogous to wound healing (Forrester et al., 1991; Geary et al., 1998). Neointima, a structurally distinct layer from the media, is produced, rather than increasing medial layer thickness.

Fluid flow generated wall shear stress has been suggested as a key mediator in restenosis development, with neointima being a tissue response to un-physiological wall shear stress (see, for example Wentzel et al. (2003)). This hypothesis was tested by Caiazzo et al. (2009, 2011), using a computational model in which SMC proliferation was limited by high wall shear stress. They found that the restenosis growth arrested when the wall shear stress reached the prescribed homeostatic value. Such a directly regulated lesion would not be a danger, unless the fluid flow homeostatic stimulus changed to some un-physiological value. This means that such phenomenological linking between fluid flow and tissue growth provides little predictive power, unless the nature of the changes in the homeostatic stimulus value is understood. If a more mechanistic modelling approach were used, the endothelium could be studied and included as an interacting component of the artery, alongside the injury model described here.

6.2 Limitations

The injury prediction relies on the accuracy of the finite element model. The models used in this thesis assumed the arterial tissue to behave as

an isotropic, hyperelastic, homogeneous cylinder. While this provided a first approximation for injury distribution within the stent, much work has been done in the research community on refining the accuracy of stent implantation models. In particular, the modelling of the anisotropic artery layers and plaque would improve the stress calculations. This complexity would require a further understanding of the injury/damage behaviour of these materials.

Injury was predicted using a compressive stress threshold (chapter 3), and a remaining-life damage mechanics model (chapter 4). This prediction could be improved by accumulating more data on the compressive thresholds and damage accumulation within arterial tissue. Other injury prediction models may provide a more accurate prediction, such as a model to predict tissue rupture, or low-cycle fatigue models.

In the studies performed as part of this thesis, two data sets for arterial tissue were used. In the first study (chapter 3), the artery was modelled based on the material properties of human arterial tissue, combined with a compressive stress threshold from rat skeletal muscle. While this enabled an estimation of the amount of cell death - and hence injury - it could not capture mechanical tissue damage, or a continuous damage distribution in the artery. Study 2 (chapter 4) improved upon this model by using a damage-mechanics approach based on data for porcine coronary artery tissue. While, ideally, both the damage accumulation data and the tissue properties would be from humans (and layer-specific), no human damage accumulation data is currently available. Instead, the porcine damage accumulation data was used in conjunction with porcine arterial tissue

data. Due to the higher stiffness of human tissue, combining this model with porcine damage data would lead to much higher injury in the arteries, and further reduce the differences between stents. While both of these studies provided reasonable estimates of injury in the artery, more accurate models may be needed to further refine the predictions.

Inflammation was modelled in this thesis using phenomenological models; in chapter 3, as an initial amount of inflammation (MDF_{init} and G_{init}), and in the other sections as a set of ordinary differential equations. This allowed the study of the effects that varying the inflammatory response had on restenosis. In future, the inflammation step could be reimplemented with a more mechanistic model, by introducing new cell types and algorithms based on inflammatory cells. This may allow the use of data on inflammatory cells to inform the model.

While the lattice model already produces much complex behaviour at the tissue level, many aspects of the arterial wall system have not been included. The relationships that were modelled were selected based on the experimental literature, and could be expanded. The direct mechanoregulation of SMCs and the organisation of tissue into anisotropic layers may become important if simulations are run over longer time periods. The environmental variables (ECM, MDF and G) are generic species which represent many diverse components of the arterial system. As more quantitative information on these components becomes available, it could be integrated into the framework described here.

6.3 Role of Inflammation in Restenosis Development

In this thesis, the inflammation response to injury was explicitly included in the simulation of restenosis; in the first study, through the initial amounts of matrix degrading factor and growth stimulus and, in the other studies, as a set of ordinary differential equations. The amount of inflammation response was simulated as a phenomenological set of variables adapted to some experimental findings. Even with this phenomenological model, interesting relationships were found. The duration and intensity of the inflammatory response to injury was shown to have an effect on the amount of restenosis, which agrees with the correlation found *in vivo* (Cipollone et al., 2001). The results from the first study (Chapter 3) showed that the differences in restenosis between stents was affected by the level of inflammation. If this finding is corroborated *in vivo*, we may need to know the inflammatory phenotype of the patient in order to accurately predict stent relative efficacies. This result could help explain why results found in animal models, which could be assumed to have a lower inflammation response than aged patients, do not often translate to the clinic (Johnson et al., 1999). If this is the case, and if inflammation varies within a population, it suggests a role for screening for inflammatory phenotype before implantation. It may also pave the way for population-based pre-clinical trials *in silico*. Instead of a deterministic comparison of stent designs based on mechanical and geometric analyses, a randomly varying population could be simulated to predict the end point of the clinical trial.

This could show which stents behave better in a random population, or help with the design of patient-specific stents, as well as identifying at-risk patients who may not be suitable for stent implantation.

The second study (Chapter 4) showed that inflammation increased the correlation between expansion ratio and subsequent restenosis. This finding suggests that as inflammation response increases, the stent design becomes less important, while the level of expansion takes a larger role in stimulating restenosis, which may have important implications for device and treatment design. For example, the patient's inflammatory reaction may dictate which device is best, or if implantation pressure needs to be limited, or if other treatment types are more suitable.

6.4 Modelling the Extracellular Environment

This study represents the first time extracellular biochemical stimuli have been included in a simulation of restenosis. The model included a variable for extracellular matrix, a growth stimulus variable and a matrix degradation variable. These represent biological factors that have been shown to have an important role in restenosis development (see Fig. 6.1).

The extracellular matrix has been shown to affect SMC phenotype (Thyberg, 1996), and so plays a key role in the regulation of tissue growth. The ECM is also a major constituent of neointima in terms of tissue volume, and neointima can progress even with relatively low proliferation rates (O'Brien et al., 2000), indicating the need to model its production explicitly.

The growth stimulus represents an attempt to model the time-course of smooth muscle cell proliferation. The proliferation of SMCs had been shown to require external stimuli (Thyberg et al., 1990), and to be controlled by reducing the amount of that stimulus (Lindner and Reidy, 1991). As stent design may affect where, how much and for how long these factors are released, knowledge of them is essential to accurately predicting the tissue response. The matrix degrading factor (MDF) represents a key link between inflammation and SMC phenotype in that MDF degrades ECM, which leads to a phenotype change (Fig. 6.1). Phenotype modulation is an essential step in neointima formation, and may be controlled by many factors, but one important factor is ECM composition.

The inclusion of these extracellular stimuli represents a new technique for modelling the restenotic response as a network of interacting variables. It opens the way for the simulation of treatment methods which alter these parameters, such as drug eluting stents and balloons. These devices allow the local delivery of anti-proliferative agents to the vessel wall, either from the stent struts, or the surface of a balloon. The key variables in these techniques are the spatial and temporal distribution of the drug in the tissue. Up until now, it has not been possible to look at drug elution, injury and cell activity together, except in animal models, where the reaction to anti-proliferative drugs is very different to humans (Schwartz et al., 2004). With the techniques described in this work, the effects of drugs can be simulated by modelling a drug as another interacting, diffusing species.

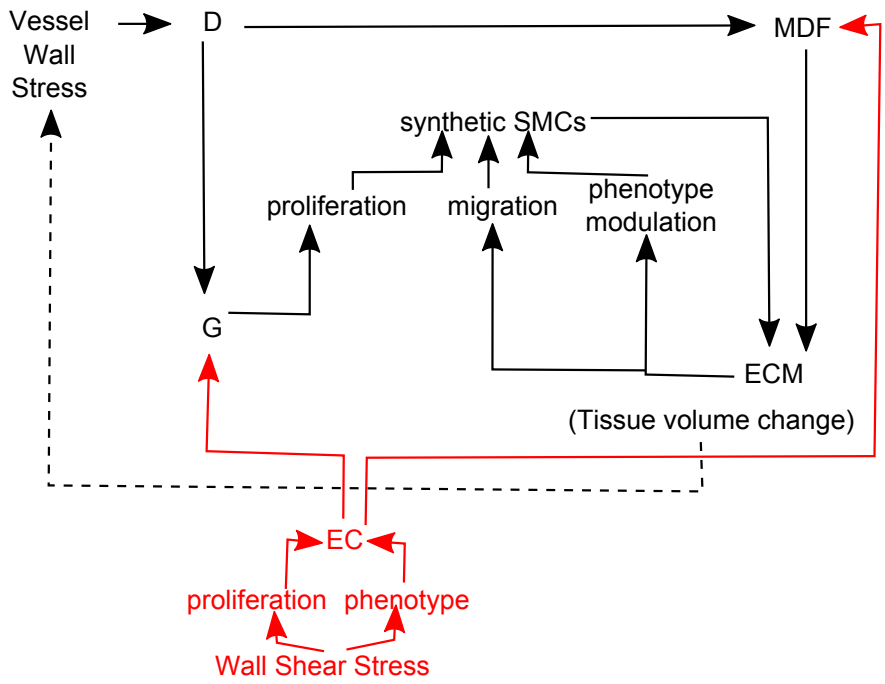

Figure 6.1: System diagram of the mechanoregulation of arterial tissue, showing the cascade response to injury, and showing how fluid flow and chronic stimuli might be incorporated. The solid black arrows show the model described in this thesis. Vessel wall stresses induce injury (D), which promotes inflammatory factors (G and MDF). The MDF in turn alters the extracellular matrix (ECM), which leads to SMC phenotype modulation. Growth factor stimulates these SMCs to proliferate, and the ECM is increased, leading to tissue growth. The dashed line represents the path for mechanoregulatory feedback, whereby tissue alterations modify the stress regime. The red paths indicate a possible approach for including fluid-flow regulation, through the proliferation and regulation of ECs, and the production of inflammatory factors.

6.5 Discrete, Dynamical Modelling

At the tissue level, we can measure stress (predicted using continuum assumptions), and the growth of the material boundary. Many tissue-level

growth models seek to model this boundary growth as a stress-regulating phenomenon at the continuum level (Alastrué et al., 2008; Kuhl et al., 2007; Rachev et al., 2000). Such a modelling approach assumes that the arterial tissue tends towards a homeostatic equilibrium using negative feedback to reduce deviations; a behaviour usually represented with low-order mathematical laws (Murray, 2002). One of the central difficulties with homeostasis-type models when describing the effect of a mechanical perturbation is that they tend to predict that the system returns, or strives to return, to the original/optimal stimulus. In contrast, many biological systems can be seen as an interaction of autonomous entities linked in a discrete, dynamic process (Weinans and Prendergast, 1996). The behaviour of the system is represented as a network of interacting agents (cells) and environmental stimuli. The agents alter their behaviour based on the local environmental cues, and any tissue-level phenomena are as a result of the self-organising properties of the system. The great benefit of this sort of modelling is that the behaviour of the whole model need not be represented with a mathematical analogue. Rather, the behaviour of the model can be far more complex than the individual components making up the model, or any postulated mathematical form. The stochastic nature of the cell behaviours (proliferation, migration, etc.) can also be included, leading to stochastic model predictions more representative of an organism's response.

Continuum modelling remains a useful assumption for many aspects of mechanobiological modelling. In this work, continuum stress assumptions were used as a basis for the computation of stress in the arterial tissue,

which was then calculated using the finite element numerical method. The damage, MDF and ECM variables are also considered as continuum variables, with their values 'sampled' at all lattice sites. These continuum assumptions suit current numerical methods and experimental data on material's elastic and damage properties.

6.6 Mechanobiological Modelling as a Design Tool

The end goal of angioplasty and stenting procedures is to produce a long-term, stable, patent lumen geometry. Stent designs can achieve this by:

- Improving the scaffolding behaviour to maximise post-implantation geometry, thereby trying to offset the neointima produced,
- Minimising the amount of injury caused to the vessel in order to provoke a minimal wound healing response,
- Neutralising the injury response with pharmacological agents.

Each design consideration, such as the numbers or connectivity of struts, affects each of these characteristics, and so it is very difficult to predict the effect of a design change when using preclinical models which treat these characteristics in isolation. The results from this thesis show that strut numbers have a large effect on restenosis, while stent cell design has a less dramatic effect. However, these types of design rules may be very specific to the application, particularly the geometry of the host artery.

For this reason, the mechanobiological modelling approach investigated here represents an early step towards a design tool capable of predicting the restenotic response to a stent. This could then be used to optimised a stent design and to inform guidelines in general stent design.

Chapter 7

Conclusions

7.1 Main findings of this work

The aim of this thesis was to test the hypothesis that arterial neointima formation in response to stent implantation and balloon angioplasty is injury-driven. A computational model was developed based on this hypothesis using discrete cell-based simulations in a lattice, applied to several biomechanical procedures, and compared to experimental studies. The main conclusions of this work are:

- An injury-driven model of restenosis development predicts phenomena at the tissue level concurrent with pathological studies of restenosis *in vivo*: non-linear lesion growth with time, higher neointima at stent struts, a correlation between the number of struts and restenosis, and between the level of stent expansion and restenosis.

- The inflammatory reaction of the artery affects the amount of resteno-

sis produced by stenting, with higher, more chronic, inflammation reactions producing more neointima.

- The differences between stent designs in the amount of restenosis they induce is affected by the intensity of the inflammation reaction. A higher intensity reaction masks the differences between stent designs.
- The extent of stent expansion affects the amount of restenosis produced, with this correlation increasing with the intensity of the inflammatory response.
- The first study produced larger differences between two stents differing in *strut number* than the third study did between three stents with the same strut numbers, but differing stent *cell geometries*. This indicates that the number of struts is a key design consideration.
- The design of treatments for ischaemic heart disease could be improved by optimising for long-term outcomes through the application of computational simulation techniques. The approach has the capacity to include the effects of drugs on the development of neointima.

7.2 Future work

This work represents an early step in the development of computational techniques for the study of restenosis, and for the preclinical prediction of mechanically-induced tissue growth. Some of the most important next steps include:

- Gathering more information on the injury produced by mechanical loading. The damage mechanics data used in this study could be reinforced with more testing over more stress ranges, on human arterial tissue, and on individual tissue layers and plaques. Other damage models and tests could be investigated and performed, such as creep damage tests or tearing analyses. The levels of stress could be related to cell death in tissue samples *in vitro*, such has been performed by Gefen et al. (2008) on tissue constructs of skeletal muscle. This would entail exposing tissue to measurable loading while measuring cell death using markers for cell death. This could be related to continuum stress measures, such as minimum principal stress, calculated in a Finite Element model, establishing the relationship between stress and cell damage.

- Quantifying the relationship between injury and the subsequent inflammation cascade must be elaborated and quantified. This would require measuring markers of inflammation *in vivo* after quantifiable injury is imparted. For example, balloon expansion to specified diameters, followed by measurement of monocyte infiltration. *In vitro* organ culture may also be a useful method for measuring the initial response of arterial tissue.

- Adapting the procedure to patient-specific applications. This will allow more detail of the arterial geometry and distribution of cells in a patient to be included in the model. This sort of analysis may reveal sensitivities which do not arise in the idealised model. The

model could also be applied to a clinical trial-type scenario, where patient parameters vary randomly according to clinical statistics.

- Investigating fluid flow stimuli. The endothelium model from the first study could be adapted to be mechanoregulated by fluid flow-induced shear stresses, calculated using a computational fluid dynamics model, such as the Lattice Boltzmann Method used by Caiazzo et al. (2011). The biological action of the endothelium could be implemented as a source of growth factor and matrix degrading factor at the lumen surface as a function of wall shear stress (Fig. 6.1).

- The injury prediction may also be updated over the simulation if the magnitudes of stress indicate a chronic source of injury. This would require stress-update steps and a modelling technique for the removal of degraded tissue and addition of new material to the artery wall, as these processes would alter the stress regime in the tissue.

- Including drug elution. As described in the above discussion, drug elution from the surface of the stent, and its interaction with the biological components could be studied by introducing a new, diffusible species.

- Refining the inflammation model. This could be refined to explicitly model the activities of inflammatory cells based on experimental findings *in vivo* and *in vitro* using new cell types and behavioural algorithms.

Bibliography

Alastrué, V., Martínez, M. a. and Doblaré, M. (2008), "Modelling adaptative volumetric finite growth in patient-specific residually stressed arteries.", *Journal of Biomechanics* , Vol. 41, pp. 1773–81.

Alber, M., Kiskowski, M., Glazier, J. and Jiang, Y. (2002), "On cellular automaton approaches to modeling biological cells", *IMA VOLUMES IN MATHEMATICS AND ITS APPLICATIONS* , Vol. 134, Citeseer, pp. 1–40.

Allender, S., Scarborough, P., Peto, V. and Rayner, M. (2008), "European Cardiovascular Disease Statistics, 2008 edition. European Heart Network, Brussels, 2008", *Health Economics* .

Bailón-Plaza, A. and van der Meulen, M. (2003), "Beneficial effects of moderate, early loading and adverse effects of delayed or excessive loading on bone healing", *Journal of Biomechanics* , Vol. 36, Elsevier, pp. 1069–1077.

Bailón-Plaza, A. and van der Meulen, M. C. (2001), "A mathematical

framework to study the effects of growth factor influences on fracture healing.", *Journal of Theoretical Biology* , Vol. 212, pp. 191–209.

Bedoya, J., Meyer, C. A., Timmins, L. H., Moreno, M. R. and Moore, J. E. (2006), "Effects of stent design parameters on normal artery wall mechanics.", *Journal of Biomechanical Engineering* , Vol. 128, pp. 757–65.

Bendeck, M. P., Zempo, N., Clowes, a. W., Galardy, R. E. and Reidy, M. a. (1994), "Smooth muscle cell migration and matrix metalloproteinase expression after arterial injury in the rat.", *Circulation Research* , Vol. 75, pp. 539–45.

Bennett, M. and O'Sullivan, M. (2001), "Mechanisms of angioplasty and stent restenosis: implications for design of rational therapy", *Pharmacology & Therapeutics* , Vol. 91, pp. 149–166.

Blackledge, H. and Squire, I. (2009), "Improving long-term outcomes following coronary artery bypass graft or percutaneous coronary revascularisation: results from a large, population-based cohort with first intervention 19952004", *Heart* , Vol. 95, BMJ Publishing Group Ltd and British Cardiovascular Society, p. 304.

Boyle, C. J., Lennon, a. B., Early, M., Kelly, D. J., Lally, C. and Prendergast, P. J. (2010), "Computational simulation methodologies for mechanobiological modelling: a cell-centred approach to neointima development in stents.", *Philosophical Transactions of the Royal Society*

of London. Series A, Mathematical, physical, and engineering sciences , Vol. 368, pp. 2919–35.

Byrne, D. P. (2008), Computational modelling of bone regeneration using a three-dimensional lattice approach, PhD thesis, Trinity College Dublin, Dublin.

Byrne, D. P., Lacroix, D., Planell, J. A., Kelly, D. J. and Prendergast, P. J. (2007), "Simulation of tissue differentiation in a scaffold as a function of porosity, Young's modulus and dissolution rate: application of mechanobiological models in tissue engineering", *Biomaterials* , Vol. 28, pp. 5544–5554.

Caiazzo, A., Evans, D., Falcone, J., Hegewald, J., Lorenz, E., Stahl, B., Wang, D., Bernsdorf, J., Chopard, B., Gunn, J., Hose, R., Krafczyk, M., Lawford, P., Smallwood, R., Walker, D. and Hoekstra, A. (2009), "Towards a complex automata multiscale model of in-stent restenosis", *Computational Science ICCS 2009* , Springer, pp. 705–714.

Caiazzo, A., Evans, D., Falcone, J.-L., Hegewald, J., Lorenz, E., Stahl, B., Wang, D., Bernsdorf, J., Chopard, B., Gunn, J., Hose, R., Krafczyk, M., Lawford, P., Smallwood, R., Walker, D. and Hoekstra, A. (2011), "A Complex Automata approach for in-stent restenosis: Two-dimensional multiscale modelling and simulations", *Journal of Computational Science* , Vol. 2, Elsevier B.V., pp. 9–17.

Casscells, W. (1992), "Migration of smooth muscle and endothelial cells. Critical events in restenosis", *Circulation* , Vol. 86, pp. 723–729.

Central Statistics Office of Ireland, C. (2006), 'Principal Causes of Death'.

Chamley-Campbell, J. H., Campbell, G. R. and Ross, R. (1981), "Phenotype-dependent Response of Cultured Aortic Smooth Muscle to Serum Mitogens Spontaneous Change in Phenotype", *Journal of Cell Biology* , Vol. 89, pp. 379–383.

Checa, S. and Prendergast, P. J. (2009), "A mechanobiological model for tissue differentiation that includes angiogenesis: a lattice-based modeling approach.", *Annals of biomedical engineering* , Vol. 37, pp. 129–45.

Chopard, B. and Droz, M. (1998), *Cellular automata modelling of physical systems*.

Cipollone, F., Marini, M., Fazia, M., Pini, B., Iezzi, A., Reale, M., Paloscia, L., Materazzo, G., D'Annunzio, E., Conti, P. and Others (2001), "Elevated circulating levels of monocyte chemoattractant protein-1 in patients with restenosis after coronary angioplasty", *Arteriosclerosis, thrombosis, and vascular biology* , Vol. 21, Am Heart Assoc, p. 327.

Codling, E. a., Plank, M. J. and Benhamou, S. (2008), "Random walk models in biology.", *Journal of the Royal Society, Interface* , Vol. 5, pp. 813–34.

Cowin, S. C. and Hegedus, D. H. (1976), "Bone remodeling I: theory of adaptive elasticity", *Journal of Elasticity* , Vol. 6, Springer Netherlands, pp. 313–326.

Davis, C., Fischer, J., Ley, K. and Sarembock, I. J. (2003), "The role of

inflammation in vascular injury and repair.", *Journal of Thrombosis and Haemostasis* , Vol. 1, pp. 1699–709.

De Beule, M., Mortier, P., Carlier, S. G., Verhegghe, B., Van Impe, R. and Verdonck, P. (2008), "Realistic finite element-based stent design: The impact of balloon folding", *Journal of Biomechanics* , Vol. 41, pp. 383–389.

Dean, C. J., Morton, a. C., Arnold, N., Hose, D. R., Crossman, D. C. and Gunn, J. (2005), "Relative importance of the components of stent geometry to stretch induced in-stent neointima formation.", *Heart* , Vol. 91, pp. 1603–4.

DiMilla, P. A., Stone, J. A., Quinn, J. A., Albelda, S. M. and Lauffenburger, D. A. (1993), "Maximal migration of human smooth muscle cells on fibronectin and type IV collagen occurs at an intermediate attachment strength", *Journal of Cell Biology* , Vol. 122, pp. 729–737.

Dormann, S. and Deutsch, A. (2002), "Modeling of self-organized avascular tumor growth with a hybrid cellular automaton.", *In Silico Biology* , Vol. 2, pp. 393–406.

Drasdo, D. (2005), "Coarse graining in simulated cell populations", *Advances in Complex Systems* , Vol. 8, Singapore: World Scientific, p. 319.

Drasdo, D., Kree, R. and McCaskill, J. (1995), "Monte Carlo approach to tissue-cell populations", *Physical review. E, Statistical, nonlinear, and soft matter physics* , Vol. 52, APS, p. 6635.

Duraiswamy, N., Schoephoerster, R. T., Moreno, M. R. and Moore, J. E. (2007), "Stented Artery Flow Patterns and Their Effects on the Artery Wall", *Annual Review of Fluid Mechanics* , Vol. 39, pp. 357–382.

Early, M. and Kelly, D. J. (2010), "The role of vessel geometry and material properties on the mechanics of stenting in the coronary and peripheral arteries", *Proceedings of the Institution of Mechanical Engineers, Part H: Journal of Engineering in Medicine* , Vol. 224, pp. 465–476.

Early, M., Lally, C., Prendergast, P. J. and Kelly, D. J. (2009), "Stresses in peripheral arteries following stent placement: a finite element analysis.", *Computer Methods in Biomechanics and Biomedical Engineering* , Vol. 12, pp. 25–33.

Edelman, E. and Rogers, C. (1999), "Stent-versus-stent equivalency trials: Are some stents more equal than others?", *Circulation* , Vol. 100, Am Heart Assoc, p. 896.

Esper, R. J., Nordaby, R. A., Vilarino, J. O., Paragano, A., Cacharron, J. L. and Machado, R. A. (2006), "Endothelial dysfunction: a comprehensive appraisal", *Cardiovascular Diabetology* , Vol. 5, p. 4.

Evans, D. J. W., Lawford, P. V., Gunn, J., Walker, D., Hose, D. R., Smallwood, R. H., Chopard, B., Krafczyk, M., Bernsdorf, J. and Hoekstra, A. (2008), "The application of multiscale modelling to the process of development and prevention of stenosis in a stented coronary artery.", *Philosophical Transactions of the Royal Society of London. Series A,*

Mathematical, physical, and engineering sciences , Vol. 366, pp. 3343–60.

Farb, A., Sangiorgi, G., Carter, A. J., Walley, V. M., Edwards, W. D., Schwartz, R. S. and Virmani, R. (2007), "Pathology of acute and chronic coronary stenting in humans.", *Circulation* , Vol. 99, pp. 44–52.

Farb, A., Weber, D., Kolodgie, F., Burke, A. and Virmani, R. (2002), "Morphological predictors of restenosis after coronary stenting in humans", *Circulation* , Vol. 105, Am Heart Assoc, p. 2974.

Fingerle, J., Au, Y., Clowes, A. and Reidy, M. (1990), "Intimal lesion formation in rat carotid arteries after endothelial denudation in absence of medial injury", *Arteriosclerosis, Thrombosis, and Vascular Biology* , Vol. 10, Am Heart Assoc, p. 1082.

Forrester, J. S., Fishbein, M., Helfant, R. and Fagin, J. (1991), "A paradigm for restenosis based on cell biology: clues for the development of new preventive therapies", *Journal of the American College of Cardiology* , Vol. 17, pp. 758–769.

Frost, H. M. (1989), "The biology of fracture healing. An overview for clincians. Part 1", *Clin. Orthop. Relat. Res.* , Vol. 248, pp. 283–293.

Galle, J., Loeffler, M. and Drasdo, D. (2005), "Modeling the effect of deregulated proliferation and apoptosis on the growth dynamics of epithelial cell populations in vitro.", *Biophysical journal* , Vol. 88, pp. 62–75.

Garasic, J. M., Edelman, E. R., Squire, J. C., Seifert, P., Williams, M. S.

and Rogers, C. (2000), "Stent and artery geometry determine intimal thickening independent of arterial injury.", *Circulation* , Vol. 101, pp. 812–8.

García, J. (2002), "Bone remodelling simulation: a tool for implant design", *Computational Materials Science* , Vol. 25, pp. 100–114.

Geary, R., Nikkari, S., Wagner, W., Williams, J., Adams, M. and Dean, R. (1998), "Wound healing: a paradigm for lumen narrowing after arterial reconstruction", *Journal of Vascular Surgery* , Vol. 27, Elsevier, pp. 96–108.

Gefen, A., van Nierop, B., Bader, D. and Oomens, C. W. (2008), "Strain-time cell-death threshold for skeletal muscle in a tissue-engineered model system for deep tissue injury.", *Journal of Biomechanics* , Vol. 41, pp. 2003–12.

Gervaso, F., Capelli, C., Petrini, L., Lattanzio, S., Di Virgilio, L. and Migliavacca, F. (2008), "On the effects of different strategies in modelling balloon-expandable stenting by means of finite element method.", *Journal of Biomechanics* , Vol. 41, pp. 1206–12.

Gijsen, F., Migliavacca, F., Schievano, S., Socci, L., Petrini, L., Thury, A., Wentzel, J., van der Steen, A., Serruys, P. and Dubini, G. (2008), "Simulation of stent deployment in a realistic human coronary artery", *BioMedical Engineering OnLine* , Vol. 7, p. 23.

Glagov, S. (1994), "Current Perspectives Intimal Hyperplasia , Vascular

Modeling , and the Restenosis Problem", *Circulation* , Vol. 89, pp. 2888–2891.

Glagov, S., Zarins, C. K., Masawa, N., Xu, C. P., Bassiouny, H. and Giddens, D. P. (1993), "Mechanical functional role of non-atherosclerotic intimal thickening", *Frontiers Med. Biol. Eng.* , Vol. 5, pp. 37–43.

Glazier, J. and Graner, F. (1993), "Simulation of the differential adhesion driven rearrangement of biological cells", *Physical review. E, Statistical, nonlinear, and soft matter physics* , Vol. 47, APS, p. 2128.

Groves, P., Banning, A., Penny, W., Lewis, M., Cheadle, H. and Newby, A. (1995), "Kinetics of smooth muscle cell proliferation and intimal thickening in a pig carotid model of balloon injury", *Atherosclerosis* , Vol. 117, Elsevier, pp. 83–96.

Gunn, J., Arnold, N., Chan, K. H., Shepherd, L., Cumberland, D. C. and Crossman, D. C. (2002), "Coronary artery stretch versus deep injury in the development of in-stent neointima", *Heart* , Vol. 88, pp. 401–405.

Hansson, G. K. (2005), "Inflammation, atherosclerosis, and coronary artery disease", *New England Journal of Medicine* , Vol. 352, pp. 1685–1695.

Harnek, J., Zoucas, E., Carlemalm, E. and Cwikiel, W. (1999), "Differences in endothelial injury after balloon angioplasty, insertion of balloon-expanded stents or release of self-expanding stents: An electron microscopic experimental study", *Cardiovasc Intervent Radiol* , Vol. 22, pp. 56–61.

Hayward, I., Bridle, K., Campbell, G. R., Underwood, P. and Campbell, J. H. (1995), "Effect of extracellular matrix proteins on vascular smooth muscle cell phenotype", *Cell Biology International* , Vol. 19, Elsevier, pp. 727–734.

Hedin, U., Bottger, B., Forsberg, E., Johansson, S. and Thyberg, J. (1988), "Diverse effects of fibronectin and laminin on phenotypic properties of cultured arterial smooth muscle cells.", *Journal of Cell Biology* , Vol. 107, Rockefeller Univ Press, p. 307.

Hirst, S. J., Twort, C. H. and Lee, T. H. (2000), "Differential effects of extracellular matrix proteins on human airway smooth muscle cell proliferation and phenotype.", *American Journal of Respiratory Cell and Molecular Biology* , Vol. 23, pp. 335–44.

Hoffmann, R., Jansen, C., Konig, A., Haager, P. K., Kerckhoff, G., Vom Dahl, J., Klauss, V., Hanrath, P. and Mudra, H. (2001), "Stent design related neointimal tissue proliferation in human coronary arteries - An intravascular ultrasound study", *European Heart Journal* , Vol. 22, pp. 2007–2014.

Hoffmann, R., Mintz, G. S., Haager, P. K., Bozoglu, T., Grube, E., Gross, M., Beythien, C., Mudra, H., vom Dahl, J. and Hanrath, P. (2002), "Relation of stent design and stent surface material to subsequent in-stent intimal hyperplasia in coronary arteries determined by intravascular ultrasound", *American Journal of Cardiology* , Vol. 89, pp. 1360–1364.

Holzapfel, G. A., Sommer, G., Gasser, C. T. and Regitnig, P. (2005), "De-

termination of layer-specific mechanical properties of human coronary arteries with nonatherosclerotic intimal thickening and related constitutive modeling", *American Journal of Physiology-Heart and Circulatory Physiology* , Vol. 289, pp. H2048–H2058.

Holzapfel, G. a., Stadler, M. and Schulze-Bauer, C. a. J. (2002), "A layer-specific three-dimensional model for the simulation of balloon angioplasty using magnetic resonance imaging and mechanical testing", *Annals of Biomedical Engineering* , Vol. 30, pp. 753–767.

Holzapfel, G., Gasser, T. and Ogden, R. (2000), "A new constitutive framework for arterial wall mechanics and a comparative study of material models", *Journal of elasticity* , Vol. 61, Springer, pp. 1–48.

Huiskes, R., Weinans, H., Grootenboer, H. J., Dalstra, M., Fudala, B. and Slooff, T. J. (1987), "Adaptive bone-remodeling theory applied to prosthetic-design analysis", *Journal of Biomechanics* , Vol. 20, pp. 1135–1150.

Humphrey, J. D. (2008), "Vascular adaptation and mechanical homeostasis at tissue, cellular, and sub-cellular levels.", *Cell biochemistry and biophysics* , Vol. 50, pp. 53–78.

Johnson, G. J., Griggs, T. R. and Badimon, L. (1999), "The Utility of Animal Models in the Preclinical Study of Interventions to Prevent Human Coronary Artery Restenosis: Analysis and Recommendations", *Thromb Haemost* , Vol. 81, pp. 835–843.

Kandzari, D. E., Tcheng, J. E. and Zidar, J. P. (2002), "Coronary artery stents: Evaluating new designs for contemporary percutaneous intervention", *Catheterization and Cardiovascular Interventions* , Vol. 56, pp. 562–576.

Kansal, a. R., Torquato, S., Harsh GR, I. V., Chiocca, E. a. and Deisboeck, T. S. (2000), "Simulated brain tumor growth dynamics using a three-dimensional cellular automaton.", *Journal of Theoretical Biology* , Vol. 203, pp. 367–82.

Kastrati, a., Mehilli, J., Dirschinger, J., Pache, J., Ulm, K., Schühlen, H., Seyfarth, M., Schmitt, C., Blasini, R., Neumann, F. J. and Schömig, a. (2001), "Restenosis after coronary placement of various stent types.", *American Journal of Cardiology* , Vol. 87, pp. 34–9.

Khayyeri, H., Checa, S., Tägil, M., Aspenberg, P. and Prendergast, P. J. (2011), "Variability observed in mechano-regulated in vivo tissue differentiation can be explained by variation in cell mechano-sensitivity.", *Journal of Biomechanics* , Vol. 44, pp. 1051–8.

Khayyeri, H., Checa, S., Tägil, M. and Prendergast, P. J. (2009), "Corroboration of mechanobiological simulations of tissue differentiation in an in vivo bone chamber using a lattice-modeling approach.", *Journal of Orthopaedic Research* , Vol. 27, pp. 1659–66.

Kipshidze, N., Dangas, G., Tsapenko, M., Moses, J., Leon, M. B., Kutryk, M. and Serruys, P. (2004), "Role of the endothelium in modulating neointimal formation: vasculoprotective approaches to attenuate

restenosis after percutaneous coronary interventions", *Journal of the American College of Cardiology* , Vol. 44, pp. 733–739.

Kornowski, R., Hong, M. K., Tio, F. O., Bramwell, O., Wu, H. and Leon, M. B. (1998), "In-stent restenosis: contributions of inflammatory responses and arterial injury to neointimal hyperplasia", *Journal of the American College of Cardiology* , Vol. 31, pp. 224–230.

Kuhel, D. G. (2002), "Distinction in Genetic Determinants for Injury-Induced Neointimal Hyperplasia and Diet-Induced Atherosclerosis in Inbred Mice", *Arteriosclerosis, Thrombosis, and Vascular Biology* , Vol. 22, pp. 955–960.

Kuhl, E., Maas, R., Himpel, G. and Menzel, A. (2007), "Computational modeling of arterial wall growth. Attempts towards patient-specific simulations based on computer tomography.", *Biomechanics and Modeling in Mechanobiology* , Vol. 6, pp. 321–31.

Kuhl, E., Menzel, a. and Steinmann, P. (2003), "Computational modeling of growth", *Computational Mechanics* , Vol. 32, pp. 71–88.

Lacroix, D., Prendergast, P. J., Li, G. and Marsh, D. (2002), "Biomechanical model to simulate tissue differentiation and bone regeneration: application to fracture healing", *Medical and Biological Engineering and Computing* , Vol. 40, pp. 14–21.

Lally, C., Dolan, F. and Prendergast, P. J. (2005), "Cardiovascular stent design and vessel stresses: a finite element analysis.", *Journal of Biomechanics* , Vol. 38, pp. 1574–81.

Lally, C., Kelly, D. J. and Prendergast, P. J. (2006), *Stents*, in Encyclopedia of Biomedical Engineering, Wiley.

Lally, C. and Prendergast, P. J. (2006), *Simulation of In-stent Restenosis for the Design of Cardiovascular Stents*, in Mechanics of Biological Tissue, Springer-Verlag, pp. 255–267.

Lander, A. D. (2004), "A calculus of purpose.", *PLoS biology* , Vol. 2, p. e164.

Lee, Y., Pan, J., Hathaway, R. and Barkey, M. (2005), *Fatigue Testing and Analysis, Theory and Practice*, Elsevier.

Lennon, A., Khayyeri, H., Xue, F. and Prendergast, P. (2011), *Biomechanical Modelling of Cells in Mechanoregulation*, Vol. 4, Springer, p. 297.

Libby, P., Schwartz, D., Brogi, E., Tanaka, H. and Clinton, S. K. (1992), "A cascade model for restenosis. A special case of atherosclerosis progression.", *Circulation* , Vol. 86, pp. III47–52.

Linder-Ganz, E., Engelberg, S., Scheinowitz, M. and Gefen, A. (2006), "Pressure-time cell death threshold for albino rat skeletal muscles as related to pressure sore biomechanics", *Journal of Biomechanics* , Vol. 39, pp. 2725–2732.

Lindner, V. and Reidy, M. (1991), "Proliferation of smooth muscle cells after vascular injury is inhibited by an antibody against basic fibroblast growth factor", *Proceedings of the National Academy of Sciences of the United States of America* , Vol. 88, National Acad Sciences, p. 3739.

Liu, S. Q., Ruan, Y. Y., Tang, D., Li, Y. C., Goldman, J. and Zhong, L. (2002), "A possible role of initial cell death due to mechanical stretch in the regulation of subsequent cell proliferation in experimental vein grafts", *Biomechanics and Modeling in Mechanobiology* , Vol. 1, pp. 17–27.

McLoughlin, R. (2008), Tensile fatigue behaviour of porcine coronary arterial tissue in the longitudinal and circumferential directions, Master's thesis, University of Dublin, Dublin.

Merks, R. and Glazier, J. (2005), "A cell-centered approach to developmental biology", *Physica A: Statistical Mechanics and its Applications* , Vol. 352, pp. 113–130.

Mi, Q., Riviere, B., Clermont, G., Steed, D. L. and Vodovotz, Y. (2007), "Agent-based model of inflammation and wound healing: insights into diabetic foot ulcer pathology and the role of transforming growth factor-beta 1", *Wound Repair and Regeneration* , Vol. 15, pp. 671–682.

Migliavacca, F., Petrini, L., Colombo, M., Auricchio, F. and Pietrabissa, R. (2002), "Mechanical behavior of coronary stents investigated through the finite element method", *Journal of Biomechanics* , Vol. 35, pp. 803–811.

Migliavacca, F., Petrini, L., Massarotti, P., Schievano, S., Auricchio, F. and Dubini, G. (2004), "Stainless and shape memory alloy coronary stents: a computational study on the interaction with the vascular wall", *Biomechanics and Modeling in Mechanobiology* , Vol. 2, pp. 205–217.

Moore, M., Goldman, J., Patel, A., Chien, S. and Liu, S. (2001), "Role of tensile stress and strain in the induction of cell death in experimental vein grafts", *Journal of Biomechanics* , Vol. 34, pp. 289–297.

Moreira, J. and Deutsch, A. (2002), "Cellular automation models of tumor development: a critical review", *Advances in Complex Systems* , Vol. 5, pp. 247–268.

Moretti, M., Prina-Mello, A., Reid, A., Barron, V. and Prendergast, P. J. (2004), "Endothelial cell alignment on cyclically-stretched silicone surfaces", *Journal of Materials Science: Materials in Medicine* , Vol. 15, pp. 1159–1164.

Morton, A. C., Crossman, D. and Gunn, J. (2004), "The influence of physical stent parameters upon restenosis.", *Pathologie-Biologie* , Vol. 52, pp. 196–205.

Murray, J. D. (2002), *Mathematical Biology I: An Introduction*, 3rd edn, Springer.

O'Brien, E. R., Urieli-Shoval, S., Garvin, M. R., Stewart, D. K., Hinohara, T., Simpson, J. B., Benditt, E. P. and Schwartz, S. M. (2000), "Replication in restenotic atherectomy tissue.", *Atherosclerosis* , Vol. 152, pp. 117–26.

Peck, S. L. (2004), "Simulation as experiment: a philosophical reassessment for biological modeling", *Trends in Ecology & Evolution* , Vol. 19, pp. 530–534.

Pérez, M. A. and Prendergast, P. J. (2007), "Random-walk models of cell dispersal included in mechanobiological simulations of tissue differentiation.", *Journal of Biomechanics* , Vol. 40, pp. 2244–53.

Prendergast, P. J. (2009), Papers in Biomechanics and Bioengineering, Scd, University of Dublin.

Prendergast, P. J., Checa, S. and Lacroix, D. (2010), "Computational Modeling in Biomechanics", *Bioengineering* , Springer Netherlands, Dordrecht.

Prendergast, P. J., Huiskes, R. and Soballe, K. (1997), "Biophysical Stimuli on Cells During Tissue Differentiation at Implant Interfaces", *Journal of Biomechanics* , Vol. 30, pp. 539–548.

Prendergast, P. J., Lally, C., Daly, S., Reid, A. J., Lee, T. C., Quinn, D. and Dolan, F. (2003), "Analysis of Prolapse in Cardiovascular Stents: A Constitutive Equation for Vascular Tissue and Finite-Element Modelling", *Journal of Biomechanical Engineering* , Vol. 125, p. 692.

Rachev, A., Manoach, E., Berry, J. and Moore, J. E. (2000), "A model of stress-induced geometrical remodeling of vessel segments adjacent to stents and artery/graft anastomoses.", *Journal of Theoretical Biology* , Vol. 206, pp. 429–43.

Reneman, R. S., Arts, T. and Hoeks, A. P. (2006), "Wall shear stress–an important determinant of endothelial cell function and structure–in the arterial system in vivo. Discrepancies with theory", *Journal of Vascular Research* , Vol. 43, pp. 251–269.

Resnick, N., Yahav, H., Shay-Salit, A., Shushy, M., Schubert, S., Zilberman, L. and Wofovitz, E. (2003), "Fluid shear stress and the vascular endothelium: for better and for worse", *Progress in biophysics and molecular biology* , Vol. 81, Elsevier, pp. 177–199.

Rogers, C., Welt, F. G., Karnovsky, M. J. and Edelman, E. R. (1996), "Monocyte Recruitment and Neointimal Hyperplasia in Rabbits: Coupled Inhibitory Effects of Heparin", *Arteriosclerosis, Thrombosis, and Vascular Biology* , Vol. 16, pp. 1312–1318.

Ruimerman, R., Hilbers, P., van Rietbergen, B. and Huiskes, R. (2005), "A theoretical framework for strain-related trabecular bone maintenance and adaptation", *Journal of Biomechanics* , Vol. 38, pp. 931–941.

Schulz, C., Herrmann, R., Beilharz, C., Pasquantonio, J. and Alt, E. (2000), "Coronary stent symmetry and vascular injury determine experimental restenosis", *Heart* , Vol. 83, BMJ Publishing Group Ltd and British Cardiovascular Society, p. 462.

Schwartz, R. S., Chronos, N. A. and Virmani, R. (2004), "Preclinical restenosis models and drug-eluting stents: still important, still much to learn.", *Journal of the American College of Cardiology* , Vol. 44, pp. 1373–85.

Schwartz, R. S., Chu, A., Edwards, W. D., Srivatsa, S. S., Simari, R. D., Isner, J. M. and Holmes, D. R. (1996), "A proliferation analysis of arterial neointimal hyperplasia: lessons for antiproliferative restenosis therapies", *International Journal of Cardiology* , Vol. 53, pp. 71–80.

Scott, N. A. (2006), "Restenosis following implantation of bare metal coronary stents: pathophysiology and pathways involved in the vascular response to injury.", *Advanced drug delivery reviews* , Vol. 58, pp. 358–76.

Simpson, M., Merrifield, A., Landman, K. and Hughes, B. (2007), "Simulating invasion with cellular automata: Connecting cell-scale and population-scale properties", *Physical review. E, Statistical, nonlinear, and soft matter physics* , Vol. 76, pp. 1–11.

Thanyasiri, P., Kathir, K., Celermajer, D. S. and Adams, M. R. (2007), "Endothelial dysfunction and restenosis following percutaneous coronary intervention.", *International Journal of Cardiology* , Vol. 119, pp. 362–7.

Thyberg, J. (1996), "Differentiated properties and proliferation of arterial smooth muscle cells in culture.", *International Review of Cytology* , Vol. 169, pp. 183–265.

Thyberg, J., Blomgren, K., Roy, J., Tran, P. and Hedin, U. (1997), "Phenotypic modulation of smooth muscle cells after arterial injury is associated with changes in the distribution of laminin and fibronectin", *Journal of Histochemistry and Cytochemistry* , Vol. 45, Histochemical Soc, p. 837.

Thyberg, J., Hedin, U., Sjolund, M., Palmberg, L. and Bottger, B. (1990), "Regulation of differentiated properties and proliferation of arterial smooth muscle cells", *Arteriosclerosis, Thrombosis, and Vascular Biology* , Vol. 10, Am Heart Assoc, p. 966.

Timmins, L., Moreno, M., Meyer, C., Criscione, J., Rachev, A. and Moore, J. (2007), "Stented artery biomechanics and device design optimization",

Medical and Biological Engineering and Computing , Vol. 45, Springer, pp. 505–513.

Tracy, R. (1997), "Declining density of intimal smooth muscle cells as a precondition for atheronecrosis in the coronary artery", *Virchows Archiv* , Vol. 430, Springer, pp. 155–162.

van Oers, R. F. M., Ruimerman, R., Tanck, E., Hilbers, P. A. J. and Huiskes, R. (2008), "A unified theory for osteonal and hemi-osteonal remodeling.", *Bone* , Vol. 42, pp. 250–9.

Walker, D. C., Southgate, J., Hill, G., Holcombe, M., Hose, D. R., Wood, S. M., Mac Neil, S. and Smallwood, R. H. (2002), "The epitheliome: agent-based modelling of the social behaviour of cells.", *Bio Systems* , Vol. 76, pp. 89–100.

Weinans, H. and Prendergast, P. J. (1996), "Tissue adaptation as a dynamical process far from equilibrium", *Bone* , Vol. 19, pp. 143–149.

Welt, F. G. P., Tso, C., Edelman, E. R., Kjelsberg, M. a., Paolini, J. F., Seifert, P. and Rogers, C. (2003), "Leukocyte recruitment and expression of chemokines following different forms of vascular injury.", *Vascular Medicine* , Vol. 8, pp. 1–7.

Welt, F. G. and Rogers, C. (2002), "Inflammation and restenosis in the stent era", *Arteriosclerosis, Thrombosis, and Vascular Biology* , Vol. 22, pp. 1769–1776.

Wentzel, J., Gijsen, F., Stergiopulos, N., Serruys, P., Slager, C. and Krams,

R. (2003), "Shear stress, vascular remodeling and neointimal formation", *Journal of Biomechanics* , Vol. 36, pp. 681–688.

Wentzel, J., Kloet, J., Andhyiswara, I., Oomen, J., Schuurbiers, J., de Smet, B., Post, M., de Kleijn, D., Pasterkamp, G., Borst, C., Slager, C. and Krams, R. (2001), "Shear-stress and wall-stress regulation of vascular remodeling after balloon angioplasty - Effect of matrix metalloproteinase inhibition", *Circulation* , Vol. 104, pp. 91–96.

White, C., Haidekker, M. and Bao, X. (2001), "Temporal gradients in shear, but not spatial gradients, stimulate endothelial cell proliferation", *Circulation* , Vol. 103, pp. 2508–2513.

Windecker, S. and Meier, B. (2001), "All stents are not alike or is the difference in the eye of the observer only?", *European Heart Journal* , Vol. 22, pp. 1973–7.

Zahedmanesh, H. (2011), Finite Element and Mechanobiological Modelling of Vascular Devices, Phd, Dublin City University.

Zarins, C. K., Zatina, M. A., Giddens, D. P., Ku, D. N. and Glagov, S. (1987), "Shear stress regulation of artery lumen diameter in experimental atherogenesis", *Journal of Vascular Surgery* , Vol. 5, pp. 413–420.

Zempo, N., Koyama, N., Kenagy, R. D., Lea, H. J. and Clowes, a. W. (1996), "Regulation of vascular smooth muscle cell migration and proliferation in vitro and in injured rat arteries by a synthetic matrix metalloproteinase inhibitor.", *Arteriosclerosis, thrombosis, and vascular biology* , Vol. 16, pp. 28–33.

Zhuang, Y. J., Singh, T. M., Zarins, C. K. and Masuda, J. (1998), "Sequential increases and decreases in blood flow stimulates progressive intimal thickening", *Eur. J. Vasc. Endovasc. Surg.* , Vol. 16, pp. 301–310.

Zohdi, T. I., Holzapfel, G. A. and Berger, S. A. (2004), "A phenomenological model for atherosclerotic plaque growth and rupture", *Journal of Theoretical Biology* , Vol. 227, pp. 437–443.

Zygourakis, K., Bizios, R. and Markenscoff, P. (1991), "Proliferation of anchorage-dependent contact-inhibited cells: I. Development of theoretical models based on cellular automata", *Biotechnology and Bioengineering* , Vol. 38, pp. 459–470.